NORTHWESTERN UNIVERSITY

Mechanistic Modeling of Polymer Pyrolysis: Investigation of Intrinsic Kinetics, Reaction Pathways, and Structural Heterogeneities

A DISSERTATION

SUBMITTED TO THE GRADUATE SCHOOL

IN PARTIAL FULFILLMENT OF THE REQUIREMENTS

for the degree

DOCTOR OF PHILOSOPHY

Field of Chemical and Biological Engineering

By

Seth Elon Levine

EVANSTON, ILLINOIS

December 2008

ABSTRACT

Mechanistic Modeling of Polymer Pyrolysis: Investigation of Intrinsic Kinetics, Reaction Pathways, and Structural Heterogeneities

Seth Elon Levine

Resource recovery is a promising category of polymer recycling where polymeric waste is converted via thermal or chemical means to monomer and chemical feedstocks. Specifically, pyrolysis is an attractive method because of its simplicity and ability to handle a heterogeneous feedstock. Polymer pyrolysis is characterized by a complex free radical reaction network, which often yields a diverse product spectrum. While polymer pyrolysis has been studied for over 60 years, there are still questions about the kinetics and mechanisms of these reaction systems. We have utilized detailed mechanistic modeling to gain insight into the kinetics and mechanisms of polystyrene (PS), polyethylene (PE), and poly(styrene peroxide) (PSP) pyrolysis.

Mechanistic models based on the method of moments were developed to study PS and PE pyrolysis. Using the PS pyrolysis model, the possible reaction pathways for styrene dimer formation were examined. Net rate analysis demonstrated that the 7,3-hydrogen shift pathway was dominant for dimer formation, while the benzyl radical addition pathway became more competitive as temperature increased. Additionally, the PS pyrolysis model was used to determine an overall activation energy of 53.3 +/- 1.3 kcal mol^{-1}, which was free of transport effects. The PE pyrolysis model was utilized to study the temporal evolution of the diverse product spectrum from PE decomposition. Net rate analysis was utilized to compare the general

reaction pathways of product formation. Random scission was found to be dominant, while the backbiting pathway played a complementary role for product formation during PE pyrolysis.

The method of moments modeling framework was extended by developing an algorithm to track backbone triad concentrations within polymer pyrolysis models. The algorithm was validated using the PS pyrolysis model. A PSP pyrolysis model was constructed using this algorithm and was of manageable size, but because of the stiffness of the model equations, it could not be solved. To address this difficulty, a kinetic Monte Carlo model for PSP pyrolysis was constructed. The model was used to test the traditional mechanism for PSP pyrolysis. A new reaction pathway relying on successive hydrogen abstraction reactions was found to be viable for formation of the minor products of PSP pyrolysis.

ACKNOWLEDGEMENTS

I would not be here today without the support of a myriad of people who have assisted me in many different ways during my time as a graduate student. I would like to acknowledge and thank the friends, family, and mentors who has played a role in my life during the past five years.

I have had the pleasure to work under the guidance of Linda Broadbelt. Linda has provide a perfect combination of freedom to pursue my research project on my own while still providing much needed insight and a guiding hand to keep me on track. Her research group has been a wonderful environment to work in for the past five years. Linda's unshakable confidence in me as a researcher has been invaluable especially when my own doubts were affecting my work. I want to thank Linda for being such a tireless mentor to me.

I would also like to thank the members of my research committee, John Torkelson, Joseph Fitzpatrick, and Vassily Hatzimanikatis, for the valuable comments and guidance they have provided me during my research career. They have aided not just in focusing my research but also in making me a better presenter so that my ideas and conclusions are conveyed in a clearer and more certain fashion. I would also like to acknowledge Harold Kung for his mentoring of me when I participated in the Teaching Apprenticeship Program. His feedback made me a better teacher and lecturer.

I would like to thank the members of both the Snurr and Broadbelt research groups for helpful questions and feedback during five years of group meetings together. I have always enjoyed group meeting (even if I occasionally fall asleep during them) as a great chance to hear about different research and to provide and receive valuable criticism. I would like to acknowledge Shumaila Khan, Maria Curet-Arana, Andrew Cho, Debarshi Majumder, Jim

Pfaendtner, Simon Albo, Chris Henry, Joanna Gonzalez, Rodney Priestley, Xinrui Yu, Chunyi Sung, Stacey Finley, Andrew Adamczyk, Gloria Emberger, Lin Wang, Xiaoying Bao, Ivan Konstantinov, Patrick Ryan, Kate Bjorkman, Rafael Alcala, Raj Assary my colleagues over these five years in the Broadbelt group (I apologize if I have forgotten anyone). I would particularly like to thank Jim, Simon, Rodney, Cho, Xinrui, Stacey, Ivan, and Patrick for their friendship over the years. My time in grad school would not have been the same without the friendship of Sofia Garcia, Shara Dellatore, Houston Frost, Rodney, Cho, Chris Ellison, and Stan Rendon.

I would like to thank Dr. David Shor for helping me work through some tough times I have had during graduate school. You have been a valuable listener and source of guidance when I have been confused.

I would not be here today without my amazing family. My parents, Marty and Carole Levine, have been amazing inspirations and cheerleaders for me my entire life. They have always been available to me when I need some parental advice or just some of my Mom's cookies. Whether it was brewing beer with my brother Noah or playing a random game with my brother Ben or being asked a random math/science question by my sister-in-law Michelle my siblings have been wonderful friends. I love you all very much and thank you for always being there for me no matter what.

I would also like to thank my close friends, Mark and Danielle Kestnbaum, Joey Hailpern and Inbal Fraiman, and David Rubin. I have known all of you for most of my life. You guys have always been there for me to have a good time or just to listen to me vent over the years. Leaving you guys is one of the hardest parts of finishing my graduate career and leaving Chicago (along with leaving my family as well).

Last, and definitely not least, I want to thank my wife, Stacey. She is the single best thing that has happened to me in the past five years. She gave me a partner in life. She has supported me, more than anyone should have to, when I have been stressed and completely self-involved finishing my research. For her support I will forever be grateful. I could not have done this without her support.

Dedicated to Dr. Mephie Ngoi, my high school chemistry teacher, who inspired my love of science and encouraged me to reach for these heights

GLOSSARY

Backbiting: An intramolecular hydrogen shift reaction or a general reaction pathway in polymer degradation where a intramolecular hydrogen shift reaction is followed by a β-scission reaction.

Chain length distribution: Range and concentration of chain sizes that make up a polymeric species.

Dead polymer chain: A polymer chain without a free radical moiety.

End-chain radical: A polymer chain with a free radical moiety at a chain end position.

Kinetic Monte-Carlo: A stochastic framework for modeling chemical reaction systems originally developed by Gillespie (1976).

Method of moments: Use a series of values (moments) to describe a distribution. Infinite moments are needed to fully determine the distribution, but significant information about the distribution can be known from a small number of moments.

Mid-chain radical: A polymer chain with a free radical moiety at a position along the polymers backbone other than the chain ends.

Net rate analysis: Method of comparing competing reactions by looking at the rate in terms of the forward reaction rate minus the reverse reaction rate for each competing reaction.

Perl (PERL): A high level computer programming language, particularly useful for manipulation of text files. Perl programs are usually referred to as PERL scripts.

Primary recycling: Reuse of a waste material without significant modification or processing, such as refilling a plastic bottle to use it as a water bottle.

Quaternary recycling: Energy recovery from waste material usually through incineration.

Random scission: A general reaction pathway in polymer degradation where an intermolecular hydrogen transfer reaction is followed by a β-scission reaction.

Reaction channel: Possible reaction route available in a chemical reaction mechanism

Resource recovery: Conversion of a waste material back into the raw materials that were used to originally make the waste material usually by thermal or chemical methods.

Secondary recycling: Reprocessing of a waste material to convert it into a new product without breaking down the material to its raw materials.

Tertiary recycling: Resource recovery of waste material usually through thermal or chemical methods.

Triad: Three consecutive backbone atoms in a polymer chain.

Unzipping: A general reaction pathway in polymer degradation where a polymer chain undergoes end-chain β-scission yielding monomer.

NOMENCLATURE

A	frequency factor, s^{-1} or L mol^{-1} s^{-1}
b_{ij}	conditional probability for bond fission based on involved backbone triads
D	dead polymer chain concentration
D_i	i^{th} moment for dead polymer chains
D_n	dead polymer of length n
E_a	activation energy, kcal mol^{-1}
E_0	intrinsic barrier, kcal mol^{-1}
h_{ij}	conditional probability for hydrogen abstraction based on involved backbone triad
ΔH_{rxn}	heat of reaction, kcal mol^{-1}
i	general counter symbol
k_{BB}	rate coefficient for backbiting (1,5-hydrogen shift), s^{-1}
$k_{E-\beta}$	rate coefficient for end-chain β-scission, s^{-1}
k_f	forward rate coefficient, units depend on reaction order
k_i	first order rate coefficient, s^{-1}
k_{ii}	second order rate coefficient involving the same species, L mol^{-1} s^{-1} or $particles^{-1}$ s^{-1}
k_{ij}	second order rate coefficient involving different species, L mol^{-1} s^{-1} or $particle^{-1}$ s^{-1}
k_r	reverse rate coefficient, units depend on reaction order
M_n	number average molecular weight, g mol^{-1}
M_w	weight average molecular weight, g mol^{-1}
M_0	monomer molecular weight, g mol^{-1}
n	polymer chain length
N_A	Avagadro's number, molecules mol^{-1}

P_n polymer concentration of length n, mol L^{-1}

p_r probability of reaction r occurring

Re_i i^{th} moment for end-chain polymeric radicals

Re_x end-chain polymeric radical of length x

R_i rate of i^{th} reaction, mol L^{-1} s^{-1} or particles s^{-1}

R_r rate of reaction r, mol L^{-1} s^{-1} or particles s^{-1}

r_{LMWP} rate of low molecular weight product (other than styrene) formation, mol L^{-1} s^{-1}

r_{STY} rate of styrene formation, mol L^{-1} s^{-1}

s_i conditional probability for β-scission based on involved backbone triad

T total number of possible reactions

t time, s

V volume, L

x_1 random number between zero and one

x_2 random number between zero and one

α transfer coefficient

μ_i i^{th} moment

τ kinetic Monte Carlo time step

TABLE OF CONTENTS

LIST OF TABLES

LIST OF FIGURES

CHAPTER 1

INTRODUCTION

1.1 MOTIVATION

Polymeric materials are used in an increasingly broad range of applications, from the wide array of plastic packaging seen in everyday life to a variety of automotive parts to construction and electronic applications. The diversity of use for this important class of materials has made polymers one of the fastest-growing segments of the chemical industry since World War II (Rosen 1993). The large volume of polymeric materials produced and utilized has also meant that polymers make up an increasingly large fraction of municipal solid waste (MSW). Between 1995 to 2005 polymeric materials increased from 9.5% to 11.8% by weight of the total MSW (EPA 1996, 2006) before recycling. Chemical stability, which is often seen as one of their most valuable properties, is the source of the major complaint that polymers do not degrade readily and are difficult to recycle (Rosen 1993). The difficulty in recycling polymers is illustrated by the fact that in 2005 polymers were the least recycled sector of MSW with just over 5.7% of the discarded polymeric materials recycled (EPA 2006), meaning that the bulk of the polymeric waste was landfilled. Without improved recycling techniques, the valuable resources that comprise synthetic polymers will end up being wasted, taking up more of our increasingly scarce landfill space.

A large part of the reason that polymers are not recycled in greater amounts is the heterogeneity of the polymeric waste and the difficulty of recycling these materials (Scheirs and

Kaminsky 2006). The diverse makeup of the polymeric materials in MSW in 2005 is shown in Figure 1.1 (EPA 2006). Most of the polymeric waste is made up of commodity polymers such as high-density polyethylene and polystyrene. Currently high-density polyethylene (HDPE) and polyethylene terephthalate (PET) are the only types of polymeric waste that are recycled in significant amounts, with 8.8% of the HDPE and 18.8% of the PET in MSW currently recycled. No other type of plastic has more than 3% of its waste material recycled (EPA 2006).

Recycling methods can be divided into four basic categories: (1) primary recycling or reuse, (2) secondary recycling or reprocessing, (3) tertiary recycling or resource recovery, and (4) quaternary recycling or energy recovery. Most effort to expand polymeric recycling is focused on secondary and tertiary recycling. Primary recycling is difficult to institute on a large scale because it relies on reuse by individual consumers after the original purpose of the polymeric material is fulfilled. Further, the reused waste material quickly finds its way back into the waste stream, since most polymeric objects will only be reused a few times. Quaternary recycling, which is familiarly known as incineration, of polymers to recover energy is seen as having environmental and health concerns which make public opinion of expansion of polymer incineration highly unfavorable (Aguado 1999). PET and HDPE, the two most recycled polymers, are currently both recycled primarily through reprocessing methods. Reprocessed polymers have a limited market because of both a deterioration of the material properties in the reprocessed material as well as a need in many polymer applications for extremely clean and pure material, for example food packaging and electronics applications. Reprocessing also requires a very homogeneous feed because reprocessed mixed plastic waste is only usable in the most undemanding of applications (Scheirs and Kaminsky 2006). Since secondary recycling of

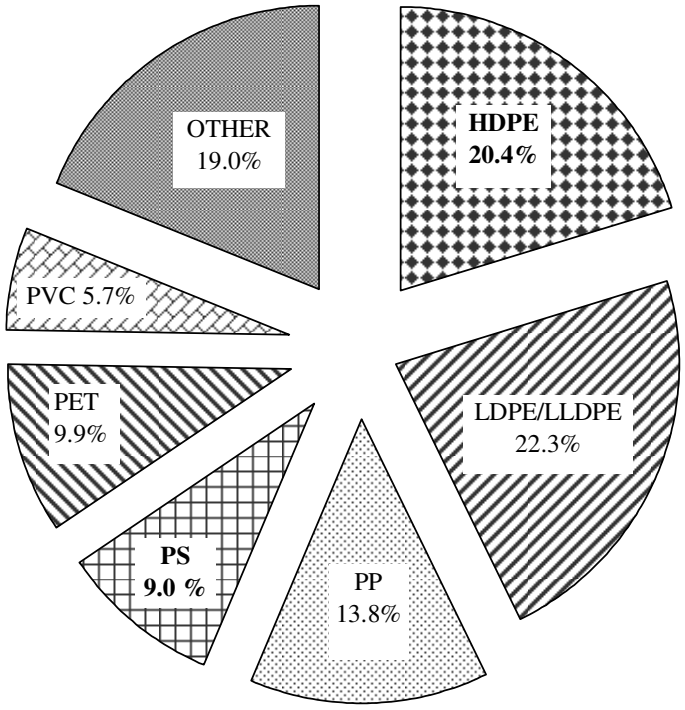

Figure 1.1: Composition by weight of 2005 polymeric waste in MSW (EPA 2006). HDPE = high-density polyethylene; LDPE = low-density polyethylene; LLDPE = linear low-density polyethylene; PP = polypropylene; PS = polystyrene; PET = polyethylene terephthalate; PVC = polyvinyl chloride.

polymeric waste is so limited in its application, a large amount of research effort has been devoted to the promising area of resource recovery as a way of expanding polymer recycling.

Resource recovery is the conversion of polymeric waste into useful chemical and fuel feedstocks that can be used in the chemical industry. This conversion is usually accomplished via thermal or chemical methods. Resource recovery techniques include catalytic degradation, solvolysis, and pyrolysis. Catalytic degradation is also promising because it can handle a heterogeneous polymer feed. It has limitations related to finding a suitable catalyst that actively degrades the various polymers in the waste feed as well as the normal difficulties of either separating the catalyst after reaction if a homogeneous catalyst is used or achieving high utilization of active sites if a heterogeneous catalyst is used. Solvolysis works very well for a few polymers, but it is only suitable for step-growth polymers since the solvolysis process involves reversing step-growth polymerization chemistry. Since PET is the only major component of the polymeric MSW shown in Figure 1.1 that is a suitable candidate for solvolysis, its widespread use as a recycling technique without improved separation techniques for the polymeric MSW is not likely. The sorting of polymeric MSW, which is still often done by hand, is one the highest costs involved in polymer recycling (Aguado 1999). Pyrolysis, or the heating of a material in the absence of oxygen, is an attractive method of resource recovery because of its simplicity. This simplicity means that it is a technology that can be developed to handle the highly heterogeneous feedstock that makes up polymeric MSW.

Polymer pyrolysis has been studied for over 60 years (Jellinek 1944, 1948a), but it has only been in the last 20 or 30 years that the method has been seen as a possible recycling technique (Aguado 1999). In order to develop this technology fully, a comprehensive understanding of the kinetic and mechanistic details involved in the pyrolysis of the various

components that make up polymeric waste is needed. Polymer pyrolysis is characterized by a complex free-radical reaction network, usually made up of thousands of species and reactions, which often yields a diverse product spectrum. Even with over 60 years of research trying to understand the kinetics and reaction pathways to the various products formed, there are still many questions that exist for most major polymers. A clear understanding of the mechanism and kinetics of polymer pyrolysis systems is needed to fully develop this technology. The mechanistic and kinetic knowledge can be utilized to optimize the reaction conditions for a given feedstock. The information can also be used to find reaction conditions that promote the formation of desired products over the less useful products of polymer pyrolysis. Mechanistic modeling is a powerful tool for gaining insight into this complex chemistry.

Previously, mechanistic models have been developed which demonstrated excellent predictive ability for pyrolysis of polystyrene, polypropylene, and binary pyrolysis of polystyrene and polypropylene (Kruse et al. 2005; Kruse et al. 2003b, 2003c; Kruse et al. 2001; Kruse et al. 2002). The modeling framework developed for these studies can be further extended beyond providing predictive ability for polymer pyrolysis to provide insight into the kinetics and mechanisms of these complex reaction processes. By including necessary detail within the models, proper analysis of the model results can yield improved understanding of the reaction pathways and general mechanistic detail involved in the pyrolysis of specific polymers. The kinetic details for polymer pyrolysis can also be investigated using detailed mechanistic models. Longstanding questions that exist in the study of polymer pyrolysis can be addressed with this work.

1.2 OUTLINE OF RESEARCH

The purpose of this research was to extend the modeling framework to allow for greater mechanistic and kinetic understanding of polymer pyrolysis. The research focused on refining the existing polystyrene pyrolysis model as well as developing models for polyethylene pyrolysis and poly(styrene peroxide) pyrolysis. The extension of the polystyrene model was done first in order to develop the analysis techniques to use the model results to understand the kinetic and mechanistic details of the system to answer longstanding questions that exist in the literature about this system. Additional structural detail was added to the polystyrene model to demonstrate the cost and benefit of incorporating this additional detail in a continuum model. To further test the analysis techniques and the mechanistic insight that can be garnered through the use of these models, a mechanistic model for polyethylene pyrolysis was constructed. Finally, a stochastic kinetic model based on the principles of Monte Carlo for poly(styrene pyrolysis) was developed. This both allowed for the existing mechanistic assumptions put forth in the literature for this system to be tested. It also was an excellent opportunity to demonstrate the value of a kinetic Monte Carlo model for a specific polymer degradation system.

Chapter 2 of this thesis provides the background information for the pyrolysis systems studied and for the modeling techniques utilized in this research. It begins by reviewing the experimental history for polystyrene pyrolysis, paying particular attention to the understanding of the overall mechanism and other areas of interest that have been debated. Next, a similar discussion for polyethylene and poly(styrene peroxide) is presented. Finally, the method of moments and kinetic Monte Carlo modeling methods are discussed.

Chapter 3 discusses the refinement of the polystyrene pyrolysis model to employ additional reaction pathways to styrene dimer formation as well as a reevaluation of the rate

parameters utilized within the model. This updated model is used to understand how dimer is formed. Chapter 4 further exploits this model to determine a definitive, overall activation energy which is free of heat and mass transport limitations.

Chapter 5 discusses the development of a model for polyethylene pyrolysis. This is a system with a much more diverse product distribution than polystyrene. The model developed in this chapter is utilized to provide additional insight into how the wide array of products is formed by probing the competition between the major pathways to the large variety of products.

Chapter 6 returns to polystyrene and discusses the addition of the ability to track more structural detail in the form of backbone triads to the model. The tracking of additional structural detail can allow for an improved connection of structure to reactivity in models. While the addition of triads to polystyrene is not essential for modeling polystyrene pyrolysis, it was used as a test system for the tracking of additional structural detail.

Chapter 7 discusses the development of a poly(styrene peroxide) model that utilizes a kinetic Monte Carlo (KMC) formulation. This was done to overcome the high degree of stiffness that made solving a poly(styrene peroxide) continuum model prohibitive. The poly(styrene peroxide) model was utilized to gain insight into the proposed mechanism based on existing literature results. It is also a demonstration of the value of KMC modeling for polymer degradation.

Finally, the results of the research discussed in the previous chapters are summarized in Chapter 8, highlighting the major conclusions of each piece of this research. Future directions of research based on the results of this work are discussed. These include the development of a model that handles complex mixtures and the extension of the modeling techniques developed and utilized in this work beyond synthetic polymer systems to biomass pyrolysis.

CHAPTER 2

BACKGROUND

2.1 POLYSTRENE PYROLYSIS

Beginning with the pioneering work of Jellinek (1944, 1948a, 1948b, 1949a, 1949b) and Madorsky and Straus (1948) 60 years ago, researchers have worked to gain a detailed understanding of the mechanistic and kinetic inner workings of polystyrene pyrolysis. The early mechanistic picture developed by Jellinek for polystyrene pyrolysis was a simple random fission mechanism. It quickly became clear that a basic random fission mechanism was not correct because the experimental styrene yields were orders of magnitude higher than the amount a simple random fission mechanism would predict (Cameron and MacCallum 1967; Jellinek 1948b, 1949a, 1949b; Madorsky 1964; Madorsky and Straus 1948). While it was obvious that the mechanism for polystyrene pyrolysis was more complex than originally believed, a clear picture of the mechanism was slow to be developed, with the view shifting from a random fission mechanism to some form of a reverse polymerization mechanism (Cameron and MacCallum 1967).

Gaining an understanding of the mechanistic picture of polystyrene pyrolysis was complicated by the idea that weak links in polystyrene chains play an important role in the degradation. The effect of weak links was first discussed by Jellinek (1948b, 1949b) as a way of explaining the rapid rate of degradation seen in the initial stages of polystyrene pyrolysis that slowed considerably as the pyrolysis continued. Considerable research effort was applied to identify the nature of the weak links. Proposed weak link heterogeneities included mid-chain

unsaturations, branch points, peroxide linkages, and initiator residues (Cameron and Kerr 1968, 1970; MacCallum 1965). While many of the proposed weak links have been studied experimentally (Cameron et al. 1984; Cameron and Kerr 1970; Cameron and McWalter 1982; Cameron et al. 1978; Krstina et al. 1989), the exact nature of the weak links has not been identified. Anionic polymerized polystyrene has been shown to lack the weak links that are seen in thermally polymerized polystyrene. This is believed to be mainly due to the low temperature conditions used during anionic polymerization (Cameron et al. 1978).

Utilizing anionic polystyrene allowed a more detailed mechanism for polystyrene pyrolysis to be developed (Cameron et al. 1978) without consideration of weak links. The mechanism proposed by Cameron et al. focused mainly on explaining the molecular weight decay observed during anionic polystyrene pyrolysis. This mechanism can be seen in Figure 2.1. This mechanism utilized several basic free radical reactions including bond fission, radical recombination, disproportionation, allyl bond fission, hydrogen abstraction, and mid-chain β-scission. The mechanism was missing any clear discussion of specific reactions to form volatile products. It is assumed in the Cameron et al. mechanism that the volatile products are formed from the end-chain radicals with no further insight offered beyond this (Cameron et al. 1978). The most likely pathway is end-chain β-scission to form styrene monomer, the most abundant product obtained from polystyrene pyrolysis.

Building on the mechanism developed by Cameron et al. (1978) as well as discussions about the importance of both inter- and intramolecular transfer reactions in polystyrene pyrolysis (Cameron and McWalter 1970; Richards and Salter 1967), Daoust and coworkers (1981) developed reaction pathways to volatile products formed during polystyrene pyrolysis. They found two oligomers of styrene formed during their pyrolysis experiments, dimer and trimer.

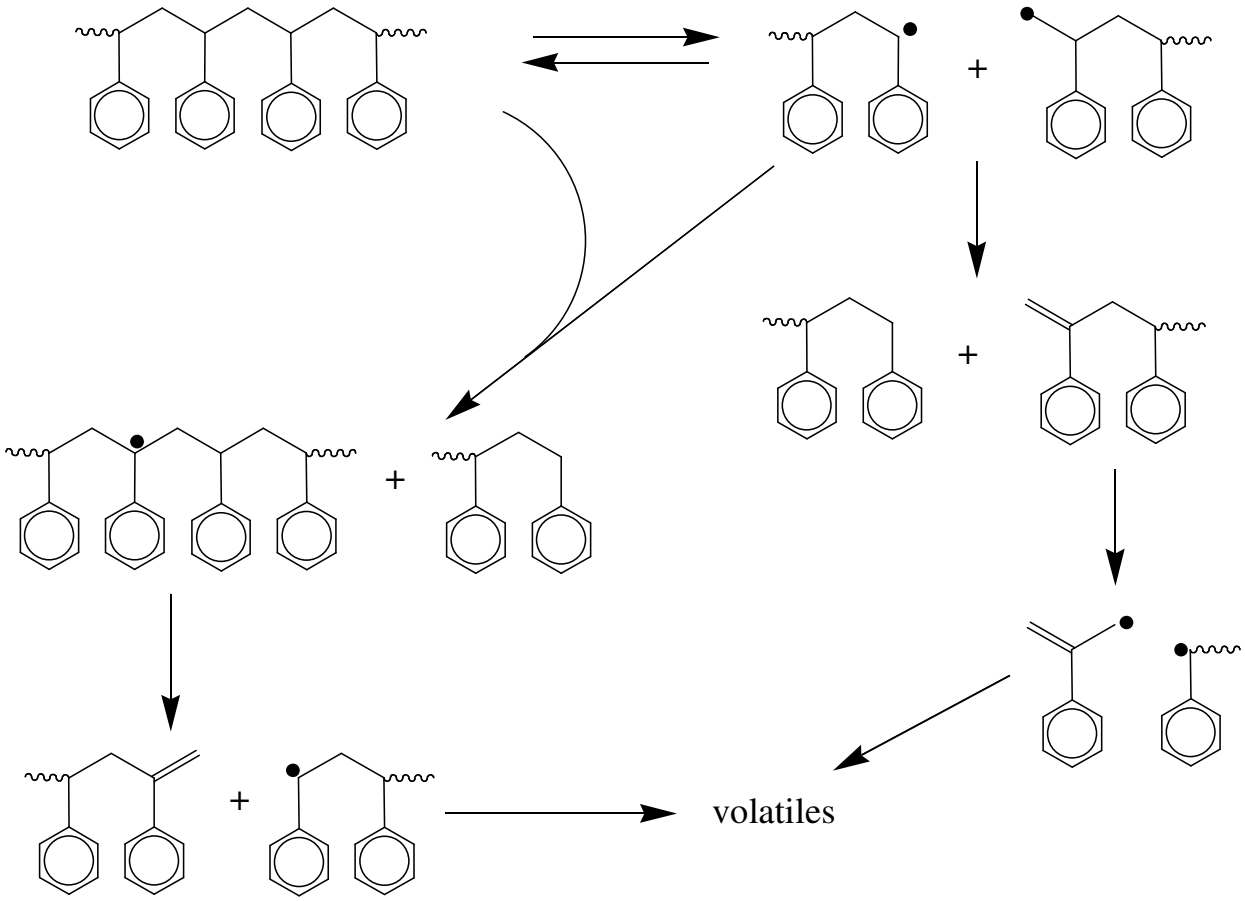

Figure 2.1: Polystyrene pyrolysis mechanism proposed by Cameron et al. (1978).

Intramolecular hydrogen shift reaction pathways were proposed for the formation of these products: 1,5-hydrogen shift to form trimer and 1,3-hydrogen shift to form dimer. These pathways could also be used to explain the formation of some non-oligomeric volatile products, 1,3-diphenylpropane and toluene (Daoust et al. 1981). These reaction pathways, coupled with unzipping to form styrene monomer, gave mechanistic routes that lead to the formation of most of the products formed during polystyrene pyrolysis.

Additional work has been done more recently to further understand the low molecular weight products formed during polystyrene pyrolysis (Kruse et al. 2001; Kruse et al. 2002; Woo et al. 1998). These studies found that there are six significant products formed during polystyrene pyrolysis: styrene monomer, styrene dimer, styrene trimer, 1,3-diphenylpropane, α-methyl styrene, and toluene. All of these products can be formed using the mechanisms and reaction pathways discussed above. Various mechanistic models have been developed which make use of these proposed mechanisms (Faravelli et al. 2003; Faravelli et al. 2001; Kruse et al. 2005; Kruse et al. 2001; Kruse et al. 2002). These models have succeeded in predicting both product evolution and molecular weight decay under a number of conditions including a range of temperatures and initial polystyrene molecular weights. For the formation of the dimer product these models either rely on 1,3-hydrogen shift (Kruse et al. 2001; Kruse et al. 2002) or neglect predicting the formation of dimer (Faravelli et al. 2003; Faravelli et al. 2001).

Recently, the traditional pathway to dimer, 1,3-hydrogen shift, has drawn the attention of researchers because, unlike 1,5-hydrogen shift, 1,3-hydrogen shift is believed to have a high energy barrier, making this reaction very difficult (Poutsma 2006). By discarding the traditionally accepted pathway to dimer, the mechanism for polystyrene pyrolysis has become an area of debate and confusion.

Determining the overall activation energy for polystyrene pyrolysis has also received considerable attention in studies of polystyrene pyrolysis. Starting from the work of Jellinek (1949b) researchers began reporting overall activation energies. Jellinek reported a value of 44.9 kcal mol^{-1}, and his work was quickly followed by values from additional researchers using different techniques and reactor types to conduct the experiments to determine the overall activation energy. A survey of the literature finds values ranging from 19.8 kcal mol^{-1} from a study using pyrolysis-gas chromatography (Cascaval et al. 1970) up to 105.1 kcal mol^{-1} from a study using both differential scanning calorimetry and differential thermogravimetry techniques (Maholtra et al. 1975). The range of 85 kcal mol^{-1} that exists in the literature demonstrates the difficulty in determining an intrinsic value for the overall activation energy of polystyrene pyrolysis. Transport effects on the kinetic studies are believed to be the cause of many of the discrepancies between the different values reported in the literature (Westerhout et al. 1997; Zhao and Bar-Ziv 2000; Zhao et al. 1998). Transport limitations have been shown to affect kinetic data obtained from polymer pyrolysis experiments even when the sample is only a few mg (Szekely et al. 1987). Polystyrene pyrolysis has a long history of study, but there are still many important areas that are not clearly understood.

2.2 POLYETHYLENE PYROLYSIS

Polyethylene pyrolysis also has a long and extensive history of study. The earliest studies were performed in the late 1940's by Jellinek (1949a) and Madorsky and coworkers (1949). These studies were concerned with developing both a kinetic and mechanistic picture of the thermal degradation of polyethylene. As was the case for polystyrene, their early data quickly demonstrated that a random bond fission mechanism was incapable of explaining the

experimentally observed products and rates of degradation. Jellinek (1949a) proposed that some version of a depropagation mechanism would be compatible with his weight loss data for polyethylene. The work done by Madorsky et al. (1949) contradicts a purely unzipping mechanism by showing, in one of the first studies of polymer degradation using a mass spectrometer, that there is a broad spectrum of products other than monomer (ethylene) produced during polyethylene pyrolysis. Extending this work, Wall and coworkers (1954) proposed that random hydrogen transfer reactions are important in polyethylene pyrolysis. The discovery of the importance of hydrogen transfer reactions significantly improved the mechanistic understanding of polyethylene thermal degradation, but the full mechanistic picture was still unclear.

As experimental techniques allowing for measurement of the degradation products produced during polymer pyrolysis improved, a more detailed picture of the polyethylene pyrolysis mechanism developed. The large number of products produced during polyethylene pyrolysis made their measurement and analysis difficult. Tsuchiya and Sumi (1968a) performed one of the earliest detailed analysis of the volatile products produced during polyethylene pyrolysis. Based on the product spectra they obtained, a basic free radical mechanism was proposed including both inter- and intramolecular hydrogen transfer reactions. Their further work looking at a broader product spectrum of up to 16 carbon atoms in the products caused them to reinforce the importance of intramolecular hydrogen transfer over intermolecular hydrogen transfer in the mechanism of polyethylene pyrolysis (Tsuchiya and Sumi 1968b). This was based on small regular peaks in their product spectrum corresponding to 1-hexene and 1-decene as well as propane, n-heptane, and n-undecane. Tsuchiya and Sumi proposed successive 1,5-hydrogen shift reactions to lead to this product spectrum. This backbiting mechanism is

shown in Figure 2.2. Tsuchiya and Sumi (1968b) discuss the competition between inter- and intramolecular hydrogen chain transfer and conclude that intramolecular transfer is dominant over intermolecular transfer during polyethylene pyrolysis based on the product yield patterns in their experiments.

Seeger and Cantow (1975) looked at a wider product spectrum of up to 30 carbon atoms in the products to gain mechanistic insight obtained from high temperature polyethylene pyrolysis. In order to obtain such a wide product spectrum, they needed to hydrogenate their products, losing differentiation between alkane, alkene, or diene products. They used a scission mechanism which is similar to that proposed by Tsuchiya and Sumi to mechanistically look at their results. This allowed a comparison of inter- and intramolecular hydrogen transfer reactions. Intermolecular transfer followed by scission leads to a statistical product distribution because all positions on the chain are equally likely to have hydrogen abstracted. Intramolecular transfer followed by scission leads to a non-statistical product distribution because specific positions on the chain are preferentially chosen for hydrogen abstraction. Their results showed that both types of hydrogen transfer were important for product formation (Seeger and Cantow 1975), which is inconsistent with the supposition of Tsuchiya and Sumi that backbiting was dominant. The study of Kiran and Gillham (1976) further showed the importance of intermolecular hydrogen transfer to product formation during polyethylene pyrolysis in an extensive product study, where products with up to 28 carbon atoms were detected, often distinguishing between alkanes and alkenes.

This picture of a free-radical mechanism with product formation from end-chain and mid-chain scission reactions where mid-chain scission reactions are preceded by either inter- or intramolecular hydrogen transfer has been widely accepted. Most studies more recently have

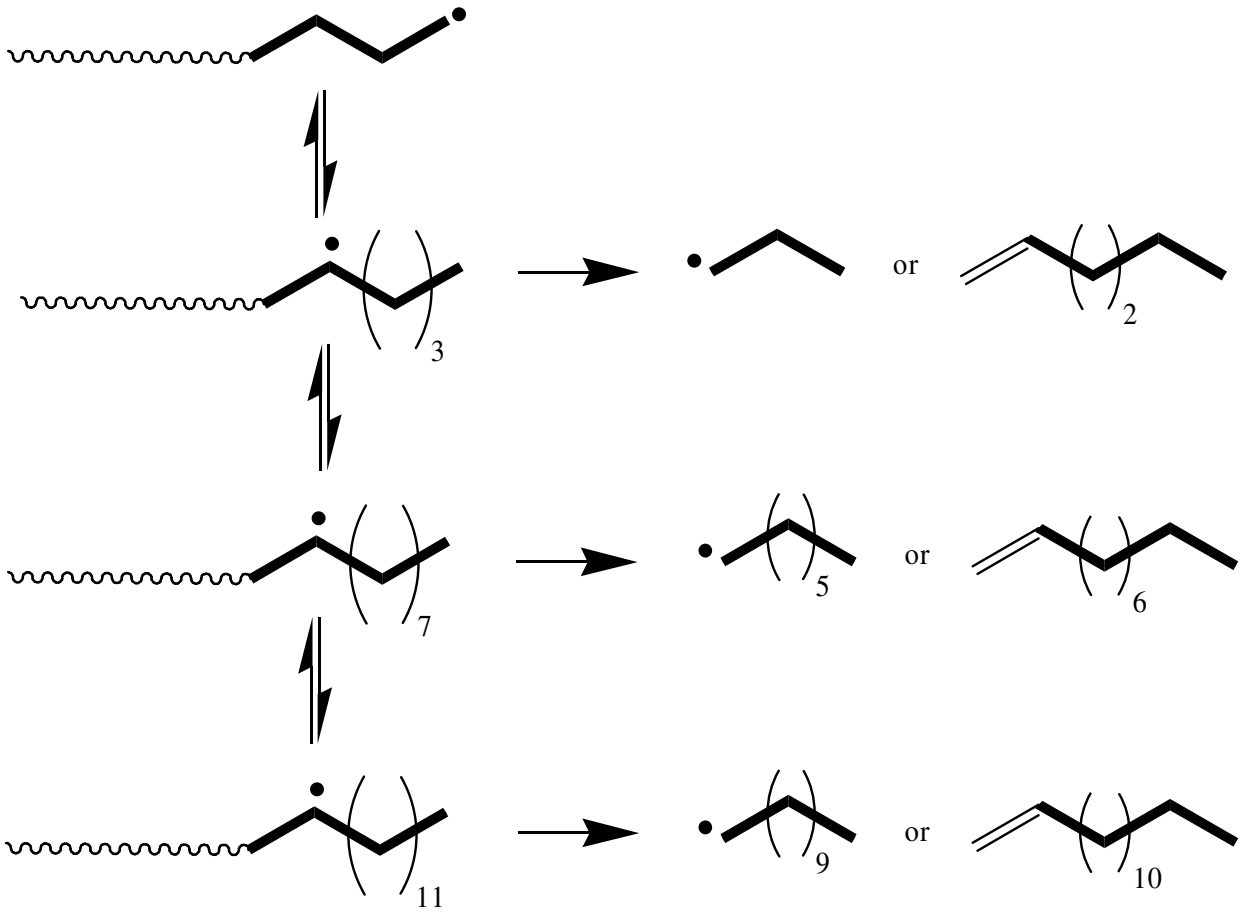

Figure 2.2: Intramolecular hydrogen transfer mechanism for specific product formation during polyethylene pyrolysis as proposed by Tsuchiya and Sumi (1968a, 1968b).

focused on quantifying the product spectrum and rates of mass loss seen during polyethylene pyrolysis (Ballice et al. 1998; Bockhorn et al. 1999; Conesa et al. 1997; De Witt and Broadbelt 2000; Jalil 2002; Westerhout et al. 1998). These studies have shown that the product distribution obtained from polyethylene is extremely diverse and often difficult to fully characterize, but is made up of n-alkanes, 1-alkenes, and at higher temperatures α,ω-dienes (Poutsma 2003). These experimental studies have not provided any additional insight into the competition between inter- and intramolecular hydrogen transfer in the polyethylene pyrolysis mechanism.

Recently, mechanistic models have been built for polyethylene pyrolysis. The first models were developed by Ranzi and coworkers (1997) and Sezgi and coworkers (1998) and focused on capturing the mass loss observed during polyethylene pyrolysis and the evolution of the molecular weight distribution, respectively. Both of these models utilized the basic radical mechanism discussed above. However, neither modeling study looked into the formation of specific products. More recently, Faravelli and coworkers built on the Ranzi model to study in a more detailed manner the product distribution obtained from polyethylene pyrolysis (Faravelli et al. 1999; Marongiu et al. 2007). They focused on final product yields and not on the time evolution of specific product formation. Faravelli and coworkers concluded that the random scission pathways were more dominant than the backbiting pathways, meaning that intermolecular transfer was more dominant than intramolecular transfer. Mastral et al. (2007) recently also developed a mechanistic model for polyethylene pyrolysis in which they made an attempt to capture some secondary reactions, specifically the formation of aromatic species. Their model focused only on final product yields and utilized lumped product groups, making mechanistic interpretation of how specific products were formed difficult. It should be further noted that inter- and intramolecular hydrogen transfer were not distinguished in the Mastral

model. The competition between inter- and intramolecular hydrogen transfer in polyethylene pyrolysis is still not fully understood.

2.3 POLY(STYRENE PEROXIDE) PYROLYSIS

Polyperoxides are an interesting class of materials because of their extremely thermally labile structure. They have found applications as macroinitiators and solid fuels because of their exothermic thermal degradation (Kishore and Mukundan 1986; Nanda and Kishore 2000b; Subramanian 2003). Poly(styrene peroxide) is particularly of interest because it has the most extensive history of experimental study of all vinyl polyperoxides. Additionally, it can be seen as the extreme case of peroxide bond heterogeneities in polystyrene, which are often proposed as a possible weak link in polystyrene. Poly(styrene peroxide) is an ideal alternating copolymer of styrene and oxygen. Poly(styrene peroxide) can be difficult to work with experimentally because it can be explosive at temperatures above 100 °C (Kishore and Mukundan 1986; Mayo and Miller 1956; Subramanian 2003).

The first study of poly(styrene peroxide) pyrolysis was performed by Mayo and Miller (1956) over 50 years ago. This study covered the thermal degradation of poly(styrene peroxide) under a wide array of degradation conditions (temperature, solvent, pressure, etc.). Their experiments focused on the product yields, and, for a selection of studies, a measure of overall degradation based on the percentage of peroxide bonds remaining in the sample (Mayo and Miller 1956). Mayo and Miller identified the major products formed during poly(styrene peroxide) pyrolysis as formaldehyde and benzaldehyde and the minor products observed as α-hydroxy acetophenone and phenyl glycol. The structure of these products is shown in Figure 2.3. A basic unzipping mechanism for the formation of formaldehyde and benzaldehyde was

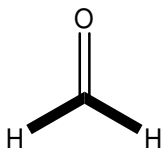

Formaldehyde

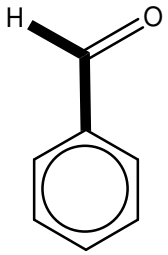

Benzaldehyde

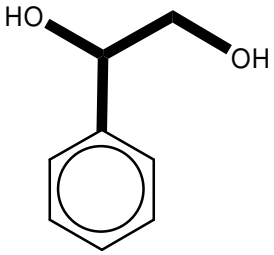

Phenyl Glycol

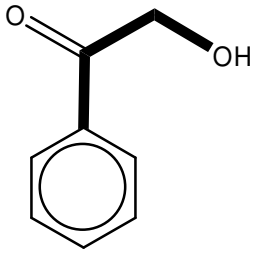

α-Hydroxy Acetophenone

Figure 2.3: Major (formaldehyde and benzaldehyde) and minor (phenyl glycol and α-hydroxy acetophenone) products observed experimentally during poly(styrene peroxide) pyrolysis.

first proposed by Mayo and Miller. Since they observed a greater formation of the minor products at lower temperatures than at the more explosive higher temperatures, Mayo and Miller (1956) proposed a mechanism based on repeated disproportionation reactions to form the minor products α-hydroxy acetophenone and phenyl glycol. The basic mechanistic picture proposed by Mayo and Miller in this original study has been utilized to interpret subsequent experimental studies on this system.

The majority of experimental studies on poly(styrene peroxide) were performed by Kishore and coworkers (Kishore 1980, 1981; Kishore and Bhanu 1985; Kishore and Mukundan 1986; Kishore et al. 1980; Kishore et al. 1996; Kishore and Ravindran 1982, 1983; Nanda and Kishore 2000a; Nanda and Kishore 2000b). Using DSC and TGA studies, Kishore and coworkers (1981, 1980) determined an overall activation energy of between 30 and 32.5 kcal/mol for poly(styrene peroxide) pyrolysis. This value is in the basic range of peroxide bond strengths, which suggested to Kishore and coworkers that peroxide bond fission was the rate-limiting step under the conditions studied. Using isothermal TGA experiments Kishore and coworkers (1980) monitored the percentage decomposition (based on mass loss) over time at temperatures ranging from 76 °C to 104 °C. This study showed a decelerating nature to the decomposition as the polymer degraded. Kishore and Ravindran (1982) performed pyrolysis-gas chromatography experiments over a wide range of temperatures to study if the mechanism changed with temperature. Their results showed that the major product distribution and consequently the mechanism stayed the same until approximately 450 °C. To date there have been no mechanistic models developed for the poly(styrene peroxide) degradation system to test the proposed mechanisms for the formation of the major products, benzaldehyde and formaldehyde, and minor products, α–hydroxy acetophenone and phenyl glycol.

2.4 MACROMOLECULE PYROLYSIS MODELING

2.4.1 Method of Moments Modeling

The method of moments has been used in polymer degradation modeling to allow models of a manageable size to be constructed while still maintaining the necessary detail to track changes in the polymer molecular weight distribution. Moments come out of probability theory and are a way of representing a distribution with a series of values. While an infinite number of moments are needed to fully determine a distribution, key information about the distribution can be determined from only a few moments (Grinstead and Laurie 1997). The method of moments has been commonly used for the modeling of polymerization through the use of moment-generating functions (Dotson et al. 1996). Most method of moment models for polymer systems utilize the zeroth, first and second moments, which are usually defined as shown in equations 2.1, 2.2, and 2.3:

$$\mu_0 = \sum_{n=1}^{\infty} P_n \qquad (2.1)$$

$$\mu_1 = \sum_{n=1}^{\infty} nP_n \qquad (2.2)$$

$$\mu_2 = \sum_{n=1}^{\infty} n^2 P_n \qquad (2.3)$$

where μ_0, μ_1, and μ_2 are the zeroth, first and second moments, n is the length of a polymer chain, and P_n is count or concentration of polymer of length n. By tracking the first three moments the number-average and weight-average molecular weights can be tracked in the model.

The extension of the method of moments to polymer degradation began with the work of McCoy and coworkers. Polymer degradation reactions can be treated similarly to polymerization reactions making the use of the method of moments seem straightforward.

However, the fission and scission reactions which are important to most polymer degradation mechanisms lead to an uncertainty about the chain lengths of the products of these reactions. To address this uncertainty McCoy (1993) used continuous kinetics which assumes the molecular weight distribution is a continuous function of chain length. This approach requires that a stoichiometric coefficient be utilized to partition chain lengths of the reactant and product species. This coefficient is based on the probability that a chain of length *n* will break to form chains of length *i* and *n-i*. Both random and proportional fission coefficients have been developed by McCoy and coworkers (McCoy 1993; Wang et al. 1995), with the random case being most relevant for polymer pyrolysis. McCoy and coworkers developed moment equations for additional important polymer degradation reactions including hydrogen abstraction (Kodera and McCoy 1997). They applied their framework to various polymer degradation systems including polystyrene and poly(styrene-allyl alcohol) (Madras et al. 1997a; Madras et al. 1997b; Wang et al. 1995).

Kruse and coworkers built on the work of McCoy by utilizing the method of moments to develop highly detailed mechanistic models for polystyrene, polypropylene, and binary polystyrene-polypropylene pyrolysis (Kruse et al. 2005; Kruse et al. 2003b, 2003c; Kruse et al. 2001; Kruse et al. 2002). In the Kruse models polymeric species were divided based on key structural features and these structural features were linked to reactivity. All reactions included in the Kruse models were elementary free-radical reactions, so clear reaction pathways to the low molecular weight products could be discerned from the model. The elementary reaction terms were used to create population balance equations using moment terms which made up the model equations.

The research of Kruse and coworkers is considered the most detailed polymer pyrolysis modeling work that has been published (Poutsma 2006). Faravelli and coworkers have also utilized the method of moments in their detailed mechanistic modeling of polymer pyrolysis (Faravelli et al. 2003; Faravelli et al. 2001; Marongiu et al. 2007), though their models lack all of the structural detail included in the models of Kruse and coworkers.

The procedure for developing the moment-based population balance equations will be illustrated using a bond fission/recombination reversible reaction (equation 2.4):

$$D_n \leftrightarrow Re_i + Re_{(n-i)} \qquad (2.4)$$

where D_n is a dead polymer chain of length n, and Re_x is an end-chain polymer radical of length i or n-i. k_f and k_r will be used for the forward and reverse rate constants, respectively. Typical mass action kinetic balance equations are first formulated for each species involved in the reactions (equations 2.5, 2.6, and 2.7):

$$\frac{d[D_n]}{dt} = -k_f((2n-1)[D_n]) + k_r[\mathrm{Re}_i][\mathrm{Re}_{(n-i)}] \qquad (2.5)$$

$$\frac{d[R_i]}{dt} = k_f((2n-1)[D_n]) - k_r[\mathrm{Re}_i][\mathrm{Re}_{(n-i)}] \qquad (2.6)$$

$$\frac{d[R_{(n-i)}]}{dt} = k_f((2n-1)[D_n]) - k_r[\mathrm{Re}_i][\mathrm{Re}_{(n-i)}] \qquad (2.7)$$

where t is time, and the 2n-1 terms come from the fact that a typical polymer chain has 2n-1 breakable bonds. The 2n-1 term can be augmented if the chain has fewer breakable bonds than a typical chain. In this form versions of these equations for all values of n and all values of i (up to i = n-1) would be necessary to fully solve the system of equations. To remove the chain length dependence these equations are converted to population balances by multiplying by the respective chain length of the differential equation to the zeroth, first or second power and

summing over all possible chain lengths for the respective chains. This procedure applied to equation 2.5 is shown in equations 2.8, 2.9, and 2.10:

$$\sum_{n=1}^{\infty}\frac{d[D_n]}{dt} = -k_f\sum_{n=1}^{\infty}((2n-1)[D_n]) + k_r\sum_{n=1\&n>i}^{\infty}([Re_i][Re_{(n-i)}]) \tag{2.8}$$

$$\sum_{n=1}^{\infty} n\frac{d[D_n]}{dt} = -k_f\sum_{n=1}^{\infty}(n(2n-1)[D_n]) + k_r\sum_{n=1\&n>i}^{\infty}(n[Re_i][Re_{(n-i)}]) \tag{2.9}$$

$$\sum_{n=1}^{\infty} n^2\frac{d[D_n]}{dt} = -k_f\sum_{n=1}^{\infty}(n^2(2n-1)[D_n]) + k_r\sum_{n=1\&n>i}^{\infty}(n^2[Re_i][Re_{(n-i)}]) \tag{2.10}$$

These equations can be rearranged to put them in terms of specific moments for the polymeric species. Differential equations for the zeroth, first, and second moments for dead polymer chains are obtained after rearranging these equations as shown in equations 2.11, 2.12, and 2.13:

$$\frac{dD_0}{dt} = -k_f(2D_1 - D_0) + k_r\frac{\mathrm{Re}_0\,\mathrm{Re}_0}{2} \tag{2.11}$$

$$\frac{dD_1}{dt} = -k_f(2D_2 - D_1) + k_r\,\mathrm{Re}_1\,\mathrm{Re}_0 \tag{2.12}$$

$$\frac{dD_2}{dt} = -k_f(2D_3 - D_2) + k_r(\mathrm{Re}_2\,\mathrm{Re}_0 + \mathrm{Re}_1\,\mathrm{Re}_1) \tag{2.13}$$

where D_0, D_1, D_2, D_3 and R_0, R_1, R_2 denote the zeroth, first, second, and third moments for dead polymer or end-chain polymer radicals, respectively. It should be noted that for this reaction pair the x+1 moment always appears in the x^{th} moment equation. The Saidel-Katz approximation (equation 2.14) is used to provide closure to these equations (Saidel and Katz 1968).

$$D_3 = \frac{2D_2D_2}{D_1} - \frac{D_2D_1}{D_0} \tag{2.14}$$

Finally, it should be noted that the stoichiometric coefficient for random fission developed by McCoy and coworkers (Wang et al. 1995) is needed to properly develop the moment equations from the end-chain radical balance equations (equations 2.6 and 2.7).

2.4.2 Kinetic Monte Carlo Modeling

Traditionally, chemical reaction models for batch reactions are made up of a set of ordinary differential equations which describe the time evolution of a particular species in the chemical reaction system. An alternative approach was originally developed by Gillespie (1976) and is generally known as kinetic Monte Carlo (KMC) modeling. KMC uses a stochastic approach to model behavior of the system of interest as opposed to a deterministic approach. Reaction rates are not used as an explicit measure of the speed of a reaction but instead are used as a measure of the probability that a reaction will occur. Instead of species concentrations, KMC models make use of discrete particles in a scaled homogeneous reaction volume. One advantage of KMC models over traditional deterministic models is the use of an iterative procedure to solve KMC models that does not require the use of a numerical solver. This means that numerical difficulties such as the stiffness of the system are not a hindrance to KMC models.

In a KMC model each possible reaction is defined by how it affects the explicit reaction system and is assigned a reaction probability. The reaction probability for a given reaction event is based on its current reaction rate as well as the sum of all the possible reaction rates as shown in equation 2.15:

$$p_r = \frac{R_r}{\sum_{i=1}^{T} R_i} \qquad (2.15)$$

where p_r is the probability of reaction r occurring, R_i is the reaction rate for reaction i, and T is the total number of all possible reactions. Using equation 2.15 all the possible reactions will have probabilities making up a reaction probability distribution for the system. A reaction is chosen to occur by selecting a random number between zero and one and seeing where in the reaction probability distribution the random number falls. This stochastic reaction selection procedure is formally defined using equation 2.16:

$$\sum_{i=1}^{r-1} p_i < x_1 < \sum_{i=1}^{r} p_i \qquad (2.16)$$

where x_1 is the random number and r is the index of the selected reaction. The final step of the KMC modeling procedure is to determine the time step to take before selecting the next reaction. The time step is based on the total rate of all possible reactions that could have occurred and another random number chosen between zero and one as shown in equation 2.17:

$$\tau = \frac{1}{\sum_{r=1}^{T} R_i} \ln\left(\frac{1}{x_2}\right) \qquad (2.17)$$

where τ is the time step and x_2 is the second random number. These three steps are repeated to move temporally through the chemical reaction system being modeled.

Normally, reaction rates and reaction rate constants are used and reported on a macroscopic per volume basis, but in a KMC model reaction rates and reaction rate constants need to be based on the total number of molecules that are in the scaled volume used in the model. To achieve this, concentrations which would be used in the macroscopic case are converted to a total number of molecules within the scaled volume. Gillespie (1976) derived the conversion relationships between macroscopic rate constants and the stochastic rate constants needed for KMC models. These relationships are shown in equations 2.18, 2.19 and 2.20:

$$k_i^{KMC} = k_i^{macro} \tag{2.18}$$

$$k_{ii}^{KMC} = \frac{2k_{ii}^{macro}}{VN_A} \tag{2.19}$$

$$k_{ij}^{KMC} = \frac{k_{ij}^{macro}}{VN_A} \tag{2.20}$$

where k_i is a rate constant for a first order reaction, k_{ii} is a rate constant for a second order reaction between the same species, k_{ij} is a rate constant for a second order reaction between different species, V is the scaled reaction volume, N_A is Avogadro's number, and the superscripts KMC and macro indicate if the rate constant is the stochastic or macroscopic version, respectively.

Recently, the KMC framework has been utilized for polymer reaction modeling. KMC models are desirable for these systems because tracking every species allows for important polymer properties to be determined explicitly. An example of this is the direct modeling of the molecular weight distribution as it evolves during polymerization, since every chain length is known in a KMC model. Al-Harthi and coworkers (2007, 2006) have developed a KMC model, based on Gillespie's formulation, for atom-transfer radical polymerization. They demonstrate that the KMC model agrees with a more conventional method of moments model and utilize the KMC model to predict the MWD as it evolves during the polymerization. Habibi and Vasheghani-Farahani (2007) recently utilized a KMC model for homo- and co-polymerization systems. They utilized the explicit nature of the KMC model to examine some aspects of monomer distribution in chains during copolymerization as well as to attempt to compare the penultimate and terminal models for copolymerization.

While polymerization has had multiple successful applications of the KMC methodology, there have been limited KMC models developed for polymer degradation. This is primarily caused by some of the computational difficulties an explicit model for polymer degradation requires. These difficulties mainly focus around the number of species and reactions that can exist during polymer degradation. As one increases the number of reactants and reaction channels in KMC models, their solution becomes slower and thus more computationally prohibitive (Gillespie 2007; McDermott et al. 1990). The work of McDermott et al. (1990) developing a Monte Carlo simulation for a model lignin polymer, poly(veratryl β-guaiacyl ether), is one of the first instances of a KMC model being utilized in the literature for a polymer degradation system. However, the KMC model developed by McDermott et al. uses a KMC framework that is different from the Gillespie formulation. In the McDermott et al. model, regular time steps are used, checking each reactive moiety in the system independently to see if a reaction occurs based its probability. After the total time of interest was reached, the system was reset to its initial state and a new reaction chain was begun. The final results of the model were the average of all of these independent reaction series. This was done to avoid listing all possible reaction events in the system as is required for the Gillespie KMC framework, which can be prohibitively large for polymer degradation systems. Acid hydrolysis of polysaccharides has also been modeled using a KMC model based on the framework used by McDermott et al. (Pinto and Kaliaguine 1991). There have been multiple studies of general polymer degradation systems using KMC models to study the evolution of the polymer molecular weight distribution (Bose and Git 2004; Giudici and Hamielec 1996; Tobita 1996a, 1996b). These studies do not utilize any specific polymer structure. Additionally, theoretical chain scission probabilities are used in place of rate coefficients. KMC modeling of peroxide-initiated degradation of polypropylene

has been used to guide kinetic parameter estimation for the scission rate constant in initiator efficiency (Huang et al. 1997; Huang et al. 1995). The work of Libanati and coworkers (1993) developing a KMC model for the pyrolysis of poly(arylether sulfones) is one of the only studies of the application of a stochastic model to the pyrolysis of specific polymer. Their KMC model used a dynamic reaction lattice to allow gelation to be modeled. The gelation was characterized using percolation theory. While these KMC models are powerful tools for studying polymer degradation, the development of detailed KMC models for specific polymer degradation systems to provide mechanistic insight has been limited.

CHAPTER 3

REACTION PATHWAYS TO DIMER IN POLYSTYRENE PYROLYSIS: A MECHANISTIC MODELING STUDY

3.1 INTRODUCTION

Polymers make up an increasingly large fraction of municipal solid waste (MSW). While polymers made up 11.8% of MSW as of 2005, only 5.7% of this amount was recycled, making them one of the sectors of MSW that is recycled to the smallest extent (EPA 2006). With fewer landfills available for disposal of MSW each year, developing effective recycling strategies for polymeric waste is becoming increasingly important. Tertiary recycling, or resource recovery, where polymeric waste is converted via thermal or chemical techniques to valuable chemical feedstocks and monomer, is a very attractive method of polymer recycling. Resource recovery offers the ability to convert waste into a reusable chemical stream to make brand new products. Pyrolysis, heating the material in the absence of oxygen, is a very attractive method of resource recovery because of its simplicity and its ability to deal with a mixed feedstock, especially a mixture of chain-growth polymers, such as polystyrene (PS) which cannot undergo solvolysis. Polystyrene alone makes up 9% of the polymer waste fraction in MSW and virtually none of this post consumer waste is currently recycled (EPA 2006). In order to develop polymer pyrolysis as an effective recycling method, greater understanding of the kinetics and mechanism is needed.

Polymer pyrolysis is characterized by large and complex free-radical reaction networks. The high molecular weight, polydisperse nature of polymers leads to reaction systems with

thousands of species and reactions. This complexity often yields a diverse product spectrum (Aguado 1999). Understanding the reaction mechanism in general and the reaction pathways to the various products in particular is essential to developing polymer pyrolysis as a viable technology. The complexity of free-radical reaction networks makes understanding the mechanism and reaction pathways via experimental studies a difficult task. Mechanistic models are powerful tools for gaining insight into the complex chemistry of polymer pyrolysis. By analyzing the results of a detailed mechanistic model in terms of net rates, the major reaction pathways to specific products can be determined.

To successfully use a mechanistic model to determine which reaction pathways are dominant, a significant level of detail must be included in the model, and the rate parameters used in the model must be well validated from experiment or reliable estimation methods. It is very difficult to determine individual rate parameters for the elementary reactions involved in polymer pyrolysis because they are rapid and compete with numerous other reactions (Poutsma 2006). Currently, published experimental values are only available for a few reaction types that occur in polystyrene pyrolysis, with most coming from polymerization experiments (Buback et al. 1995; Li et al. 2006). The limited availability of experimental rate parameters necessitates the use of estimation methods based on small molecule chemistry and parameter fitting to experimental data within acceptable physical bounds.

Pyrolysis of polystyrene affords a relatively simple product spectrum compared to pyrolysis of other commodity polymers such as polyethylene (Poutsma 2003) and polypropylene (Kruse et al. 2003b). The product spectrum is dominated by three major products: styrene monomer, dimer, and trimer, with a few minor products such as toluene, α-methyl styrene, and diphenyl propane. While this slate of products is relatively simple, the experimental literature

has reported wide ranges of product ratios among them (Poutsma 2006). Much of this disparity can be attributed to how the reaction was carried out and whether transport effects were present. This makes mechanistic modeling as a tool to understand the relative contributions of different reaction pathways to the formation of major and minor products even more attractive, since it can be ensured that only intrinsic kinetics are present.

The reaction pathways to the three major products of polystyrene pyrolysis were thought to be well understood (Faravelli et al. 2001; Kruse et al. 2001; Kruse et al. 2002; Marongiu et al. 2007). Monomer is primarily formed via chain unzipping (end-chain β-scission). Dimer and trimer were both thought to be formed via backbiting reactions followed by mid-chain β-scission of mid-chain head radicals in the third or fifth positions, respectively. These reaction pathways are depicted in Figure 3.1. While the reaction pathways depicted in Figure 3.1 for styrene and trimer formation are still widely accepted, the traditional 1,3-hydrogen shift pathway to form dimer has received considerable attention recently. Backbiting reactions are expected in high temperature polymeric reaction systems, but the 1,3-hydrogen shift reaction has a high energy barrier (Pfaendtner et al. 2006). Unlike 1,5-hydrogen shift, which has a six-membered ring as the transition state, 1,3-hydrogen shift requires a more unfavorable transition state characterized by a four-membered ring.

In our previous work in which polystyrene pyrolysis was modeled, a low energy barrier for 1,3-hydrogen shift was used, making 1,3-hydrogen shift the dominant reaction pathway to dimer (Kruse et al. 2005; Kruse et al. 2002). Two alternate reaction pathways to dimer formation during PS pyrolysis have been proposed. The benzyl radical addition pathway, which is depicted in Figure 3.2, was proposed originally by Ohtani et al. (1990) based on experimental work and recently supported by Poutsma (2006) based on theoretical and computational work.

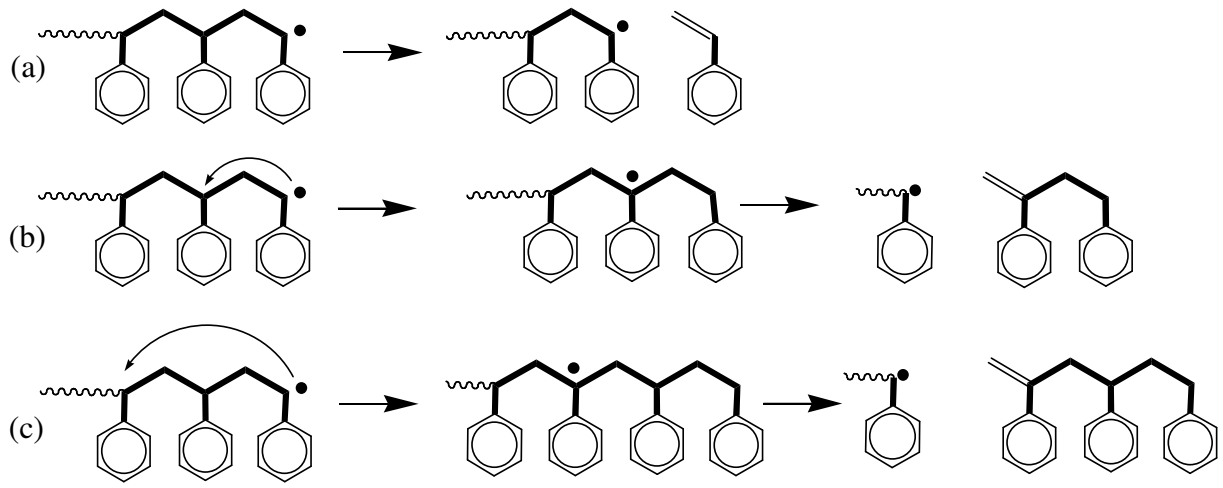

Figure 3.1: Traditional polystyrene pyrolysis reaction pathways to form (a) styrene, (b) dimer, and (c) trimer.

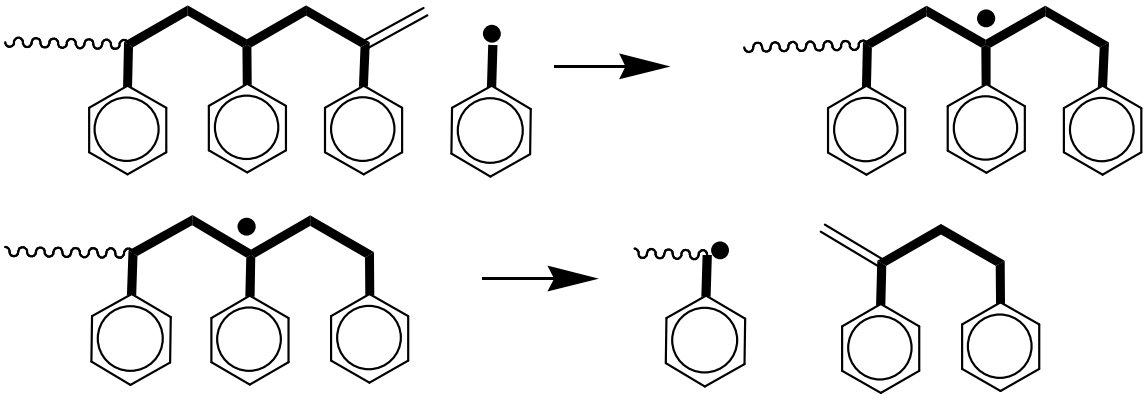

Figure 3.2: Benzyl radical addition pathway to styrene dimer.

This reaction pathway involves the radical addition of a benzyl radical to an unsaturated, primary carbon chain end. This reaction forms a mid-chain head radical in the third position which can then undergo mid-chain β-scission to form addition of a benzyl radical to an unsaturated, primary carbon chain end. This reaction forms a mid-chain head radical in the third position which can then undergo mid-chain β-scission to form dimer. This reaction was also in our previous model of polystyrene pyrolysis, but because 1,3-hydrogen shift was set to be favorable, the contribution of the benzyl radical addition pathway to dimer formation was negligible. The 7,3-hydrogen shift pathway, depicted in Figure 3.3, was proposed recently by Moscatelli et al. (2006) based on computational work to investigate high temperature styrene polymerization. This reaction pathway involves 1,7-hydrogen shift to form a mid-chain head radical at the seventh position followed by 7,3-hydrogen shift to form a mid-chain head radical at the third position. Thus, all three reaction pathways lead to dimer through β-scission of the mid-chain head radical in the third position, but they differ in how this radical is formed.

In this study, we applied our modeling framework to polystyrene pyrolysis to gain insight into the reaction pathways to dimer. In light of recent work in the literature (Moscatelli et al. 2006; Pfaendtner et al. 2006; Poutsma 2006), it was important to re-evaluate a subset of the rate parameters used in our model. For the 7,3-hydrogen shift reaction pathway, it was also necessary to add the appropriate reactions to the model to capture this chemistry. The results of the expanded mechanistic model were compared to a large selection of experimental data collected in our lab (Kruse et al. 2002) and from the literature (Bockhorn et al. 1998; Bouster et al. 1980) covering a wide range of conditions (initial molecular weights, pyrolysis temperatures, and reactor configurations). Net rate analysis was then carried out based on the results of our

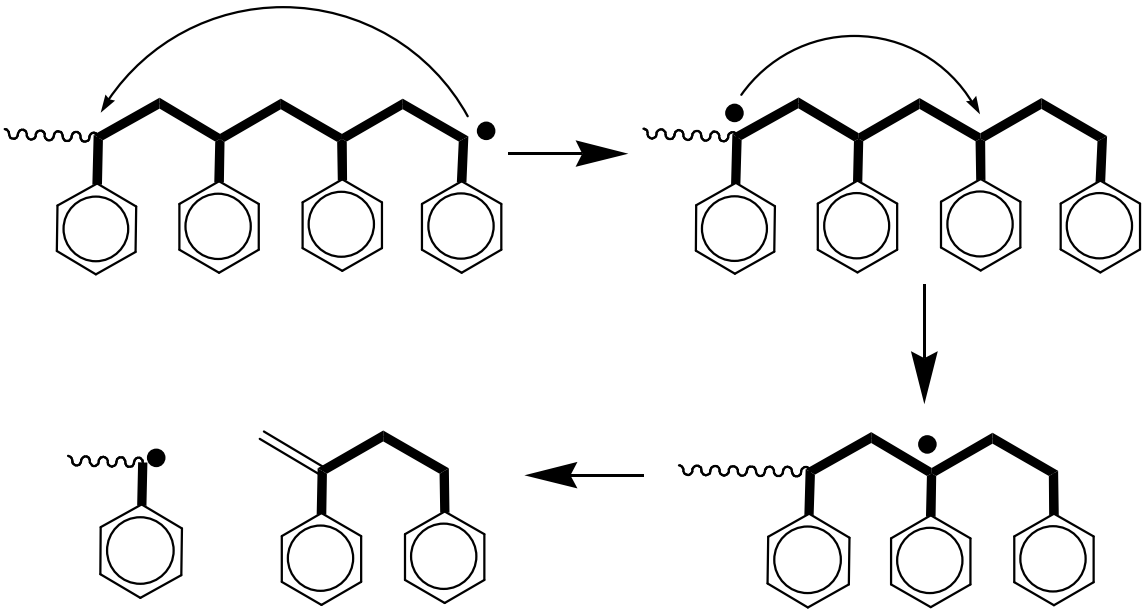

Figure 3.3: 7,3-Hydrogen shift pathway to styrene dimer.

detailed mechanistic model to determine the relative contributions of the three different reaction pathways to the formation of styrene dimer.

3.2 MODELING FRAMEWORK

3.2.1 Mechanistic Chemistry

Polymer pyrolysis involves a complex free-radical reaction mechanism consisting of thousands of reactions and species due to the high molecular weight and polydisperse nature of polymers, many different possible structural features (e.g. branches, unsaturations), and numerous reaction channels that are available to free radicals. It is impractical to build and solve an explicit model for such a system. In order to achieve a high level of detail and still maintain a manageable model size, the method of moments is utilized in our modeling framework, where the chain length distribution is captured by a series of moments instead of explicitly tracking chains of every length. To fully determine the chain length distribution, all moments are required, but substantial detail can be maintained from only the first few moments (Grinstead and Laurie 1997). The number average and weight average molecular weights can be determined knowing only the first three moments (zeroth, first, and second moments) of the system as shown in equations 3.1 and 3.2 (Dotson et al. 1996):

$$M_n = M_0 \frac{\mu_1}{\mu_0} \qquad (3.1)$$

$$M_w = M_0 \frac{\mu_2}{\mu_1} \qquad (3.2)$$

where M_n is the number-average molecular weight, M_w is the weight-average molecular weight, M_0 is the monomer molecular weight, and μ_i is the i^{th} moment. Building on the work of McCoy

and coworkers (Kodera and McCoy 1997; Madras et al. 1997a; Madras and McCoy 1999; Sterling and McCoy 2001), who used global rate coefficients to describe changes in the molecular weight distribution as a function of time, we have developed a moment-based modeling framework to build detailed mechanistic models for polymer reaction systems. Our framework has been previously applied to polystyrene pyrolysis, polypropylene pyrolysis, polypropylene-polystyrene binary pyrolysis, and the living free-radical polymerization of polystyrene (Kruse et al. 2005; Kruse et al. 2003a; Kruse et al. 2003b; Kruse et al. 2002).

To capture the mechanistic chemistry, all the species in the system are reacted according to a set of elementary reaction families before the method of moments is applied. For polystyrene pyrolysis, reactions are created for the following elementary reaction families: (1) chain fission, (2) radical recombination, (3) allyl chain fission, (4) hydrogen abstraction, (5) mid-chain β-scission (6) radical recombination, (7) end-chain β-scission, (8) disproportionation, and (9) intramolecular hydrogen transfer (1,3-, 1,5-, 1,7-, and 7,3-hydrogen shift). The original PS model did not include 1,7- and 7,3-hydrogen shift (Kruse et al. 2005; Kruse et al. 2002), but these reaction types were needed to capture the chemistry involved in the 7,3-hydrogen shift reaction pathway. To track structural detail while using the method of moments, polymeric species were distinguished based on the characteristics of the chain. These included radical position (end-chain, mid-chain, specific mid-chain, and dead chains), end type (primary "tail" or secondary "head" carbon, saturated or unsaturated), and chain structure (linear, branched, and specific low molecular weight species). Specific mid-chain radicals tracked included head radicals in the second, third, fifth, and seventh positions. These radicals were tracked separately because they lead to the formation of various low molecular weight products (LMWP) via β-scission. LMWP and low molecular weight radicals were tracked explicitly. Utilizing these

reaction families and the method of moments, a detailed description of the mechanistic chemistry was created.

3.2.2 Specification of Rate Parameters

The protocol for specifying rate parameters that was previously developed in our research group was used to specify rate parameters for each reaction in the mechanistic model (Kruse et al. 2005; Kruse et al. 2003b; Kruse et al. 2002). Rate parameters in the model were dependent on the reaction type and the structure and thermodynamics of the reactants and products involved. To establish this link between structure and reactivity, the Evans-Polanyi relationship was used primarily. The Evans-Polanyi relationship (equation 3.3) relates the activation energy of a reaction linearly to the heat of reaction (Evans and Polanyi 1938).

$$E_a = E_0 + \alpha \Delta H_{rxn} \qquad (3.3)$$

where E_a is the activation energy, E_0 is the intrinsic barrier, α is the transfer coefficient, and ΔH_{rxn} is the heat of reaction. E_0 and α are specific to the reaction type or family, while ΔH_{rxn} is specific to the reactants and products of a given reaction. Additionally, the Blowers-Masel relationship (equation 3.4) was used for intermolecular chain transfer reactions since it was developed specifically for this class of reactions (Blowers and Masel 1999).

$$E_a = \begin{cases} 0 & \Delta H_{rxn} / 4E_0 < -1 \\ E_0 (1 + \Delta H_{rxn} / 4E_0)^2 & -1 \le \Delta H_{rxn} / 4E_0 \le 1 \\ \Delta H_{rxn} & \Delta H_{rxn} / 4E_0 > 1 \end{cases} \qquad (3.4)$$

All the intramolecular hydrogen shift reactions were assigned a specific activation energy based on the work of Poutsma (2006).

Arrhenius behavior was assumed for all reactions, requiring a frequency factor and either a specific activation energy or the parameters for either the Evans-Polanyi or Blowers-Masel relationship be specified for each reaction family. These values are assigned using a hierarchical approach in which experimental data for polymeric systems are used first, and in their absence, experimental values based on small molecules and modeling studies of polymer mimics are applied (Woo et al. 1998). Heats of reaction are assigned for each reaction using a similar hierarchical approach. First, experimental values are sought, and in the absence of experimental values, Benson group additivity (Benson 1976) values or quantum chemical calculations based on small molecules that mimic the polymer are used.

Table 3.1 summarizes all of the rate parameters used in the present work. It is important to note that while many of the values are the same as those in Table 2 of Kruse et al. (2002) new reaction families were added and a subset of parameters was altered based on recent literature reports. As a result of these updates, a small number of parameters were altered slightly based on parameter estimation. In particular, benzyl radical addition was separated into a reaction family distinct from other radical addition reactions, and its frequency factor was specified based on the work of Poutsma (2006). It should be noted that the frequency factor for general radical addition was changed to be in agreement with the IUPAC value for polystyrene propagation (Buback et al. 1995). This change was also reflected in the frequency factor values for general end-chain and mid-chain β-scission which were updated to maintain thermodynamic consistency using the value for the entropy of reaction for PS polymerization (Brandrup and Immergut 1999). The reaction families of 1,7- and 7,3-hydrogen shift were added, and their activation energies were fixed based on the work of Poutsma (2006). The frequency factor for 7,3-hydrogen shift was specified also based on the work of Poutsma (2006), and the frequency factor for

Table 3.1: Representative values for rate parameters utilized in the mechanistic model of polystyrene pyrolysis

Reaction Type	Frequency Factor, A (s^{-1} or L mol^{-1} s^{-1})	Intrinsic Barrier, E_0 (kcal mol^{-1})	Transfer Coefficient, α	Representative ΔH_{rxn} (kcal mol^{-1})	Activation Energy (kcal mol^{-1})
Chain fission	$1.00x10^{15}$	2.3	1.0	65.0	67.3
Allyl chain fission	$5.50x10^{13}$	2.3	1.0	55.0	57.3
Radical recombination	$1.10x10^{11}$	2.3	0.0	-65.0	2.3
Disproportionation	$5.50x10^{9}$	2.3	0.0	NA	2.3
End-chain β-scission	$3.10x10^{12}$	11.4	0.76	16.4	23.9
Mid-chain β-scission	$3.10x10^{12}$	11.4	0.76	20.9	27.3
β-scission to LMWS[c]	$1.25x10^{13}$ [a]	11.4	0.76	19.4	26.1
Depropagation[d]	$2.80x10^{13}$ [a]	11.4	0.76	19.7	26.4
General radical addition	$4.30x10^{7}$	11.4	0.24	-20.9	6.4
Benzyl radical addition	$2.75x10^{8}$ [b]	11.4	0.24	-29.7	4.3
Hydrogen abstraction	$2.10x10^{6}$	12.0	NA	-3.12	10.5
1,5-hydrogen shift	$1.35x10^{9}$ [a]	NA	NA	NA	16.2 [b]
1,3-hydrogen shift	$5.01x10^{12}$ [b]	NA	NA	NA	37.4 [b]
1,7-hydrogen shift	$1.02x10^{9}$ [a]	NA	NA	NA	15.7 [b]
7,3-hydrogen shift	$6.31x10^{9}$ [b]	NA	NA	NA	16.6 [b]

[a]Updated values obtained using parameter estimation.
[b]Updated values obtained based on recent literature (Pfaendtner et al. 2006; Poutsma 2006).
[c]β-scission to low molecular species (LMWS) is defined as β-scission of a mid-chain radical resulting in the formation of species of chain length of four or fewer monomer units.
[d]Depropagation is the formation of monomer from low molecular weight radicals with chain length of five carbon atoms or less.

1,7-hydrogen shift was fit using parameter regression with bounds based on the work of Pfaendtner et al. (2006). The final additions to the set of reaction families were β-scission to LMWP and depropagation of low molecular weight radicals with chains lengths less than five carbon atoms to monomer, with the E_0 and α parameters fixed at the values for mid-chain β-scission from Kruse et al. (2002) and the frequency factors obtained from parameter estimation with bounds based on the work of Poutsma (2006). In the previous model, these reactions fell under the general categories of mid-chain β-scission and end-chain β-scission, and as a result their frequency factors were about an order of magnitude too low for small molecule chemistry as discussed by Poutsma (2006). The activation energies for 1,3- and 1,5-hydrogen shift were also fixed based on the work of Poutsma (2006), and their frequency factors were obtained from theoretical estimates suggested by Poutsma (2006) (1,3-hydrogen shift) and parameter estimation (1,5-hydrogen shift) with bounds based on the work of both Poutsma (2006) and Pfaendtner et al. (2006). To obtain the four frequency factors specified by parameter estimation, the model results were regressed using GREG (Stewart et al. 1992) against isothermal pyrolysis data at 350 °C for polystyrene with M_{n0} of 50,550 and M_{w0} of 57,640 previously collected in our lab (Kruse et al. 2002). The agreement between the model results and the experimental data used for parameter estimation is excellent for both molecular weight decay as well as the various LMWP mass yields, as shown in Figure 3.4. It should be noted that at 180 minutes the experimental mass yields do not match the model results as well as at earlier times. This is caused by secondary gas phase reactions that occur at long times under our experimental setup as discussed in previous work (Kruse et al. 2002).

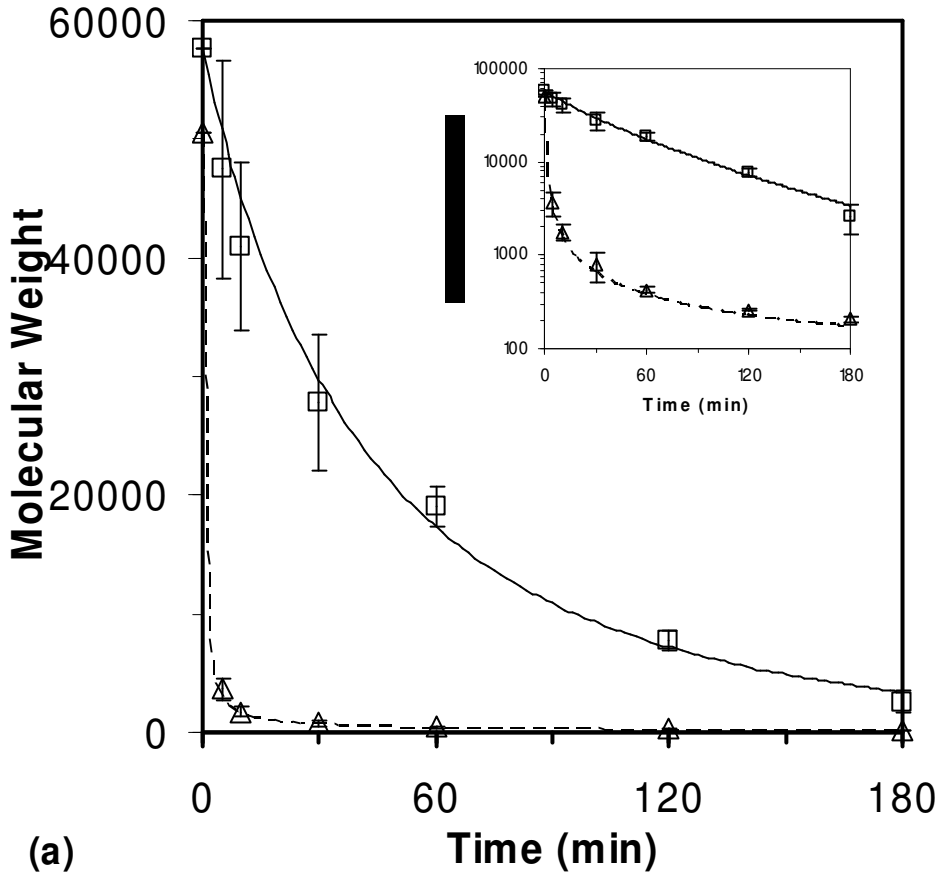

Figure 3.4: Model results compared to experimental data for pyrolysis of PS with M_{n0} = 50,550 and M_{w0} = 57,640 at 350 °C. The molecular weight changes are shown in (a) with model results shown as lines (---- M_n; —— M_w) and the experimental data as points (△ M_n; □ M_w). The low molecular weight product (LMWP) yields are shown in (b) with the model results shown as lines (---- styrene; —— dimer; — — trimer; —— total LMWP) and the experimental data shown as points (△ styrene; □ dimer; ○ trimer; ◇ total LMWP). Four of the 41 kinetic parameters were regressed to achieve this fit: frequency factors for β-scission to LMWS, depropagation of 1,3-diphenylpropyl radical to monomer, 1,5-hydrogen shift, and 1,7-hydrogen shift. The inset in (a) is the molecular weight change results plotted on a logarithmic scale to demonstrate the capture of the M_n experimental data by the model.

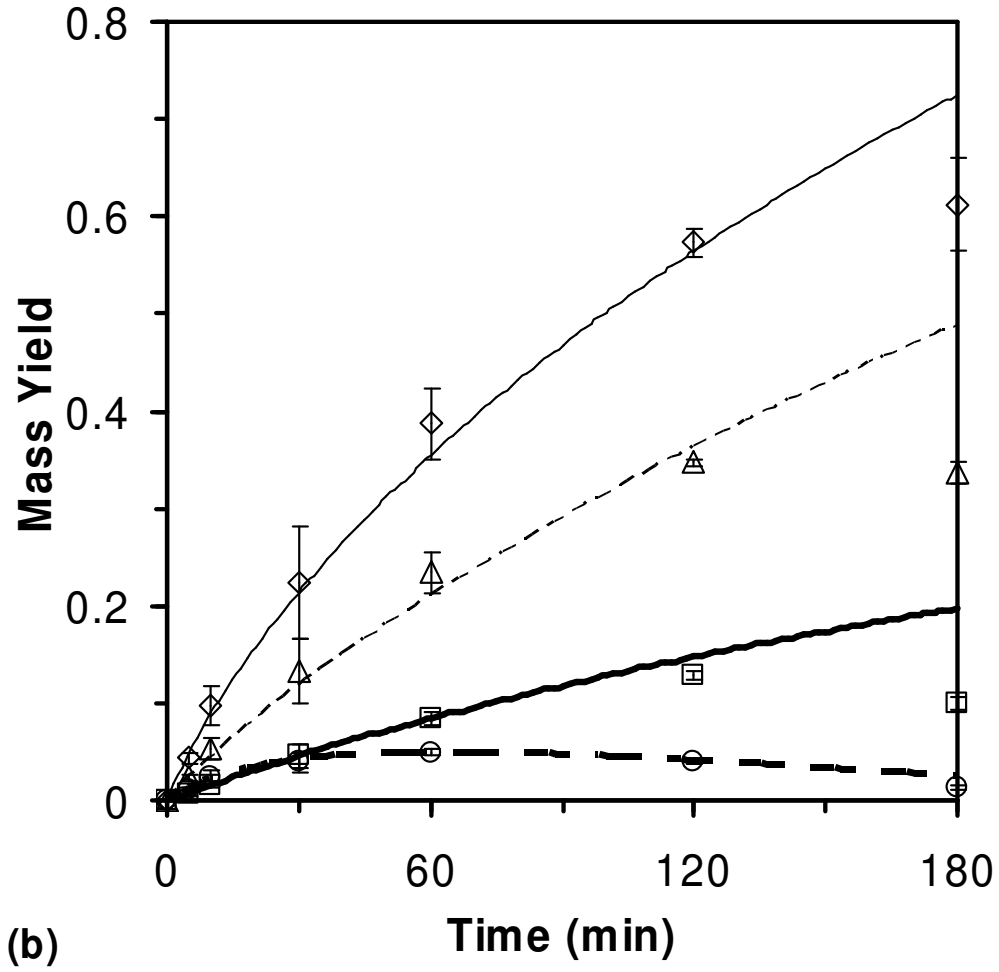

Figure 3.4: Continued

3.2.3 Model Assembly and Solution

To assist in handling the large number of reactions and species in our polymer pyrolysis models, PERL scripts were developed to automate model construction. The PERL scripts first create a list of reactions in traditional form as well as lists of species, rate constants required, variables, and algebraic equations utilized in the model. These lists are created based on the specific structural features that are being tracked in the model and the rules governing each reaction family. The PERL scripts then convert the reaction list into population balance form, which have moment operations applied to convert the reactions into the terms in the moment equations for each polymeric species. Each polymeric species is described by a differential equation for its zeroth, first, and second moments. The resultant set of stiff differential equations and the algebraic equations for other important variables was solved using DASSL (Petzold 1983). The final model tracked 75 species and included over 3500 reactions.

In solving the model, isothermal reaction conditions with heat up times dictated by the specific experiment are assumed. Volatile, low molecular weight, non-radical species are assumed to immediately leave the reacting melt and react no further based on characteristic reaction and diffusion times at the conditions of interest. Which species are volatile is specified based on the temperature. For 350 °C, species with molecular weight < 260 amu were considered volatile, while at 310 °C, species with molecular weight < 208 amu were released from the melt. All low molecular weight radical species are assumed to react before they can leave the melt based on a similar analysis. The polymer melt is treated as a homogeneous system, with no spatial concentration gradients.

3.3 RESULTS AND DISCUSSION

3.3.1 Model Verification

To validate the set of rate parameters in Table 3.1 as well as to demonstrate the broad range of conditions over which our polystyrene pyrolysis mechanistic model is predictive, model predictions were compared to experimental results collected in different laboratories and over a broad range of conditions. The model was solved with a variety of initial M_n and M_w values as well as over a range of temperatures. First, to demonstrate the ability of the model to capture reactivity over a wide range of temperatures, the model was solved for pyrolysis at 310 °C (M_{n0} of 50,550 and M_{w0} of 57,640) and 380 °C (M_{n0} of 41,200 and M_{w0} of 44,100) and compared against data collected by Kruse et al. (2002) At both temperatures, excellent agreement between the experimental results and the model predictions was obtained as shown in Figure 3.5 for 310 °C and in Figure 3.6 for 380 °C. The rates of degradation are very different at these two temperatures as evidenced by the rate of molecular weight decay and the rates of evolution of the LMWP. The model is able to capture these changes quantitatively.

To further validate the model and its rate parameters, model results were obtained for PS pyrolysis at widely different initial M_n and M_w values for pyrolysis at 350 °C and compared to experimental data reported by Kruse et al. (2002) To test the lower end of the molecular weight spectrum, pyrolysis of PS with an initial M_n of 5158 and an initial M_w of 5854 was modeled. Comparison of the model predictions and the experimental data is provided in Figure 3.7, and the agreement is excellent. To test a higher molecular weight material, pyrolysis of PS with an initial M_n of 98,100 and an initial M_w of 111,800 was modeled. Figure 3.8 shows the model predictions compared with experimental results, and again the agreement is very good. These two sets of results demonstrate the ability of the model to handle a wide range of initial

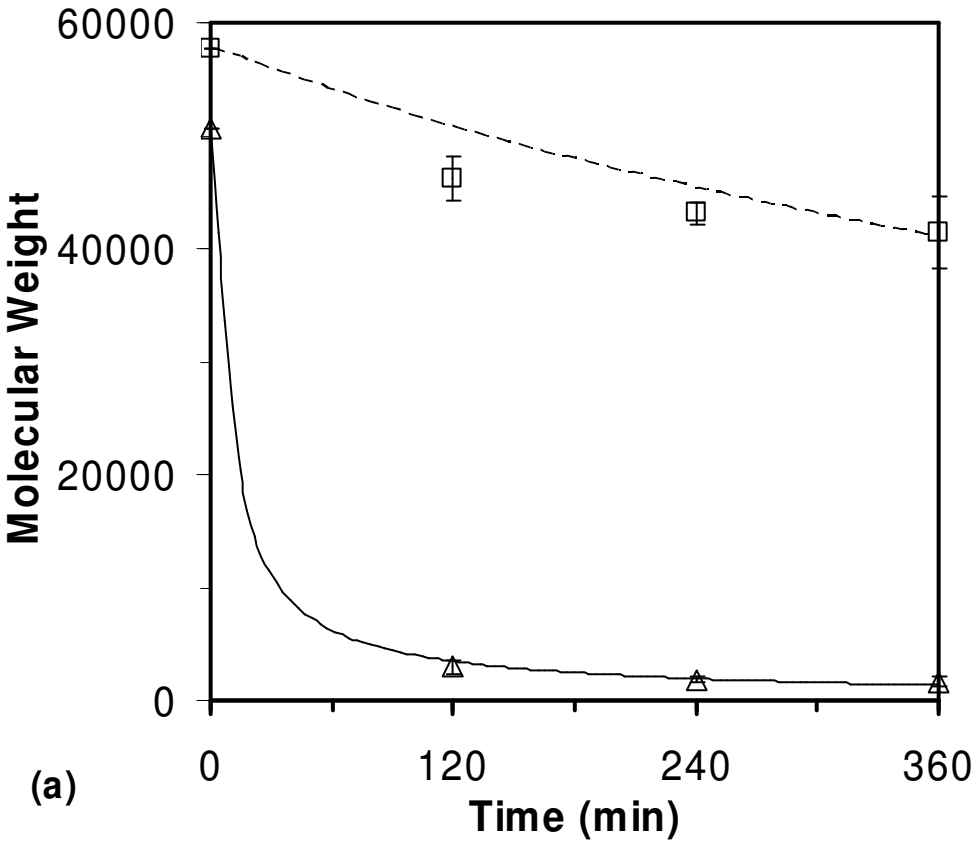

Figure 3.5: Model results compared to experimental data for pyrolysis of PS with M_{n0} of 50,550 and M_{w0} of 57,640 at 310 °C. The molecular weight changes are shown in (a) with model results shown as lines (—— M_n; ---- M_w) and the experimental data as points (△ M_n; □ M_w). The low molecular weight product (LMWP) yields are shown in (b) with the model results shown as lines (---- styrene; ——— dimer; — — trimer; —— total LMWP) and the experimental data shown as points (△ styrene; □ dimer; ○ trimer; ◇ total LMWP).

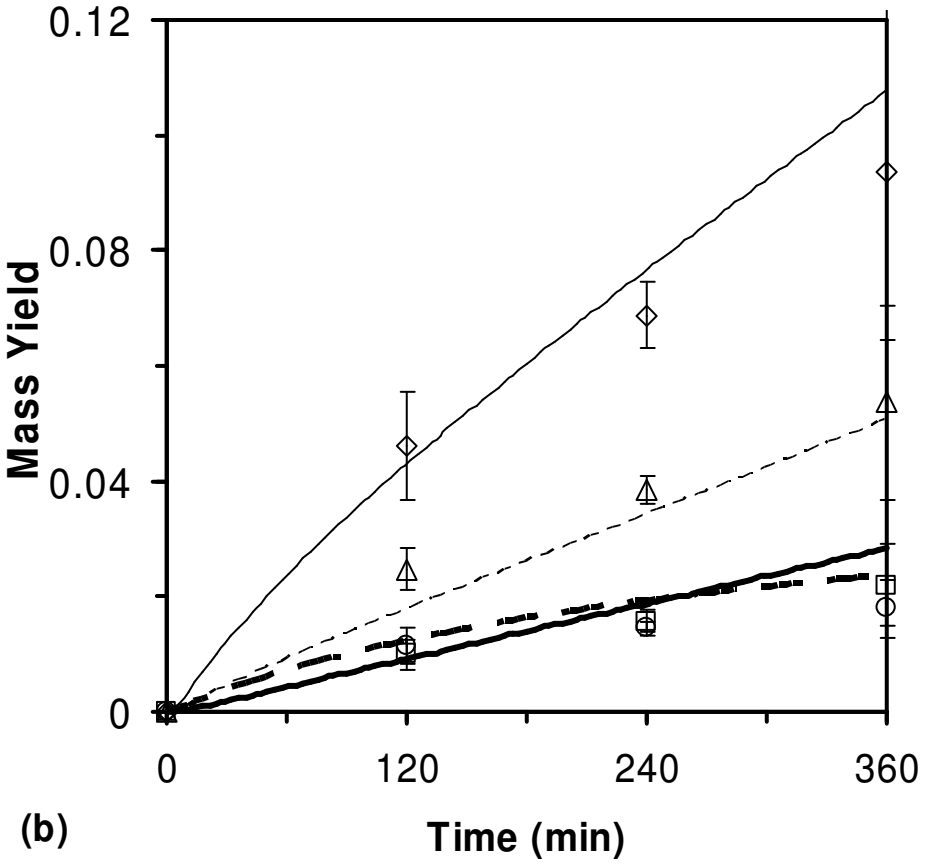

Figure 3.5: Continued.

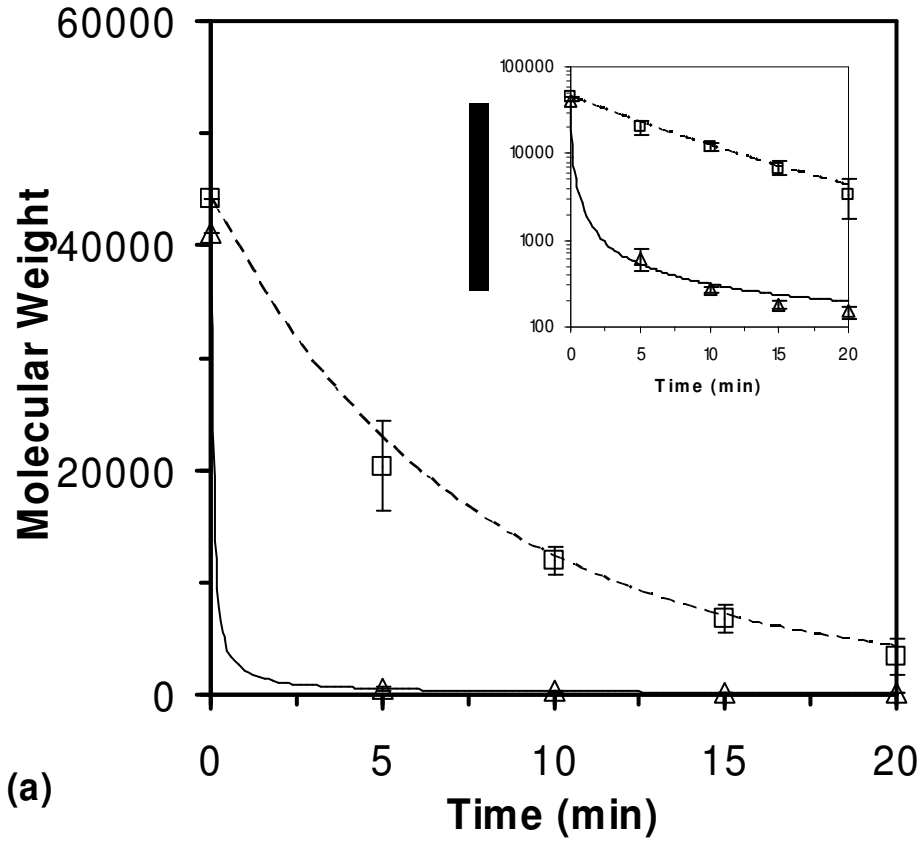

Figure 3.6: Model results compared to experimental data for pyrolysis of PS with M_{n0} of 41,200 and M_{w0} of 44,100 at 380 °C. The molecular weight changes are shown in (a) with model results shown as lines (—— M_n; ---- M_w) and the experimental data as points (△ M_n; □ M_w). The low molecular weight product (LMWP) yields are shown in (b) with the model results shown as lines (---- styrene; ▬ dimer; ▬ ▬ trimer; —— total LMWP) and the experimental data shown as points (△ styrene; □ dimer; ○ trimer; ◇ total LMWP). The inset in (a) is the molecular weight change results plotted on a logarithmic scale to demonstrate the capture of the M_n experimental data by the model.

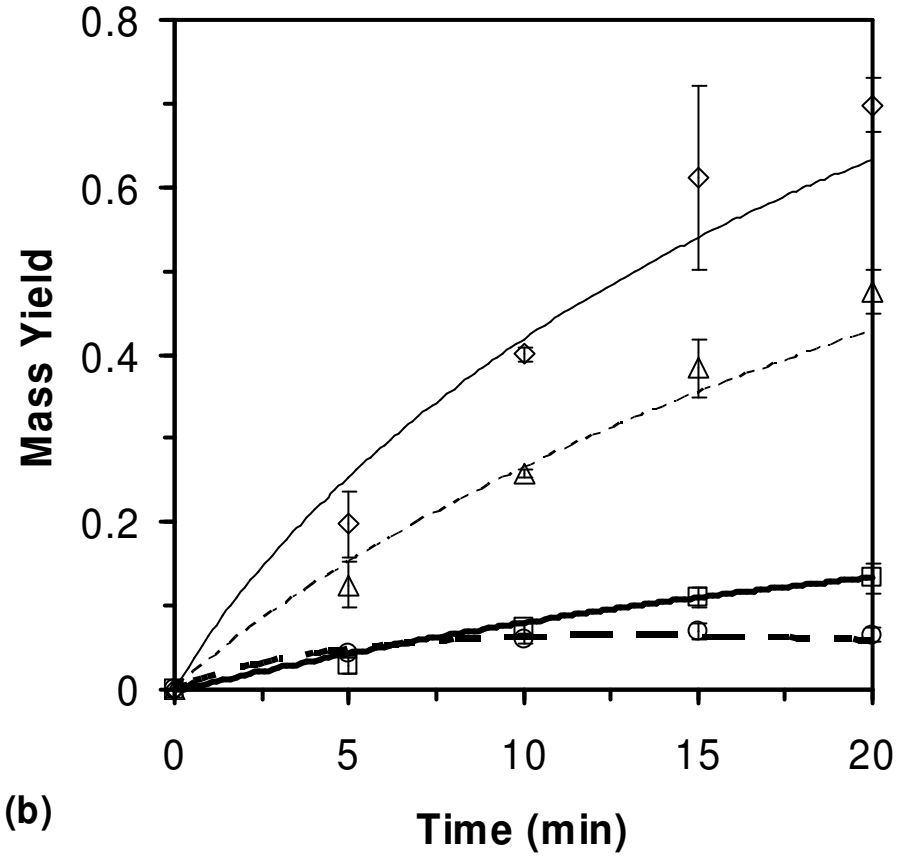

Figure 3.6: Continued.

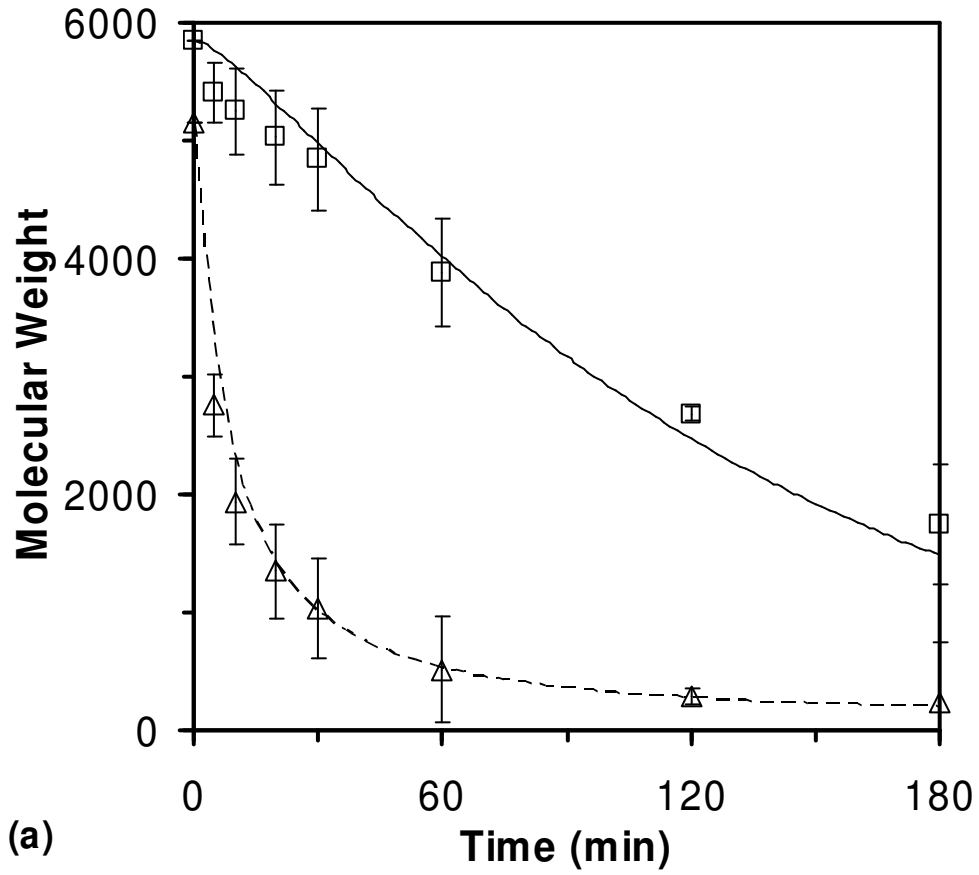

Figure 3.7: Model results compared to experimental data for pyrolysis of PS with M_{n0} of 5,518 and M_{w0} of 5,854 at 350 °C. The molecular weight changes are shown in (a) with model results shown as lines (---- M_n; —— M_w) and the experimental data as points (△ M_n; □ M_w). The low molecular weight product (LMWP) yields are shown in (b) with the model results shown as lines (---- styrene; —— dimer; — — trimer; —— total LMWP) and the experimental data shown as points (△ styrene; □ dimer; ○ trimer; ◇ total LMWP).

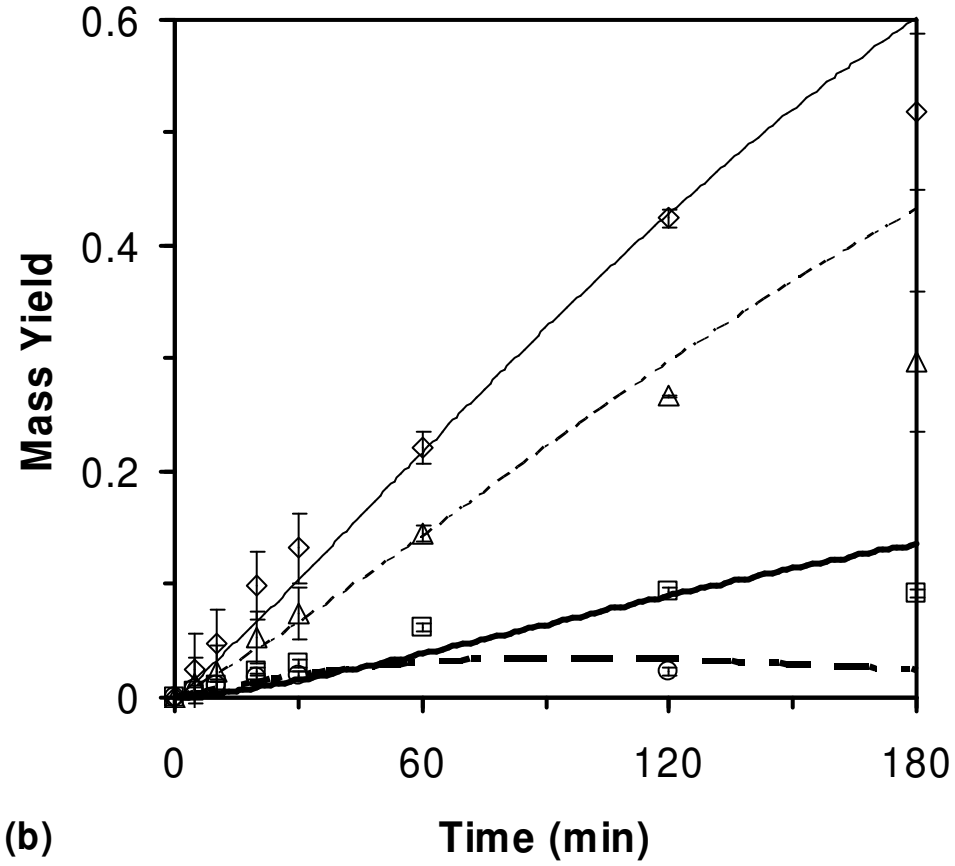

Figure 3.7: Continued.

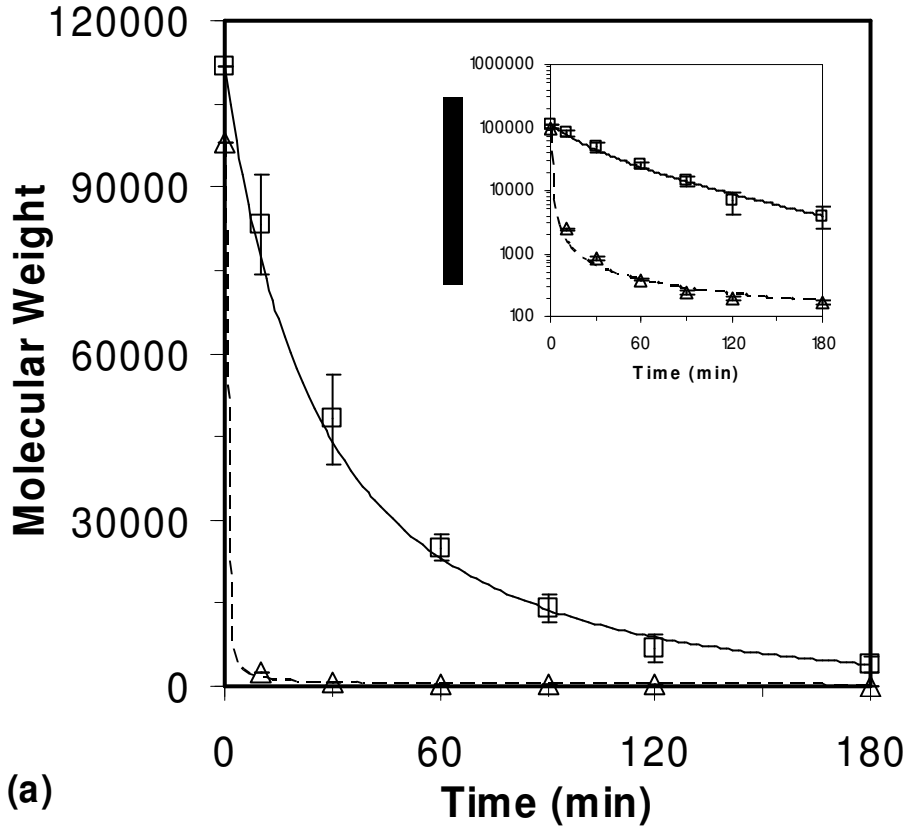

Figure 3.8: Model results compared to experimental data for pyrolysis of PS with M_{n0} of 98,100 and M_{w0} of 111,800 at 350 °C. The molecular weight changes are shown in (a) with model results shown as lines (---- M_n;—— M_w) and the experimental data as points (△ M_n; □ M_w). The low molecular weight product (LMWP) yields are shown in (b) with the model results shown as lines (---- styrene; —— dimer; — — trimer; —— total LMWP) and the experimental data shown as points (△ styrene; □ dimer; ○ trimer; ◇ total LMWP). The inset in (a) is the molecular weight change results plotted on a logarithmic scale to demonstrate the capture of the M_n experimental data by the model.

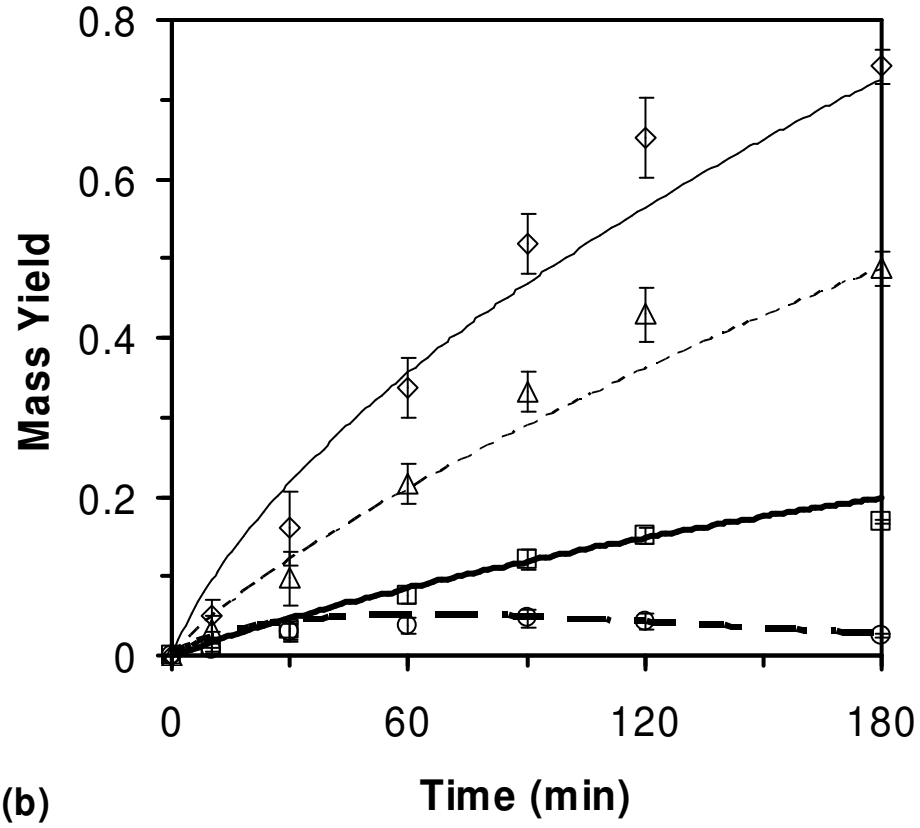

Figure 3.8: Continued.

molecular weights while still providing accurate predictions for both molecular weight decay and the LMWP yields.

The model was further tested against two data sets from the literature that were not obtained in our own laboratory. These two data sets cover various ranges of temperature as well as high molecular weights and polydispersity. The data set from Bouster et al. captures pyrolysis over a temperature range of 331-370 °C for PS with an initial M_n of 100,000 and an initial M_w of 250,000 (1980). These results were collected via isothermal thermogravimetry. The data from Bockhorn et al. analyzed PS pyrolysis over a temperature range of 360-410 °C using a sample with an initial M_n of 66,000 and an initial M_w of 186,000 (1998). These results were collected isothermally using a gradient-free reactor. It should be noted that both of these studies utilized commercially available polystyrene for their experiments. For the data of Bouster et al., a warm-up period of 15 minutes was reported, which was incorporated explicitly in the model solution. The data of Bockhorn et al. were collected with warm-up periods that depended on the temperature, and the model solution took these values into account explicitly. Comparison of the model predictions to the experimental data of Bouster et al. and Bockhorn et al. is provided in Figures 3.9 and 3.10, respectively. The agreement is very good and further demonstrates the ability of the model to capture PS pyrolysis over a wide range of temperatures, reactor configurations, and initial molecular weights.

3.3.2 Net Rate Analysis

The model results were then interrogated to identify the major pathway(s) to styrene dimer. The model includes three major reaction pathways to dimer formation: 1,3-hydrogen shift, 7,3-hydrogen shift, and benzyl radical addition. While it is expected that 1,3-hydrogen

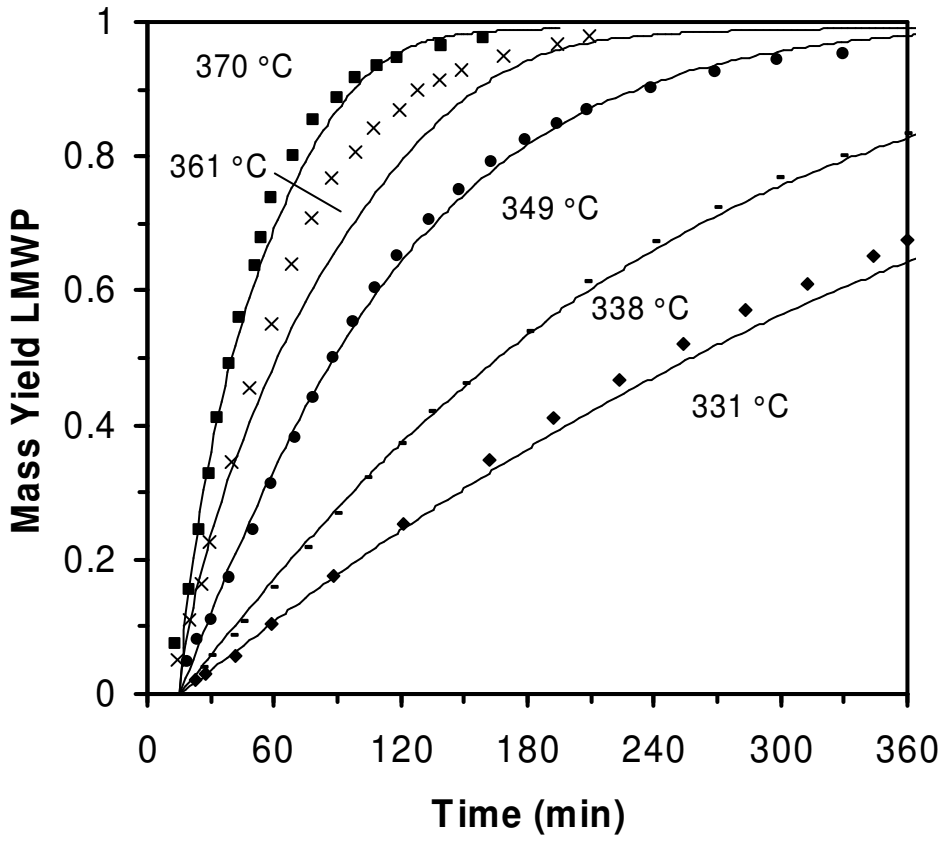

Figure 3.9: Model predictions compared with the experimental results of Bouster et al. (Bouster et al. 1980) for pyrolysis of PS with an initial M_n of 100,000. A warm-up time of 15 minutes was incorporated into the model solution in accordance with the experimental observations.

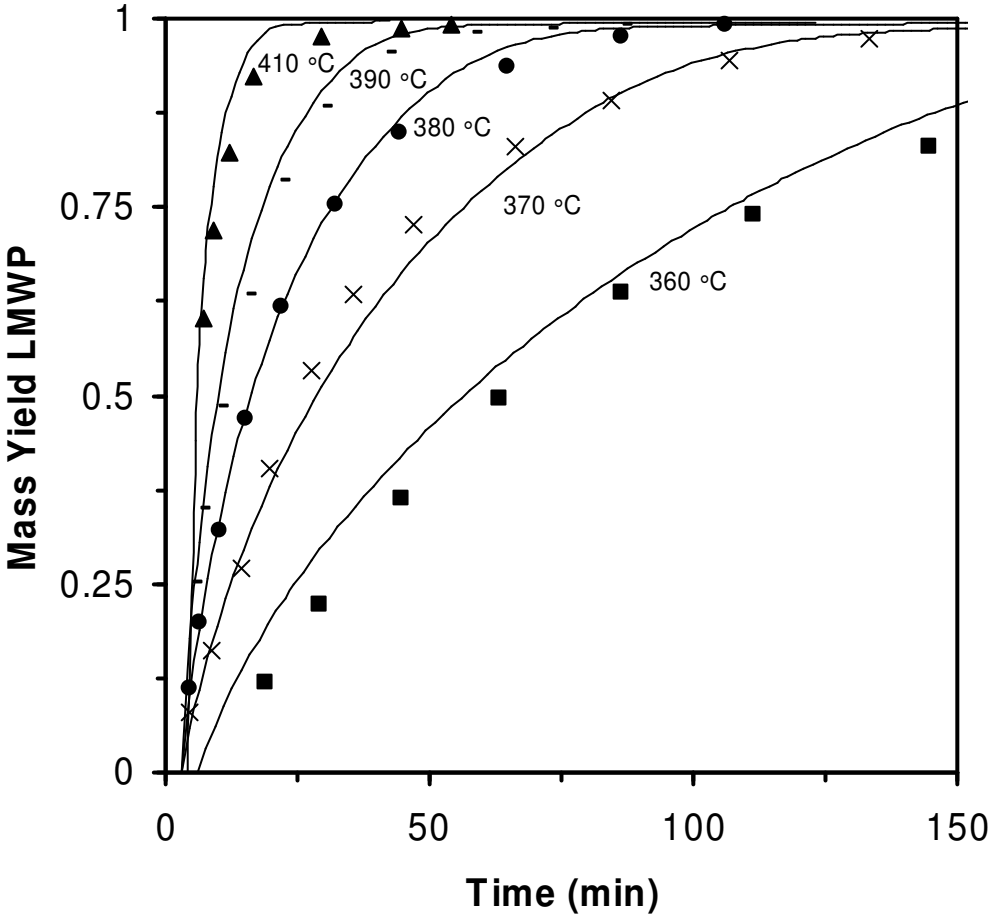

Figure 3.10: Model predictions compared with the experimental results of Bockhorn et al. (Bockhorn et al. 1998) for pyrolysis of PS with an initial M_n of 66,000. A short warm-up period was incorporated into the model solution in accordance with the experimental observations.

shift will not be an important pathway to dimer formation due to the high energy barrier of this reaction, the competitiveness of the other two reaction pathways has not been assessed and is debated. To quantify how dimer is formed, the net rates of the different pathways for the formation of the mid-chain radical with the radical center located in the third position from the chain end that is the precursor to dimer for all three reaction pathways, as shown in Figures 3.1-3.3, were calculated. Figure 3.11 plots the net rates for the three reaction pathways for pyrolysis at 310 °C and 350 °C for polystyrene with M_{n0} equal to 50550 and M_{w0} equal to 57640 and for pyrolysis at 380 °C for polystyrene with M_{n0} equal to 41200 and M_{w0} equal to 44100. It is apparent that the 7,3-hydrogen shift pathway is the dominant pathway at all three temperatures shown. 1,3-hydrogen shift is never competitive with either of the other pathways, as expected at these temperatures due to its high energy barrier. The benzyl radical addition pathway becomes increasingly more competitive as the temperature of pyrolysis increases. It should be noted that at early times (the first 136 minutes) at 310 °C the net rate for benzyl radical addition favors the reverse β-scission reaction.

The increase in the competitiveness of the benzyl radical addition pathway with increasing temperature compared to the 7,3-hydrogen shift pathway is somewhat surprising because benzyl radical addition has a much lower activation energy than 7,3-hydrogen shift as reported in Table 3.1. This points to dramatic increases in the benzyl radical concentration as the factor that accounts for the more marked increase in rate. As shown in Table 3.2, the average concentration of the benzyl radical over the reaction times examined experimentally increases by almost three orders of magnitude as the temperature increases from 310 °C to 380 °C. The concentration of polymer with unsaturated tail ends, which is the other factor in defining the rate

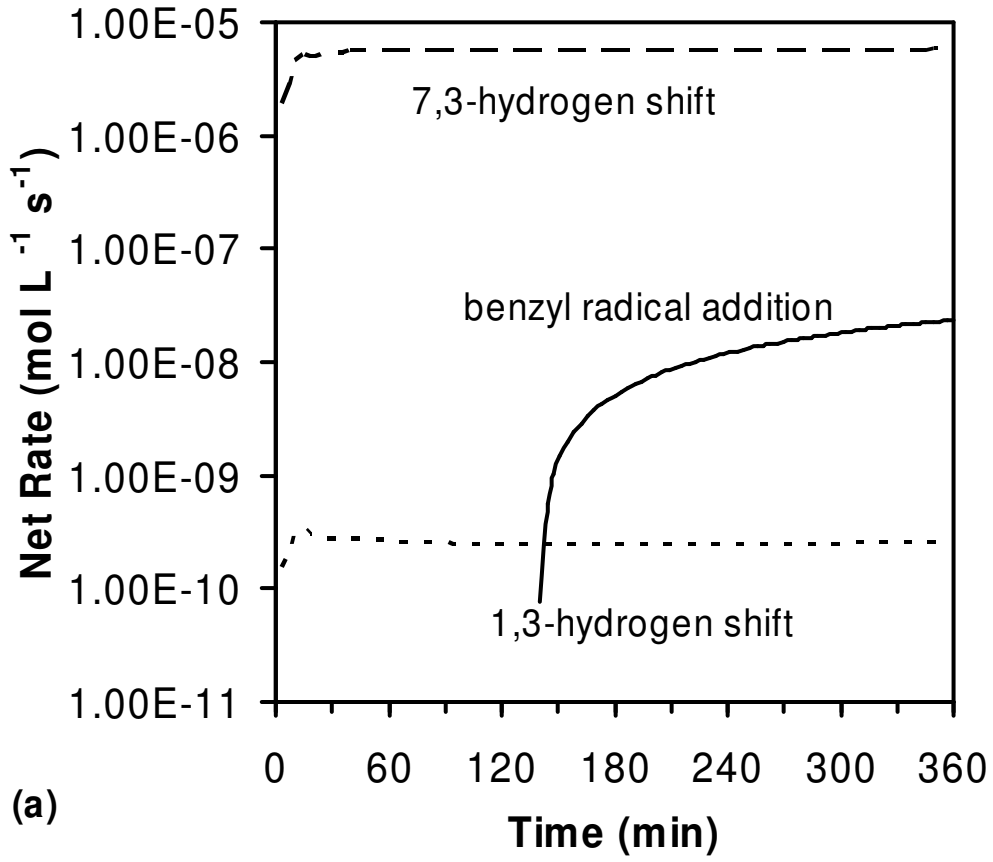

Figure 3.11: Net rates for the three different pathways for the formation of the mid-chain head radical in the third position at (a) 310 °C, (b) 350 °C, and (c) 380 °C. While 7,3-hydrogen shift is dominant at all three temperatures, benzyl radical addition becomes more important as the temperature increases. It should also be noted that at 310 °C benzyl radical addition favors the reverse β-scission reaction for the first 136 minutes of reaction time simulated.

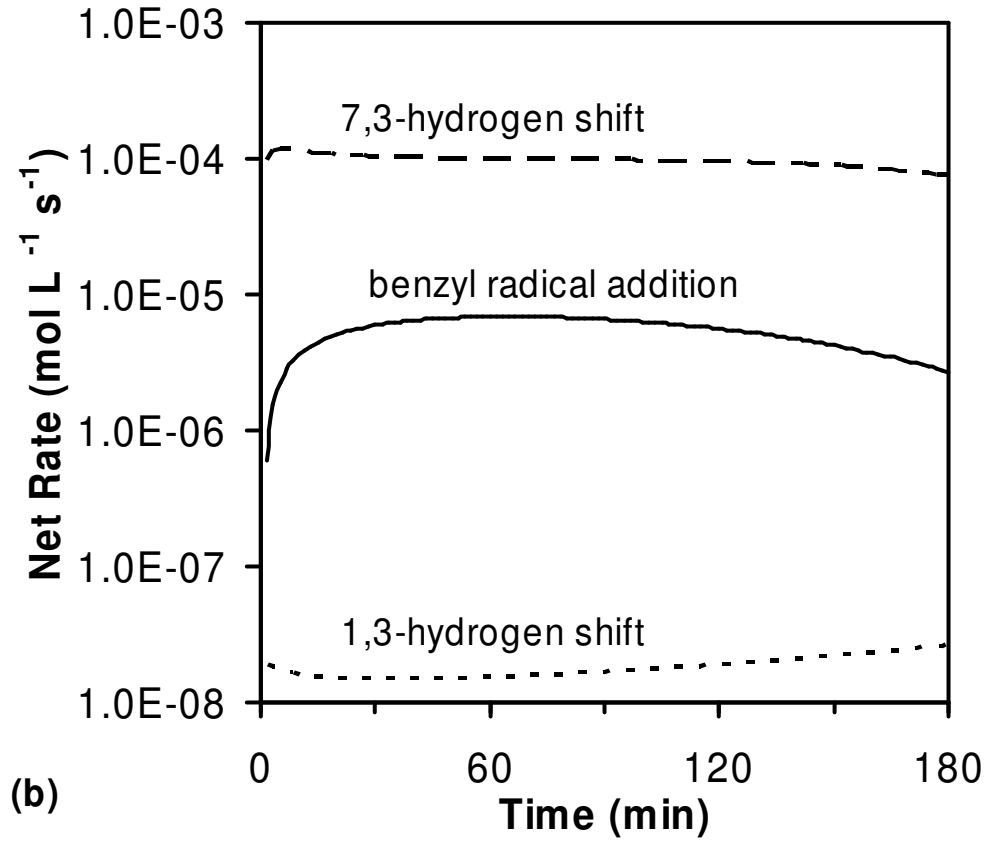

Figure 3.11: Continued.

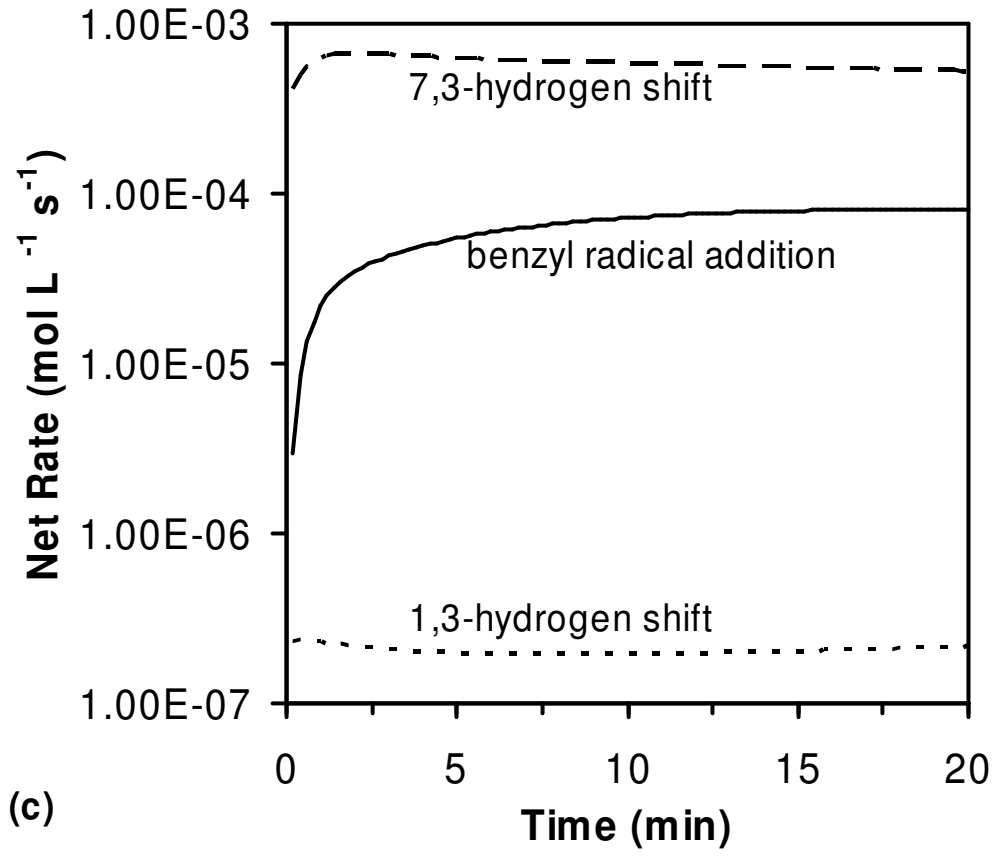

Figure 3.11: Continued

Table 3.2: Comparison of average species concentrations and rate constants for dimer formation over the temperature range from 310 to 380 °C

Temperature (°C)	Benzyl Radical Concentration[a] (mol L^{-1})	Unsaturated Tail End Concentration[a] (mol L^{-1})	7^{th} Position Mid-Chain Head Radical Concentration[b] (mol L^{-1})	$k_{benzyl\ radical\ addition}$[a] (L mol^{-1} s^{-1})	$k_{7,3\text{-}hydrogen\ shift}$[b] ($s^{-1}$)
310	4.22×10^{-13}	7.23×10^{-3}	9.33×10^{-9}	6.89×10^{6}	3.79×10^{3}
350	2.43×10^{-11}	3.52×10^{-2}	5.22×10^{-8}	8.73×10^{6}	9.50×10^{3}
380	1.97×10^{-10}	3.95×10^{-2}	1.15×10^{-7}	1.02×10^{7}	1.76×10^{4}

[a]The forward rate of the benzyl radical addition pathway is equal to $k_{benzyl\ radical\ addition} * C_{benzyl\ radical} * C_{unsaturated\ tail\ end}$.

[b]The forward rate of the 7,3-hydrogen shift pathway is equal to $k_{7,3\text{-}hydrogen\ shift} * C_{7th\ position\ mid\text{-}chain\ head\ radical}$.

of the benzyl radical addition pathway, increases by about a factor of five over the same temperature range. The concentration of mid-chain head radicals in the seventh position, which dictates the concentration-dependent portion of the rate of the 7,3-hydrogen shift pathway, only increases by a factor of approximately twelve. Thus, the more marked increase in the benzyl radical concentration is more than sufficient to compensate for the less dramatic increase in $k_{\text{benzyl radical addition}}$ compared to $k_{\text{7,3-hydrogen shift}}$ as shown in Table 3.2.

This analysis of the effect of temperature on the two primary reaction pathways to dimer formation is important because at higher temperatures the benzyl radical addition pathway may become the dominant pathway to dimer. In the work by Ohtani et al. (1990), where the benzyl radical addition pathway to dimer was proposed based on an elegant experimental study involving unlabeled PS and deuterated PS, pyrolysis was carried out at 500 °C. This is consistent with our modeling results, which suggest that benzyl radical addition will be the dominant pathway to dimer, with a minimal contribution from the 7,3-hydrogen shift pathway, at this elevated temperature. Overall, it is important to emphasize that both the 7,3-hydrogen shift pathway and the benzyl radical addition pathway are important to dimer formation during PS pyrolysis, with their relative contributions dictated by the temperature.

3.4 CONCLUSIONS

A detailed mechanistic model of polystyrene pyrolysis was developed utilizing a modeling framework based on population balances and the method of moments. The model was used to gain insight into the formation of dimer, with emphasis on the 1,3-hydrogen shift, 7,3-hydrogen shift, and benzyl radical addition pathways proposed in the literature (Moscatelli et

al. 2006; Ohtani et al. 1990; Poutsma 2006). Rate parameters were specified based on a combination of literature values and structure/reactivity correlations stemming from our previous work(Kruse et al. 2002), updated values from the literature (Moscatelli et al. 2006; Pfaendtner et al. 2006; Poutsma 2006), and parameter estimation against a limited data set. Also, greater specificity in the frequency factors for the radical addition and β-scission reaction families was included in light of recommendations by Poutsma (2006). The model and its updated parameters were validated against a wide array of experimental data sets, covering a temperature range of 100 °C and a large range of initial polymer molecular weights, and its predictive capability was demonstrated.

The validated model was then used to analyze the net rates of the competing reaction pathways to dimer. It was found that 1,3-hydrogen shift was not a competitive reaction pathway at the temperatures studied. The 7,3-hydrogen shift reaction pathway was dominant by a factor of ten or more compared to the benzyl radical addition pathway over the temperatures studied. However, the benzyl radical addition pathway became more competitive with the 7,3-hydrogen shift pathway as temperature increased due to the rapidly increasing benzyl radical concentration with temperature. Thus, the model results are consistent with the isotopic labeling studies of Ohtani et al. (1990), who proposed the benzyl radical addition pathway as the source of deuterium incorporation for pyrolysis at 500 °C. It can be concluded that the 7,3-hydrogen shift reaction pathway and the benzyl radical addition pathway are important to dimer formation during PS pyrolysis, with their relative contributions dependent on temperature.

CHAPTER 4

THE INTRINSIC ACTIVATION ENERGY OF POLYSTYRENE PYROLYSIS: A MODELING STUDY

4.1 INTRODUCTION

As the amount of municipal solid waste (MSW) generated increases each year and available landfill space dwindles, it is increasingly important to find effective recycling strategies. Polymeric materials make up a growing fraction of MSW at 11.8% (~30% by volume), while only 5.7% of this material is recycled. Polystyrene (PS) makes up 9% of plastic waste and virtually none of this post consumer waste is recycled (EPA 2006). Resource recovery, where polymeric waste is broken down by thermal or chemical techniques into valuable chemical feedstocks and monomer, is an attractive strategy for dealing with the growing amount of polymeric waste. Pyrolysis, in which the material is heated in the absence of oxygen, is an appealing resource recovery method because of its simplicity. Pyrolysis is also of interest because it can be effectively used on chain-growth polymers such as polystyrene (PS) which cannot undergo solvolysis. A greater understanding of the kinetics of polymer pyrolysis systems is important to the further development of this technology to make it a viable and economical strategy to treat polymeric waste.

Polystyrene pyrolysis has been studied for almost sixty years, starting with the pioneering work of Jellinek (1944, 1948a, 1948b, 1949a, 1949b). Throughout the long history of study of PS pyrolysis, intense effort has been put forth to understand the overall kinetics of the system as

well as the underlying mechanism. While understanding of the complexity of the chemistry has increased over time, evolving from a basic mechanism (Cameron and Kerr 1968; Jellinek 1948b; Madorsky and Straus 1948) involving random bond fission to a more detailed free-radical mechanism (Faravelli et al. 2001; Kruse et al. 2005; Kruse et al. 2002; Marongiu et al. 2007; Poutsma 2006), there are still many important aspects of PS pyrolysis which are not fully understood.

A key area of dispute in the literature is the value of the overall activation energy of PS pyrolysis. The overall activation energy is important for development of pyrolysis as a recycling strategy because it allows simple reaction models that are valuable in process design and control, where a more detailed mechanistic model is not necessary and often too slow to solve, to be utilized. The overall activation energy also offers insight into which steps in the reaction mechanism control the overall kinetics. Since Jellinek's initial work on PS pyrolysis a wide range of overall activation energies, from 19.8 to 105.1 kcal mol^{-1}, has been reported as summarized in Table 4.1 (Aguado et al. 2003; Anderson and Freeman 1961; Bockhorn et al. 1998; Cascaval et al. 1970; Fuoss et al. 1964; Jellinek 1949a; Kim et al. 2005; Kim et al. 1999; Kishore et al. 1976; Kotka et al. 1973; Kuroki et al. 1982; Madorsky 1953; Maholtra et al. 1975; Mehmet and Roche 1976; Risby and Yergey 1982). This range of over 85 kcal/mol is surprisingly large and cannot be ascribed only to experimental error.

The discrepancy seen among the values in Table 4.1 is likely due in large part to heat and mass transfer limitations confounding the intrinsic kinetics. Many of the studies reported in Table 4.1 used samples as large as a few grams, which would make them susceptible to transport effects. Problems with transport effects impacting kinetic studies of polymer degradation even when using seemingly small sample sizes has been previously documented (Szekely et al. 1987).

Table 4.1: Activation energies reported in the literature for PS pyrolysis. Note the range of over 85 kcal/mol.

Authors	Date	T (°C)	E_a (kcal/mol)
Jellinek	1950	348-400	44.9
Madorsky	1953	335-355	58.3
Anderson and Freeman	1961	246-430	46.1
		246-430	55.2 - 65.2
Fuoss et al.	1964	394	77.2
Cascaval	1970	355-810	19.8
		355-810	21.5
Kokta et al.	1973	200-500	23.9-33.4
		200-500	45.4-55.0
Kishore et al.	1976	290-390	32.0
Malhotra et al.	1975	180-390	45.2-105.1
Mehmet and Roche	1976	200-700	52.3-54.7
Bouster et al.	1980	300-400	49.0
Kuroki et al.	1982	310-390	36.3
Mertens et al.	1982	500-800	22.0
Risby et al.	1982	200-600	42.0
		200-600	39.4
Sato et al.	1983	100-600	42.3
Bockhorn and Knümann	1993	200-600	74.1
Wu et al.	1993	367-487	41.3
Westerhout et al.	1997	365-400	48.7
Bockhorn et al.	1998	360-410	41.6
Kim, Y.S. et al.	1999	370-400	53.5
Aguado et al.	2003	340-390	52.8
		500-600	19.8
		450-550	29.4
Kim, Y.C. et al.	2005	385-400	30.3
This Study	2008	286-500	53.3

The heating rate may be sufficiently slow that a steep temperature gradient in the sample exists, making data interpretation difficult, especially if there is a significant degree of degradation during the heat up period. Bubbles may also be formed in large samples, which affect the pyrolysis behavior by limiting the escape of gaseous products from the reacting melt.

The present work addressed this issue by using a mechanistic model (Kruse et al. 2005; Kruse et al. 2002; Levine and Broadbelt 2008) that is free of heat and mass transfer limitations. The objective of this study was to determine the overall activation energy for PS pyrolysis without any influence from heat and mass transfer limitations. The overall activation energy determined using our modeling techniques was then compared to values predicted using analytical Rice-Herzfeld analysis (Rice and Herzfeld 1934) of the overall kinetics to offer further insight into the complex PS pyrolysis system. The modeling framework and the analysis of kinetic data and the overall activation energy are discussed below. It is our intention to eventually utilize data collected by collaborators using a novel experimental technique that allows for rate measurements in pyrolysis systems that are free of heat and mass transport effects (Zhao and Bar-Ziv 2000; Zhao et al. 1998) to further verify the intrinsic overall activation energy determined in this study.

4.2 MODELING FRAMEWORK

4.2.1 The Method of Moments

Polymer pyrolysis involves a complex free-radical reaction mechanism consisting of thousands of species and reactions due to the fact that polymers are typically high molecular weight, polydisperse, and have many possible structural features involved during pyrolysis, as well as the numerous reaction channels available to free radicals. Therefore, it is impractical to

build an explicit model for polymer pyrolysis. To reduce the complexity and maintain a manageable model size, the method of moments was utilized, where the chain length distribution is captured by a series of values (moments), rather than explicitly including chains of every length in the model. While all the moments are needed to fully determine the chain length distribution, substantial detail can be maintained using only the first few moments (Grinstead and Laurie 1997). For example, the number average degree of polymerization and the weight average degree of polymerization for a polymer system can be determined using only the first three moments for the system (Dotson et al. 1996). Building on the work of McCoy and coworkers (Kodera and McCoy 1997; Madras et al. 1997a; Madras and McCoy 1999; Sterling and McCoy 2001), who used global rate coefficients to describe changes in the molecular weight distribution as a function of time, we have developed a framework to create detailed mechanistic models for polymer degradation systems including PS, polypropylene (PP), and binary PS-PP pyrolysis (Kruse et al. 2005; Kruse et al. 2003b; Kruse et al. 2002; Levine and Broadbelt 2008).

4.2.2 Model Assembly and Solution

To facilitate model construction, PERL scripts were devised to automatically create lists of all species, reactions in traditional form, rate constants, variables, and algebraic equations used in the model. Species are tracked in the model based on radical character (end-chain, mid-chain, dead), end units (primary or secondary carbon, saturated or unsaturated), and chain structure (linear, branched, specific low molecular weight species). For PS, reactions are created for the following elementary reaction families: (1) bond fission, (2) radical recombination, (3) hydrogen abstraction, (5) mid-chain β-scission, (6) radical addition, (7) end-chain β-scission, (8) disproportionation, and (9) hydrogen transfer (1,3-transfer, 1,5-transfer, 1,7-transfer, and 7,3-

transfer). A PERL script then transforms the traditional reaction list into population-balance equations. Moment operators are invoked to transform these reactions into terms in the moment equations for each polymeric species, comprising a set of ordinary differential equations for the zeroth, first, and second moments for each polymeric species. The concentrations of low molecular weight species are tracked explicitly with their own differential equations. The resultant set of stiff differential equations was then solved using DASSL (Petzold 1983).

The model assumes isothermal reaction conditions with no heat up time. Volatile, low molecular weight (with weight < 250 amu), non-radical species are assumed to immediately leave the reacting melt and react no further based on characteristic reaction and diffusion times at the conditions of interest. All low molecular weight radical species are assumed to react before they can leave the melt based on a similar analysis. The polymer melt is treated as a homogenous system, with no spatial concentration gradients.

4.2.3 Rate Parameter Specification

The rate parameters were specified for each reaction in the mechanistic model using the protocol we developed previously (Kruse et al. 2005; Kruse et al. 2003b; Kruse et al. 2002). Rate parameters were dependent on the reaction type and the structure of the reactants and the products. To establish this link between structure and reactivity, kinetic correlations were used. Specifically the Evans-Polanyi relationship (Evans and Polanyi 1938) (Equation 4.1):

$$E_a = E_0 + \alpha \Delta H_{rxn} \qquad (4.1)$$

was used for all reactions except for hydrogen transfer reactions, where E_a is the activation energy, E_0 is the intrinsic barrier, α is the transfer coefficient, and ΔH_{rxn} is the heat of reaction. E_0 and α are specific to the reaction family, while ΔH_{rxn} is specific to the reactants and products

of the reaction. The Evans-Polanyi relationship relates the activation energy linearly to the heat of reaction. For bimolecular hydrogen transfer reactions the Blowers-Masel relationship (Blowers and Masel 1999) (Equation 4.2) was used which was specifically developed for this family of reactions:

$$E_a = \begin{cases} 0 & \Delta H_{rxn} / 4E_0 < -1 \\ E_0 (1 + \Delta H_{rxn} / 4E_0)^2 & -1 \le \Delta H_{rxn} / 4E_0 \le 1 \\ \Delta H_{rxn} & \Delta H_{rxn} / 4E_0 > 1 \end{cases} \qquad (4.2)$$

where E_a is activation energy, E_0 is the intrinsic barrier, and ΔH_{rxn} is the heat of reaction. For intramolecular hydrogen shift reactions, specific activation energies were used based on the work of Poutsma (2006).

Arrhenius behavior was assumed for all reactions, necessitating a frequency factor and the parameters for either the Evans-Polanyi or Blowers-Masel relationship be specified for each reaction family or a specific activation energy be specified. These are determined using a hierarchical approach, first looking for applicable experimental data from the literature. In the absence of experimental data, experiments with small molecules and modeling studies of polymer mimics are used (Woo et al. 1998). To specify heats of reaction, a similar hierarchical approach is used, where experimental data is preferred and when that is not available Benson group additivity (Benson 1976) and quantum chemical calculations of small molecules that mimic the polymer are used. Recently, a detailed re-evaluation of the rate parameters for the PS pyrolysis model was conducted to study the reaction pathways to form dimer in greater detail (Levine and Broadbelt 2008). This new parameter set was used in the present study and is summarized in tabular form in Table 3.1. Using these parameters the model is able to predict

experimental results collected in our own lab (Kruse et al. 2002) and those collected in others labs (Bockhorn et al. 1998; Bouster et al. 1980).

4.2.4 Determination of Overall Reaction Rates

The PS pyrolysis model was run for a series of conditions: initial M_n of 185,000 and M_w of 203,000 at temperatures ranging from 286 to 500 °C. These initial molecular weights were utilized because they matched the M_n and M_w of the 100 μm polystyrene microspheres that will be utilized in the experimental study that our collaborators are conducting, as determined by GPC. The accuracy of the model in predicting the degradation behavior of PS pyrolysis under these basic conditions has been demonstrated previously (Kruse et al. 2005; Kruse et al. 2002).

Initial rates were used to determine the activation energy from the model, making it necessary to define a degree of degradation in the model results that would be used for initial rate calculation. To determine how significantly this choice affected the values of the rates extracted, degradation rates were determined at low molecular weight product (LMWP) mass yields of 1%, 5%, and 10%. LMWP mass yield was used as the measure of the degree of degradation since mass loss in the experimental setup of our collaborators is attributed to loss as a function of LMWP evolving out of the system. To determine the rate from the LMWP mass yield data, the LMWP mass yield was plotted as a function of time, and a line was fit centered at the percentage degradation being used to define the initial rate. For example, when 1% LMWP yield was used to define the initial rate, a line was fit to the data from ~0.5%-1.5% LMWP mass yield, with the slope of the line being equal to the overall pyrolysis rate, as shown in Figure 4.1. The range used to fit the line was chosen to give at least seven data points above and below the percentage degradation the for which the rate was being determined. All R^2 values for the linear fits were

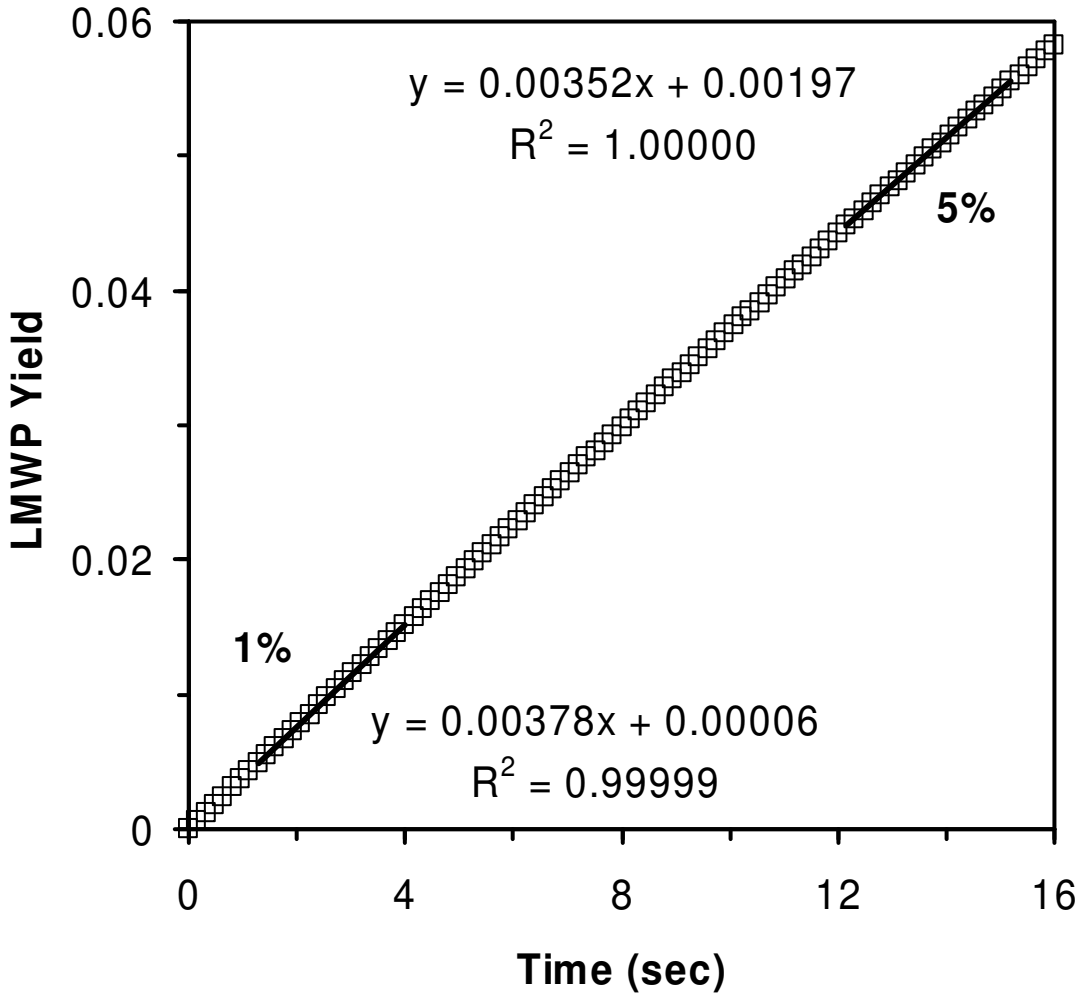

Figure 4.1: Typical figure used to determine initial rates for Arrhenius plot. This is for PS pyrolysis at 400 °C. Note the very short timescale and the minimal difference between the rates taken at 1% and 5% degradation (0.00378 mol L^{-1} s^{-1} and 0.00352 mol L^{-1} s^{-1} respectively).

above 0.999. Only small differences (typically 10-15%, with higher differences at lower temperatures) in the rate were obtained depending on what percentage of LMWP yield was used to define the initial rate. However, these differences were used to define an uncertainty for the overall activation energies reported. An Arrhenius plot using the initial rates obtained for a given LMWP yield was used to define the overall activation energy.

4.3 RESULTS AND DISCUSSION

4.3.1 Modeling Results

Three sets of modeling results were collected to create the Arrhenius plots: rates determined from 1%, 5%, and 10% degradation. All three sets of results from the model (1%, 5%, and 10% degradation) are plotted in Figure 4.2. The E_a values for the 1%, 5%, and 10% degrees of degradation were found to be 51.9, 53.6, and 54.5 kcal mol^{-1}, respectively, leading to an average overall activation energy for PS pyrolysis of 53.3 $\pm$ 1.3 kcal mol^{-1}, with the uncertainty equal to the standard deviation of the three values. Note that the value of E_a we have obtained falls squarely among the values in Table 4.1 and helps clarify which of these values are not based on intrinsic kinetics.

4.3.2 E_a Analysis

To obtain a better understanding of the kinetic origins of this activation energy, it is useful to compare it to the typical activation energies for the reactions in the PS pyrolysis mechanism. Early on in the study of polymer pyrolysis, bond fission was thought to be the controlling reaction (Jellinek 1944, 1948a, 1948b, 1949a, 1949b). Bond fission for carbon-carbon bonds in the PS backbone is characterized by an activation energy of 67.3 kcal

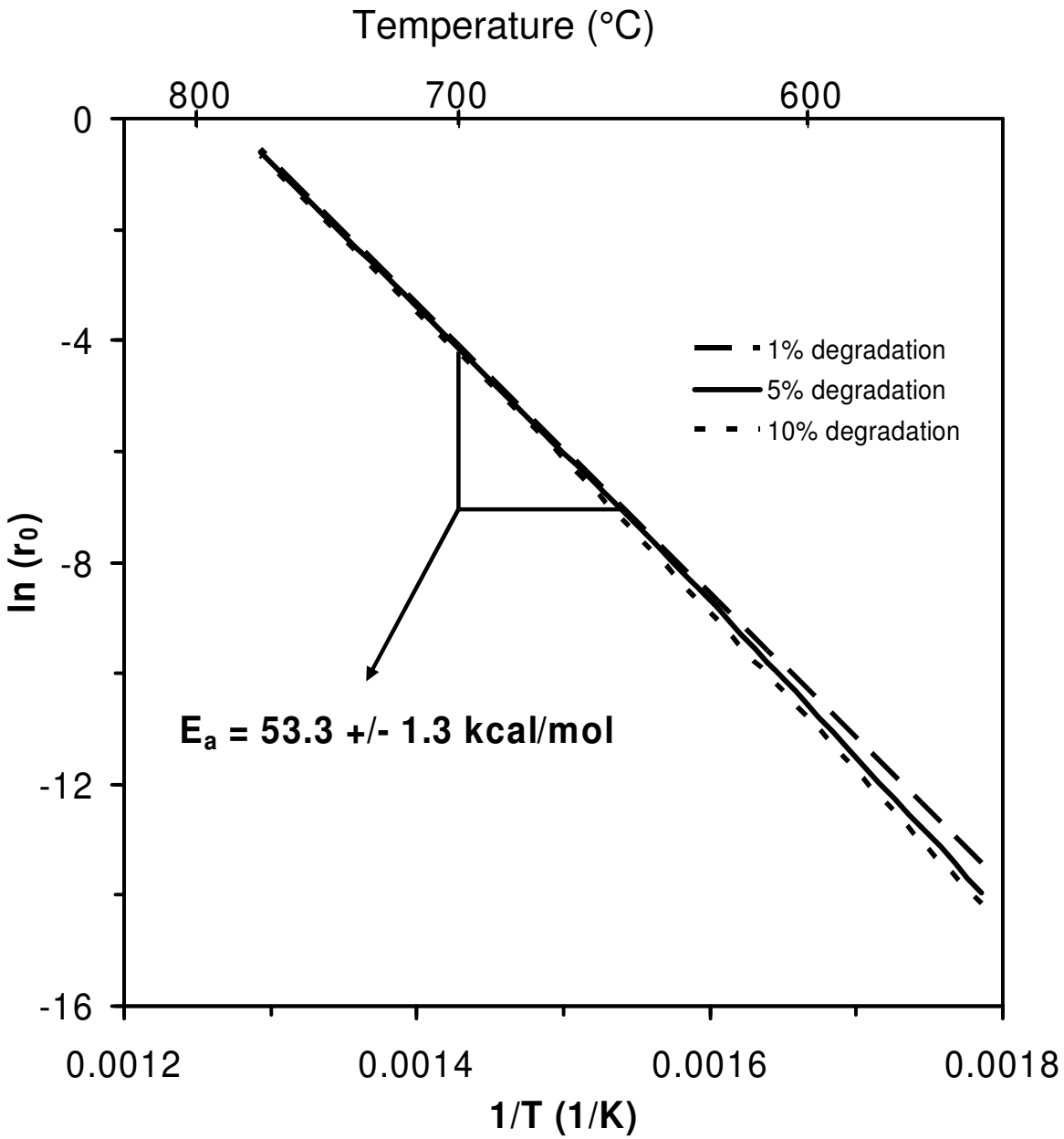

Figure 4.2: Arrhenius plot of modeling initial rates of polystyrene degradation (taken at 1, 5, and 10% degradation from the model). The Arrhenius plot gives an overall activation energy of 53.3 +/- 1.3 kcal/mol (the error is based on small changes in rate depending on what degree of degradation is used).

mol^{-1} (Aguado 1999). Thus, this reaction alone is not the controlling reaction for the PS pyrolysis process. Since free-radical chemistry is characterized by initiation, propagation, and termination reactions, it is likely that a combination of these reactions controls the degradation rate and thus defines the overall activation energy.

To further analyze the activation energy for PS pyrolysis, a Rice-Herzfeld kinetic analysis (Rice and Herzfeld 1934) was performed on a simplified mechanism for polymer pyrolysis. The simplified mechanism included seven reactions: (1) bond fission, (2) radical recombination, (3) hydrogen abstraction, (4) end-chain β-scission, (5) backbiting (hydrogen shift), (6) mid-chain β-scission, and (7) β-scission to form low molecular weight products. The system included six species: (1) dead polymer chains, (2) end-chain radicals, (3) mid-chain radicals, (4) monomer (formed via end-chain β-scission), (5) specific position mid-chain radicals which are formed via backbiting, and (6) LMWP other than monomer which is formed via reaction 7 in the simplified mechanism. Invoking the pseudo-steady state approximation and using general activation energies taken from our detailed PS pyrolysis model for corresponding reactions, analytical expressions for the rate of styrene formation and for the rate of other LMWP formation were obtained as shown in equations 4.3 and 4.4, where r_{sty} is the rate of styrene formation, r_{LMWP} is the rate of other LMWP formation, $k_{E-\beta}$ is the rate constant for end-chain β-scission, k_i is the rate constant for initiation (bond fission), k_t is the rate constant for termination (radical recombination), k_{BB} is the rate constant for backbiting (1,5-hydrogen shift) and D is the concentration of dead polymer.

$$r_{sty} = k_{E-\beta}\left(\frac{k_i D}{k_t}\right)^{1/2} \qquad (4.3)$$

$$r_{LMWP} = k_{BB}\left(\frac{k_i D}{k_t}\right)^{1/2} \qquad (4.4)$$

Based on values of E_a for recombination of 2.3 kcal mol^{-1}, backbiting of 16.2 kcal mol^{-1}, and end-chain β-scission of 23.9 kcal mol^{-1}, overall activation energies for the formation of styrene monomer of 56.4 kcal mol^{-1} and other LMWP of 48.7 kcal mol^{-1} were obtained. Our value of 53.3 kcal mol^{-1} sits in the middle of these two analytical values. Neither of these analytical activation energies is a measure of the overall activation energy because overall conversion is from polymer to all LMWP (both styrene and the other products), but it would be expected that the overall activation energy would be in the same range as these two more specific activation energies. While the simplified system used to obtain this analytical value leaves out many details of the actual pyrolysis system, for example it neglects molecular weight decay and polydispersity, lumps all non-styrene products together with no difference in how they are formed, and utilizes the pseudo-steady state assumption, it clearly demonstrates the origin of the value of our activation energy which is free from transport limitations. It also can be used to focus on details in the mechanistic model that are controlling for overall PS degradation and for product formation. The Rice-Herzfeld analysis indicates the importance of the reaction pathways to LMWP formation to the overall kinetics of the PS pyrolysis system.

This study's intrinsic activation energy of 53.3 kcal mol^{-1} allows for more detailed understanding of which previous experimental works are hindered by transport effects. Most of the values in Table 4.1 for overall polystyrene pyrolysis are lower than our value of 53.3 kcal mol^{-1} which is expected because activation energies of transport processes are lower then kinetically controlled activation energies. There is also a group of values that is in very good agreement with our activation energy which leads to the conclusion that these studies were able

to minimize heat and mass transport effects on their kinetic data. The values that our much larger than our value most likely have some other source of experimental error besides transport limitations that complicated these kinetic results.

4.4 CONCLUSIONS

We have developed and utilized a detailed mechanistic modeling framework for studying polymer pyrolysis. This framework was applied to PS pyrolysis over a wide range of temperatures. PS pyrolysis is of particular interest because it is a potential solution for recovering value from a voluminous portion of polymer solid waste. PS pyrolysis also has a long history of debate over the overall activation energy for the system, with a reported range of over 85 kcal mol^{-1}. Our detailed mechanistic model, which includes no heat or mass transfer limitations, for PS pyrolysis was utilized to obtain initial rate data that was utilized to calculate an intrinsic activation energy. The point of degradation (1-10%) at which the initial rate was determined from the model was found to have minimal impact on the value of the rate obtained, and the small differences are reflected in the uncertainty reported for the activation energy obtained from the model results.

An Arrhenius plot was created from the modeling results which yielded an overall activation energy for PS pyrolysis of 53.3 +/- 1.3 kcal mol^{-1}. As this value comes from a study which is free from heat and mass transfer effects, can be characterized as the definitive kinetic value for PS pyrolysis. Further analysis of this activation energy indicates that no single reaction family is controlling of the overall system. Rice-Herzfeld kinetic analysis of a simplified PS pyrolysis system with basic assumptions yields activation energies of 56.4 kcal mol^{-1} and 48.7 kcal mol^{-1} for styrene and other LMWP formation, respectively, which bracket the value we

determined from the detailed mechanistic model. The Rice-Herzfeld analysis indicated the importance of the reaction pathways to LMWP formation to the overall kinetics of the system. Our intrinsic activation energy allows for an understanding of how experimental studies are affected by heat and mass transport effects. The values determined from our model will be further verified utilizing the results of our collaborators' experimental study using an apparatus and technique that allows for pyrolysis which is free of heat and mass transport limitations.

CHAPTER 5

DETAILED MECHANISTIC MODELING OF HIGH-DENSITY POLYETHYLENE PYROLYSIS: LOW MOLECULAR WEIGHT PRODUCT EVOLUTION

5.1 INTRODUCTION

Polymeric materials have become essential to everyday life, being used in a variety of applications from packaging to construction to electronics. With their increasing use, the amount of polymeric materials in municipal solid waste (MSW) is becoming a growing problem. In 2005 polymeric waste made up 11.8% by weight of all MSW, yet only 5.7% of this waste was recycled (EPA 2006). With the majority of polymeric waste being landfilled coupled with a decreasing amount of available landfill space, developing effective recycling techniques for polymers is important. Resource recovery of polymeric waste is a promising, attractive method of recycling polymers, where thermal or chemical methods are used to convert the polymeric waste into valuable chemical feedstocks and monomer. Pyrolysis, heating the material in the absence of oxygen, is a promising resource recovery method because of its simplicity and ability to handle a heterogeneous feedstock like that of polymeric waste.

High-density polyethylene (HDPE) is a major component of polymeric waste, making up 20.4% (EPA 2006). It is also one of the most recycled segments of polymeric waste, with just under 9% of waste HDPE recycled (EPA 2006). The majority of the recycled HDPE is

reprocessed. Reprocessing of polymeric waste, while a well-established technology, requires expensive sorting of the polymeric waste and there are limited applications for the reprocessed polymer (Aguado 1999). Further development of resource recovery in general and pyrolysis techniques specifically is critical to increase the total amount of HDPE recycled. A greater understanding of the kinetics and mechanism of HDPE pyrolysis is needed to continue the development of this important technology.

Polymer pyrolysis mechanisms are characterized by large and complex free-radical reaction networks. The high molecular weight and polydispersity of most polymers cause their pyrolysis reaction networks to often involve thousands of species and reactions. This complexity often yields a diverse product spectrum (Scheirs and Kaminsky 2006). Understanding the interplay of the reactions comprising this complex mechanism and specifically how the products are formed is critical to improving polymer pyrolysis technologies. The complexity of the pyrolysis chemistry makes it difficult to utilize experimental methods to gain detailed mechanistic insight. Mechanistic models are important tools for gaining insight into the complex mechanisms of polymer pyrolysis.

Polyethylene pyrolysis has a long history of research (Jellinek 1949a; Madorsky et al. 1949; Wall et al. 1954), but there are still unresolved questions surrounding the mechanism and kinetics, most likely stemming from the difficulty analyzing the broad product spectrum (Poutsma 2003). The importance of both inter- and intramolecular hydrogen transfer reactions in the mechanism was recognized early in the study of polyethylene pyrolysis (Wall et al. 1954). Additional studies have attempted to look into the competition between inter- and intramolecular hydrogen transfer reactions (Kiran and Gillham 1976; Seeger and Cantow 1975; Tsuchiya and

Sumi 1968a, 1968b), but their conclusions about the relative importance of the two reaction families are inconsistent.

Polymer pyrolysis usually involves three general reaction pathways to product formation. Unzipping (UZ), or successive end-chain β-scission reactions, yields monomer from the polymer chain. UZ can be seen as the reverse of ideal free-radical polymerization. Backbiting (BB) involves specific intramolecular hydrogen transfer reactions followed by mid-chain β-scission to yield a series of specific low molecular weight products (LMWP). The products obtained from BB pathways are often referred to as non-statistical products because the formation of some products is favored over the formation of others based on the ease of different intramolecular hydrogen transfer reactions. Random scission (RS) involves intermolecular hydrogen transfer followed by mid-chain β-scission to yield a diverse array of LMWP. RS products are often referred to as statistical products because every product has an equal probability to be formed, since each abstractable hydrogen of a given type (e.g., benzylic, secondary, tertiary) on a polymer backbone is equally available as a target for intermolecular hydrogen transfer. Polyethylene is especially susceptible to both BB and RS pathways because every mid-chain hydrogen yields an equally stable secondary carbon radical. Understanding the competition between RS and BB is important for fully understanding the polyethylene pyrolysis mechanism.

There have been multiple, previous mechanistic modeling studies of polyethylene pyrolysis. Sezgi and coworkers (1998) utilized the method of moments to develop a model which focused on predicting the evolution of the molecular weight distribution during pyrolysis. Their model used lumped reactions to model the formation of LMWP so specific product yields were not predicted. Faravelli and coworkers, in a series of studies, developed multiple versions of a mechanistic model for polyethylene pyrolysis (Faravelli et al. 1999; Marongiu et al. 2007;

Ranzi et al. 1997). Initially, their model only included random scission pathways. This model was developed with a focus on the evolution of the total product yield (Ranzi et al. 1997). This model was improved with the addition of backbiting reactions allowing for more detailed product distributions to be modeled, focusing on final specific product yields (Faravelli et al. 1999). In their most recent modeling work, Faravelli and coworkers presented some analysis of the competition between RS and BB in PE pyrolysis, indicating that RS in more important for product formation (Marongiu et al. 2007). Mastral and coworkers (2007) developed a model for high temperature pyrolysis of polyethylene which included the formation of aromatics, which is often considered a secondary reaction, and utilized lumped product groups. Mastral and coworkers did not distinguish between intra- and intermolecular hydrogen transfer, which prohibited analysis of the competition between RS and BB pathways. Poutsma (2003) utilized a Monte Carlo model for the partitioning of radicals to look into the competition between UZ, BB, and RS. The Poutsma model showed that UZ was minimally important compared to BB and RS. Poutsma also concluded that both RS and BB are important for LMWP formation but that the exact competition between them is extremely difficult to determine.

In this study we have utilized our modeling framework, which has previously been applied to polystyrene pyrolysis (Kruse et al. 2003c; Kruse et al. 2001; Kruse et al. 2002; Levine and Broadbelt 2008), polypropylene pyrolysis (Kruse et al. 2003b), and binary pyrolysis of polystyrene and polypropylene (Kruse et al. 2005), to develop a detailed mechanistic model for HDPE pyrolysis. This model tracks important structural detail and links chemical structure to reactivity, allowing the model to track the formation of a broad range of LMWP. The model allows the tracking of the evolution of specific products over the course of pyrolysis, providing insight into the mechanism of formation of specific products.

5.2 MODELING FRAMEWORK

5.2.1 Level of Detail

The thousands of species and reactions in polymer pyrolysis, caused by the high molecular weight and polydisperse nature of polymers as well as the many possible structural features and numerous reaction channels available to free radicals, make constructing an explicit model computationally difficult. To achieve a high level of detail while still maintaining a reasonable model size, the method of moments is utilized to capture details about the chain length distribution as a series of moments instead of tracking every possible chain in the system. To fully capture the chain length distribution an infinite number of moments would be needed, but substantial detail can be maintained by tracking only the zeroth, first, and second moments (Grinstead and Laurie 1997). The method of moments has often been utilized for polymerization modeling (Dotson et al. 1996) and has been increasingly applied to polymer degradation systems in the past ten years. Building on the work of McCoy and coworkers (Kodera and McCoy 1997; Madras and McCoy 1999; McCoy 1993; Sterling and McCoy 2001; Wang et al. 1995), who used global rate coefficients in a method of moments model to describe changes in the molecular weight distribution as a function of time, we have developed a modeling framework based on the method of moments to develop detailed mechanistic models for polymer reaction systems. This framework has been previously applied to a variety of polymer pyrolysis systems (Kruse et al. 2005; Kruse et al. 2003b, 2003c; Kruse et al. 2001; Kruse et al. 2002; Levine and Broadbelt 2008) as well as the living free-radical polymerization of polystyrene (Kruse et al. 2003a).

To maintain a high level of detail while using the method of moments, polymeric species are tracked using the first three moments and distinguished based on the structural characteristics of the chain. The structural characteristics tracked in the HDPE model are shown in Figure 5.1

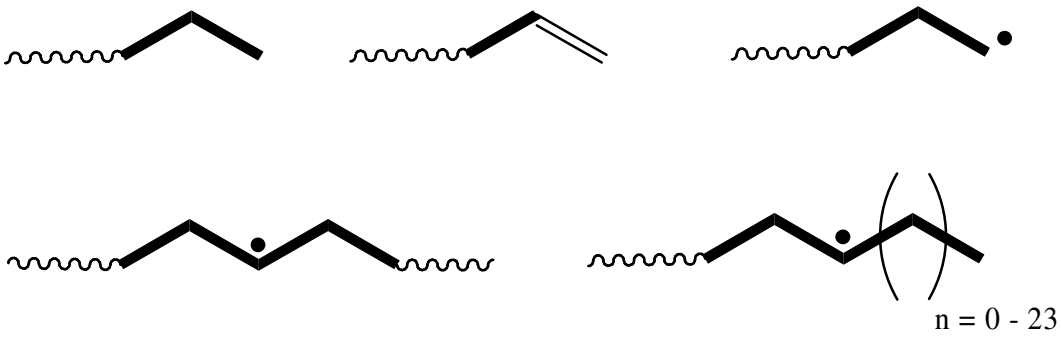

Figure 5.1: Structural detail used to distinguish polymeric species tracked in the model.

and include saturated and unsaturated end groups, end-chain radicals, general mid-chain radicals, and specific mid-chain radicals from the 2nd to the 25th position. Low molecular weight products (LMWP) and low molecular weight radicals (LMWR) are tracked explicitly. LMWP tracked included all alkanes from methane (C1) up to n-tricosane (C23) and alkenes from ethylene (C2=) up to 1-hexacosene (C26=). Tables 5.1 and 5.2 show the 23 alkane and 25 alkene products, respectively, tracked in the model and abbreviations used in this work.

The mechanistic chemistry is described by allowing all the species in the system to react according to a set of elementary reaction families before the method of moments is applied. For HDPE pyrolysis the following elementary reaction families were included in the model: (1) bond fission, (2) radical recombination, (3) allyl bond fission, (4) hydrogen abstraction, (5) mid-chain β-scission, (6) radical addition, (7) end-chain β-scission, (8) disproportionation, (9) 1,4-hydrogen shift, (10) 1,5-hydrogen shift, (11) 1,6-hydrogen shift, (12) 1,7-hydrogen shift, (13) x,x+3-hydrogen shift, (14) x,x+4-hydrogen shift, and (15) x,x+5-hydrogen shift. These reactions are depicted in Figure 5.2. Combining the above reaction families and the method of moments, a detailed representation of the mechanistic chemistry was created.

β-scission reactions are the primary routes to LMWP formation. The UZ pathway forms ethylene (C2=) through end-chain β-scission. The other LMWP are formed via mid-chain β-scission of the specific mid-chain radicals. The mid-chain β-scission products of each specific radical are depicted in Figure 5.3. The n+1 alkene product is formed directly from the β-scission of the nth position mid-chain radical. The n-2 alkyl radical is also formed by β-scission of the nth position mid-chain radical, which can then form the n-2 alkane by abstracting hydrogen from another polymer chain.

Table 5.1: Alkane species tracked in the HDPE mechanistic model

Species	Product Label
methane	C1
ethane	C2
propane	C3
n-butane	C4
n-pentane	C5
n-hexane	C6
n-heptane	C7
n-octane	C8
n-nonane	C9
n-decane	C10
n-undecane	C11
n-dodecane	C12
n-tridecane	C13
n-tetradecane	C14
n-pentadecane	C15
n-hexadecane	C16
n-heptadecane	C17
n-octadecane	C18
n-nonadecane	C19
n-eicosane	C20
n-heneicosane	C21
n-docosane	C22
n-tricosane	C23

Table 5.2: Alkene species tracked in the HDPE mechanistic model

Species	Product Label
ethylene	C2=
propylene	C3=
1-butene	C4=
1-pentene	C5=
1-hexene	C6=
1-heptene	C7=
1-octene	C8=
1-nonene	C9=
1-decene	C10=
1-undecene	C11=
1-dodecene	C12=
1-tridecene	C13=
1-tetradecene	C14=
1-pentadecene	C15=
1-hexadecene	C16=
1-heptadecene	C17=
1-octadecene	C18=
1-nonadecene	C19=
1-eicosene	C20=
1-heneicosene	C21=
1-docosene	C22=
1-tricosene	C23=
1-tetracosene	C24=
1-pentacosene	C25=
1-hexacosene	C26=

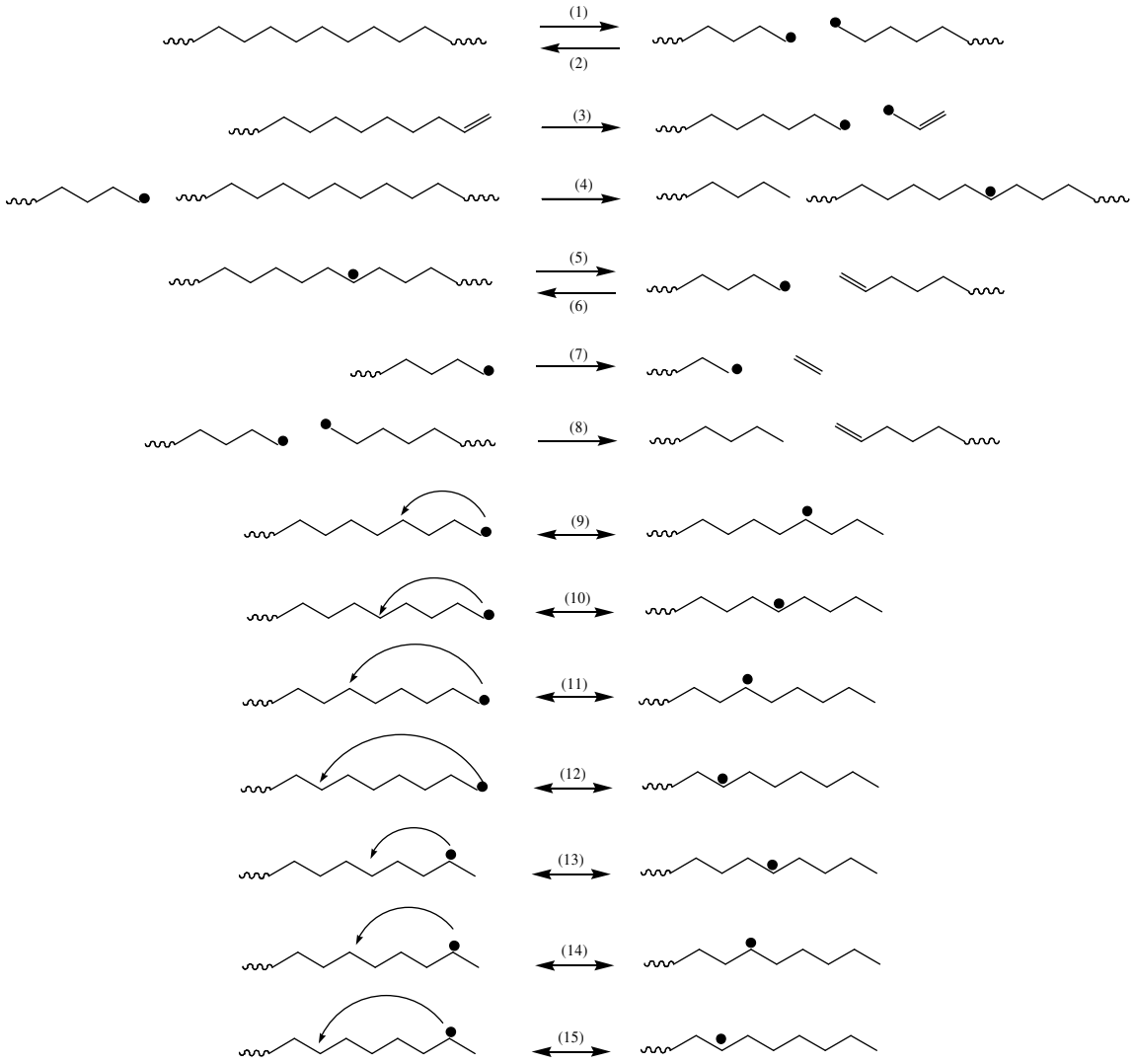

Figure 5.2: Reaction families included in the mechanistic model for HDPE.

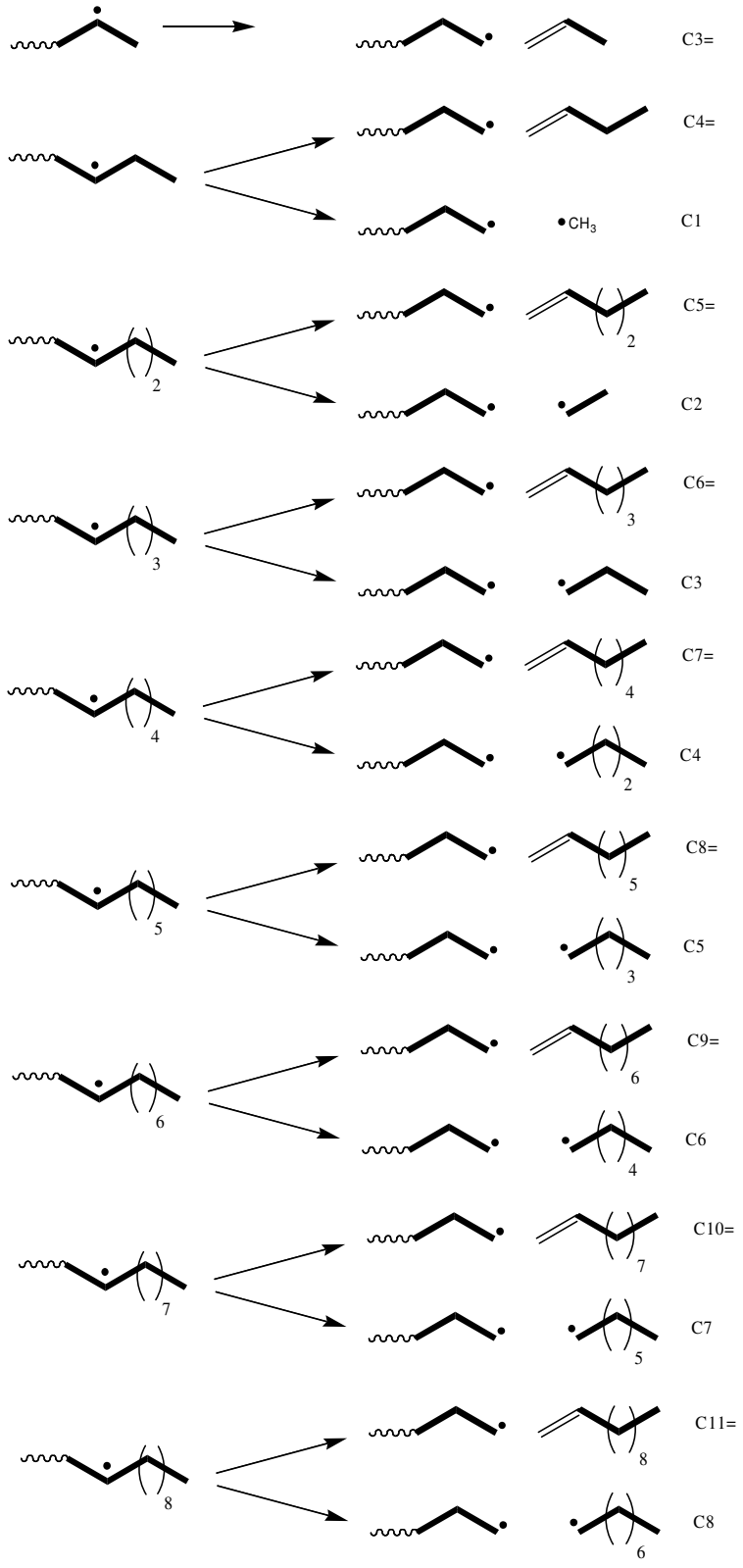

Figure 5.3: β-scission products of specific mid-chain radicals during HPDE pyrolysis

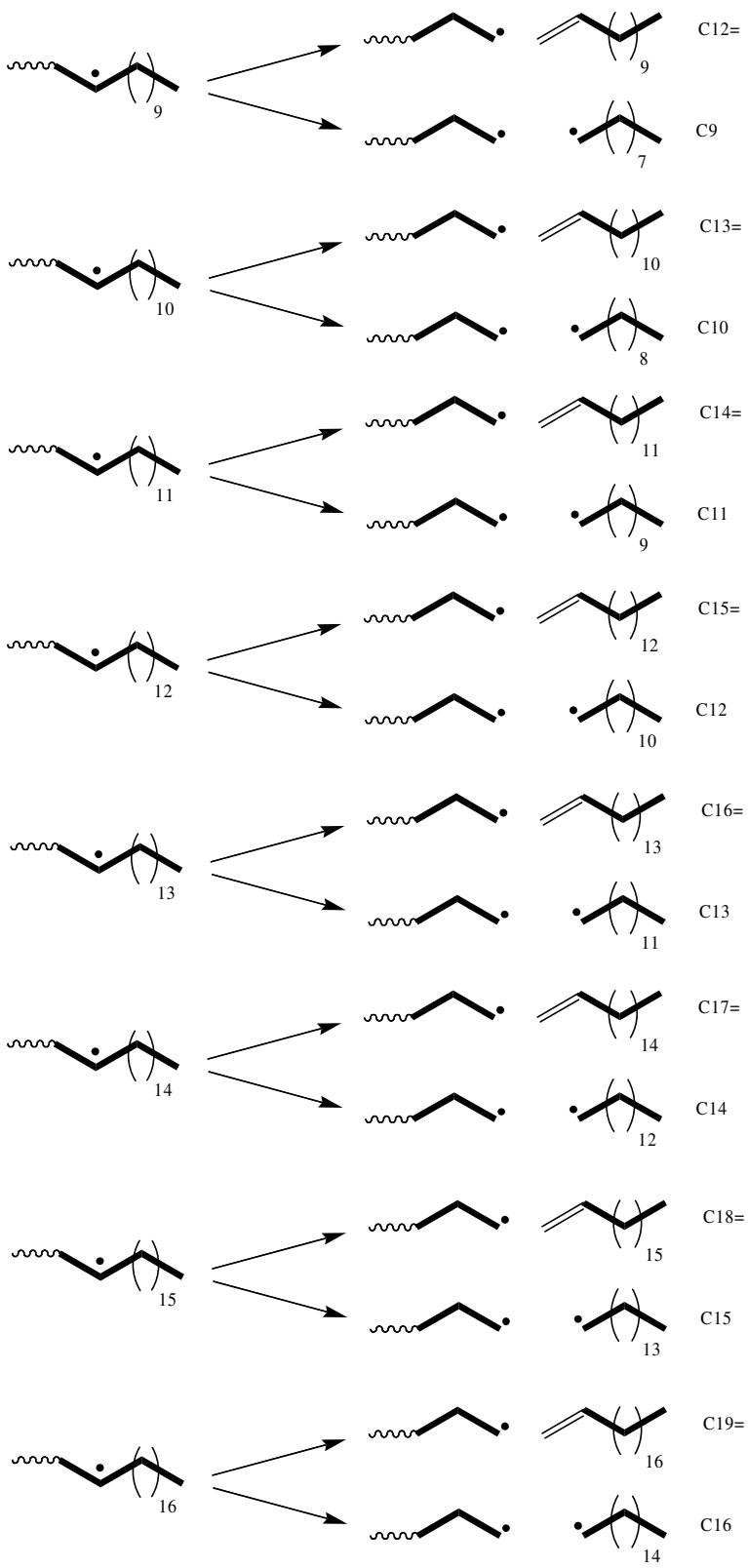

Figure 5.3: Continued

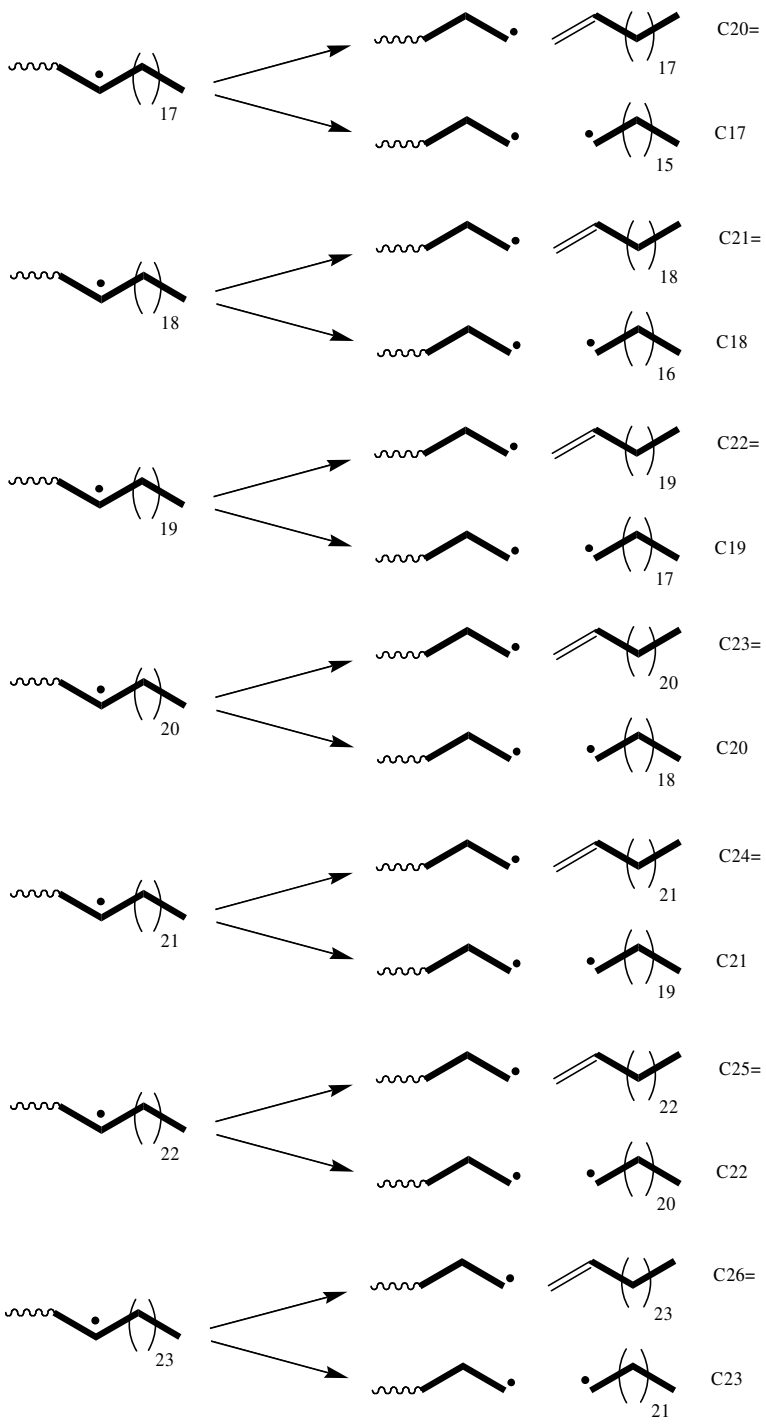

Figure 5.3: Continued

5.2.2 Specification of Rate Constants

The procedure for assigning rate constants to each reaction in the mechanistic model was developed in previous modeling work in our research group (Kruse et al. 2005; Kruse et al. 2003b; Kruse et al. 2001; Levine and Broadbelt 2008). The rate parameters were related to both the reaction type and the structure and thermodynamics of the reactants and products involved. To institute this link between structure and reactivity, the Evans-Polanyi relationship (Evans and Polanyi 1938) and the Blowers-Masel relationship (Blowers and Masel 1999) were used. The Evans-Polanyi relationship was used for all reactions other than intra- and intermolecular hydrogen transfer. The Blowers-Masel relationship was used for intermolecular hydrogen transfer. Specific activation energies were specified based on the recent estimations in the literature for all intramolecular hydrogen transfer reactions (Marongiu et al. 2007; Poutsma 2003).

For all reactions Arrhenius behavior was assumed, requiring a frequency factor and either a specific activation energy or the parameters for the Evans-Polanyi or Blowers-Masel relationship be specified for each reaction family. Table 5.3 summarizes the kinetic parameters utilized in the model. The Evans-Polanyi and Blowers-Masel parameters were taken from our previous work (Kruse et al. 2005; Kruse et al. 2003b; Kruse et al. 2002; Levine and Broadbelt 2008). The frequency factors for intra- and intermolecular hydrogen transfer were adapted from the work of Poutsma (2003) and Faravelli and coworkers (Marongiu et al. 2007). The frequency factors for bond fission, radical recombination, and disproportionation were taken from our previous work (Kruse et al. 2003b). For radical addition, the frequency factor was adapted from experimental polymerization results (Beuermann and Buback 2002). Finally, the frequency factors for the β-scission reactions were obtained by parameter estimation. These three

Table 5.3: Representative values of the kinetic and thermodynamic values utilized in the HDPE pyrolysis mechanistic model

Reaction Type	Frequency factor, A (s^{-1} or L mol^{-1} s^{-1})	Intrinsic barrier, E_0 (kcal mol^{-1}) [a]	Transfer coefficient, α[a]	Representative ΔH_{rxn} (kcal mol^{-1}) [f]	Activation Energy (kcal mol^{-1})
Chain fission	$1.00x10^{16}$ [a]	2.3	1	87.36	89.66
Allyl chain fission	$1.00x10^{16}$ [a]	2.3	1	72.9	75.2
Radical recombination	$1.10x10^{11}$ [a]	2.3	0	-87.36	2.3
Disproportionation	$1.10x10^{10}$ [a]	2.3	0	NA	2.3
End-chain β-scission	$1.32x10^{13}$ [b]	11.4	0.76	22.35	28.39
Mid-chain β-scission	$5.35x10^{14}$ [b]	11.4	0.76	23.03	28.90
β-scission to LMWS [g]	$2.33x10^{13}$ [b]	11.4	0.76	22.97	28.86
Radical addition	$2.88x10^{7}$ [c]	11.4	0.24	-23.03	5.87
Hydrogen abstraction	$2.75x10^{8}$ [d]	12.0	NA	-1.57	11.23
1,4-hydrogen shift	$1.58x10^{11}$ [d]	NA	NA	NA	20.8 [d]
1,5-hydrogen shift	$1.82x10^{10}$ [d]	NA	NA	NA	13.7 [d]
1,6-hydrogen shift	$1.05x10^{10}$ [d]	NA	NA	NA	18.3 [d]
1,7-hydrogen shift	$3.00x10^{9}$ [e]	NA	NA	NA	18.3 [e]
x,x+3-hydrogen shift	$1.00x10^{11}$ [d]	NA	NA	NA	21.2 [d]
x,x+4-hydrogen shift	$1.26x10^{10}$ [d]	NA	NA	NA	14.7 [d]
x,x+5-hydrogen shift	$7.24x10^{9}$ [d]	NA	NA	NA	18.1 [d]

[a]Values taken from our previous modeling work (Kruse et al. 2003b)
[b]Values obtained using parameter estimation
[c]Value adapted from polymerization experimental value (Beuermann and Buback 2002)
[d]Values adapted from estimations of Poutsma (2003) and Faravelli and coworkers (Marongiu et al. 2007)
[e]Values adapted based on our previous work (Levine and Broadbelt 2008) and the work of Poutsma (2006, 2003)
[f]All heats of reaction taken from literature values or estimated using Benson group additivity (Benson 1976)
[g]β-scission to low molecular weight species (LMWS) is defined as β-scission of a mid-chain radical resulting in the formation of a species with molecular weight <364 amu

frequency factors were obtained by regressing the model results using GREG (Stewart et al. 1992) against isothermal pyrolysis data for HDPE at 420 °C previously obtained in our lab (De Witt and Broadbelt 2000). The data set used in this work included yield results at 30, 90, and 150 minutes for alkanes ranging from C1 to C23 and alkenes from C2= to C23=. There were results reported for lumped species with carbon numbers above C_{23}, but it was noted in the original experimental study that they were not reliable. It should also be noted that n-hexane, 1-hexene, n-heptane, and 1-heptene yields were not reported in the experimental study due to these species being impurities in the solvent used for product extraction. The reported results for n-pentane and 1-pentene were also seen to be inaccurate due to experimental difficulties isolating these species (De Witt and Broadbelt 2000). Thus, the parameter estimation excluded the n-pentane and 1-pentene results. No molecular weight decay information was available for this study. The initial M_w of the HDPE used in the experimental study was known to be 125,000, but the initial M_n was unknown, so a polydispersity of two was assumed, giving an initial M_n of 62,500 which was used in the model. The model results changed minimally if the initial polydispersity was assumed to be 1.5.

5.2.3 Model Assembly and Solution

PERL scripts have been developed to automate model construction to aid in handling the large number of species and reactions in our pyrolysis models. The PERL scripts create lists of reactions in traditional form, species, rate constants required, variables, and algebraic equations utilized in the model. The PERL scripts create these lists based on the specific structural features included in the model, Figure 5.1, and the rules governing the elementary reaction families included in the model, Figure 5.2. The PERL scripts then convert the reaction list into

population balances using moment operations to obtain moment equations based on the reaction terms for each polymeric species. Each polymeric species is described by differential equations for the zeroth, first, and second moments. This process yields a set of stiff differential equations and algebraic equations which was solved using DASSL (Petzold 1983). The final model tracked 151 species and included over 11,000 reactions. The model is solved assuming isothermal conditions. For this modeling study species with molecular weight <364 amu were assumed to be volatile and immediately leave the reacting melt. All LMWR were assumed to react before they could diffuse out of the melt based on analysis of the relative time scales for reaction and diffusion. The reacting polymer melt was treated as a homogeneous system, with no spatial concentration gradients.

5.3 RESULTS AND DISCUSSION

5.3.1 Full LMWP Spectrum

A product spectrum of 48 products was tracked in the mechanistic model. The experimental data utilized in this modeling study included reliable values up to a carbon number of C_{23} for both alkane and alkene products. The experimental values for species with carbon numbers between C_5 and C_7 were either absent or not reliable and have been excluded from comparison to the model results. Figure 5.4 shows the comparison of the model results to the experimental data for the alkene molar yields for condensable products (C8= and higher) at degradation times of 30, 90, and 150 minutes. Molar yields are defined as moles of a product formed per initial moles of HDPE chains. The agreement between the experimental and model values for the condensable alkene molar yields is excellent. The model results are within a factor

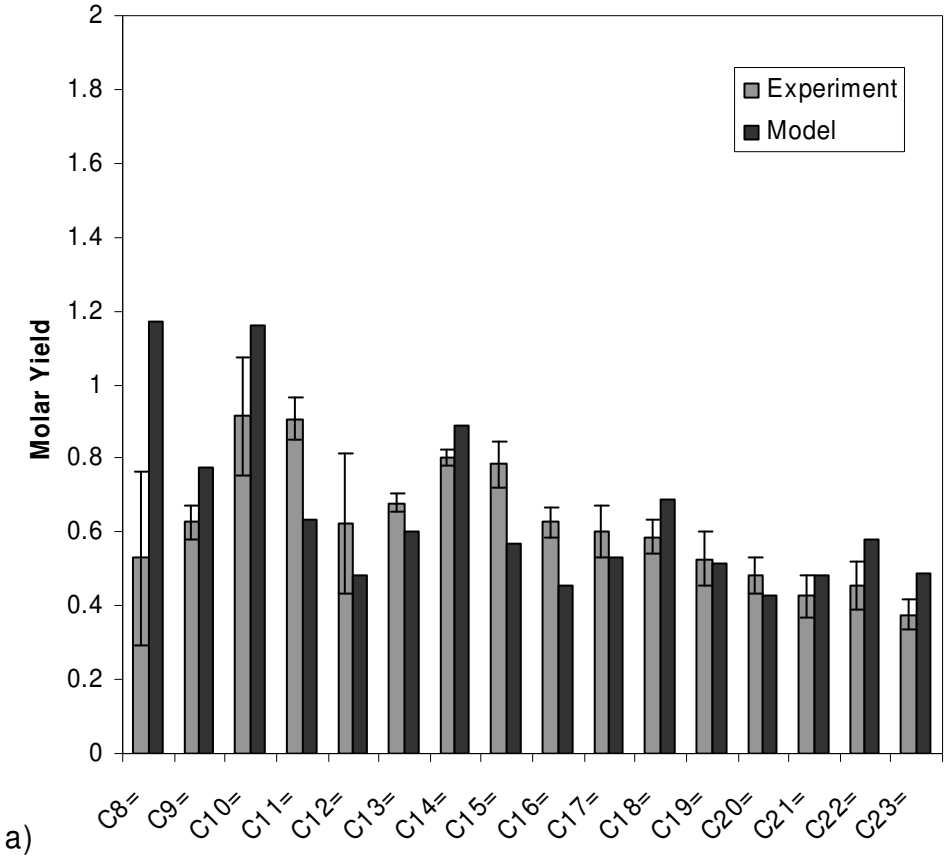

a)

Figure 5.4: Comparison of experimental and model condensable alkene yields for 125,000 M_{w0} HDPE pyrolysis at 420 °C after a) 30 min, b) 90 min, and c) 150 min of degradation. The error bars on the experimental data reflect the standard deviation of the molar yields reported for three different initial HDPE loadings in the experimental study.

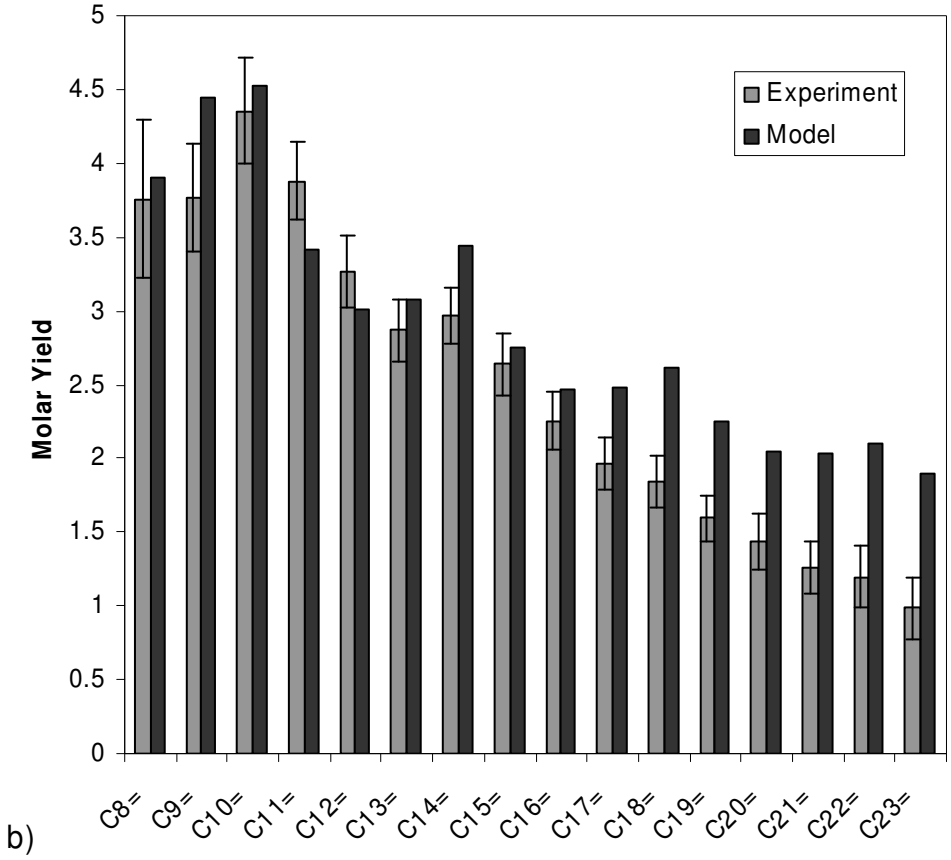

b)

Figure 5.4: Continued

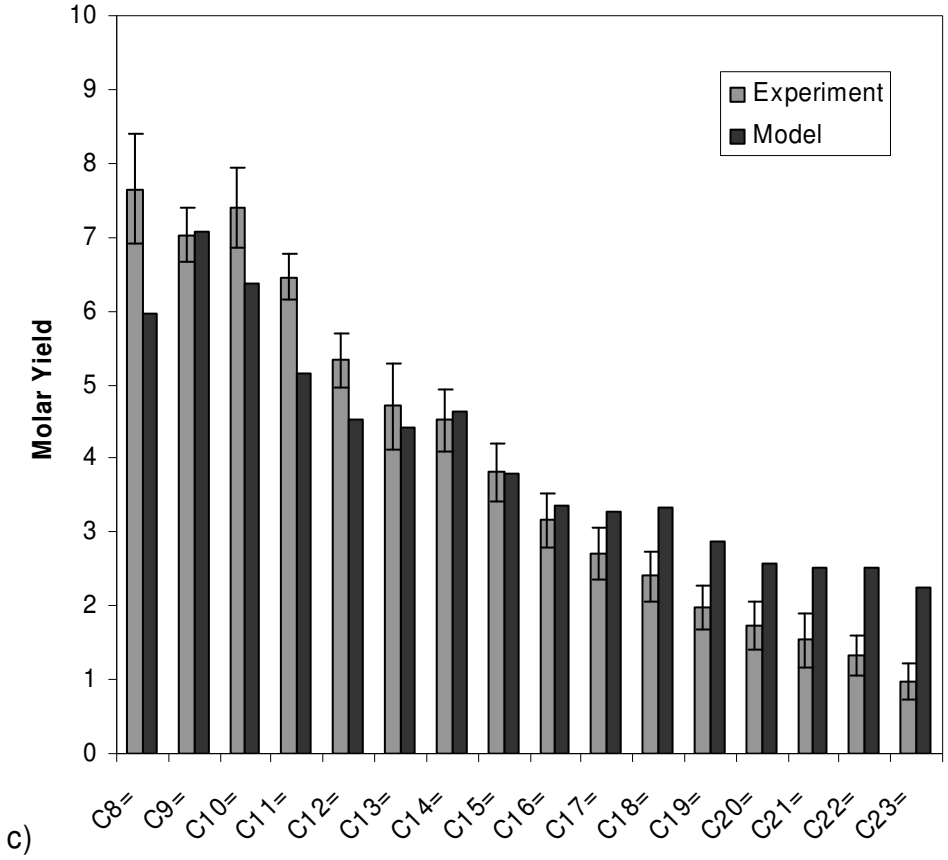

c)

Figure 5.4: Continued

of 1.35 of the corresponding experimental results, with the exception of only two data points in which the model yield was off by over a factor of two compared with the experimental result. In general, the model results nicely capture the peaked product spectrum observed experimentally, characteristic of successive x,x+4-hydrogen shift reactions. The model results also follow the decline in product yield with increasing carbon number. This behavior is more pronounced at longer times, although the decrease in the model results is not quite as marked as that observed experimentally.

The condensable alkane molar yields (C8 and above) at degradation times of 30, 90, and 150 minutes for the experimental and model results are compared in Figure 5.5. The model and experimental values are in excellent agreement. The model results are within a factor of 1.3 of the corresponding experimental results for all data points except in one instance in which the model yield is off by over a factor of two compared with the experimental result. The behavior of the condensable alkane molar yields is similar to that of the condensable alkenes. The model again is able to capture the peaked behavior seen in the experimental results as a function of carbon number as well as the falloff in product yield as a function of carbon number at longer reaction times.

The decline in the molar yields of both alkanes and alkenes as carbon number increases at longer times can be partially attributed to the decay of the polymer molecular weight during the degradation. As the molecular weight declines, it becomes less probable to form the higher carbon number products because chains may not be long enough to have all the necessary positions available to form a given product. While the model predicts a rapid decline of the molecular weight initially, which is consistent with literature reports (Wall et al. 1954), the lack

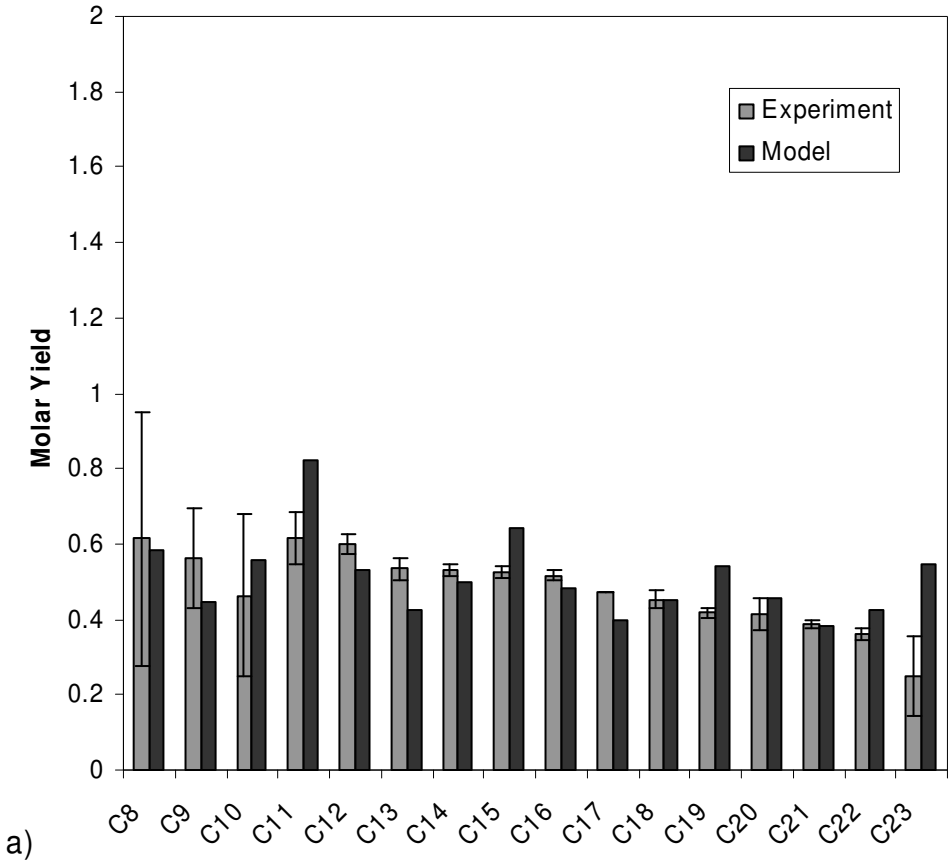

Figure 5.5: Comparison of experimental and model condensable alkane yields for 125,000 M_{w0} HDPE pyrolysis at 420 °C after a) 30 min, b) 90 min, and c) 150 min of degradation. The error bars on the experimental data reflect the standard deviation of the molar yields reported for three different initial HDPE loadings in the experimental study.

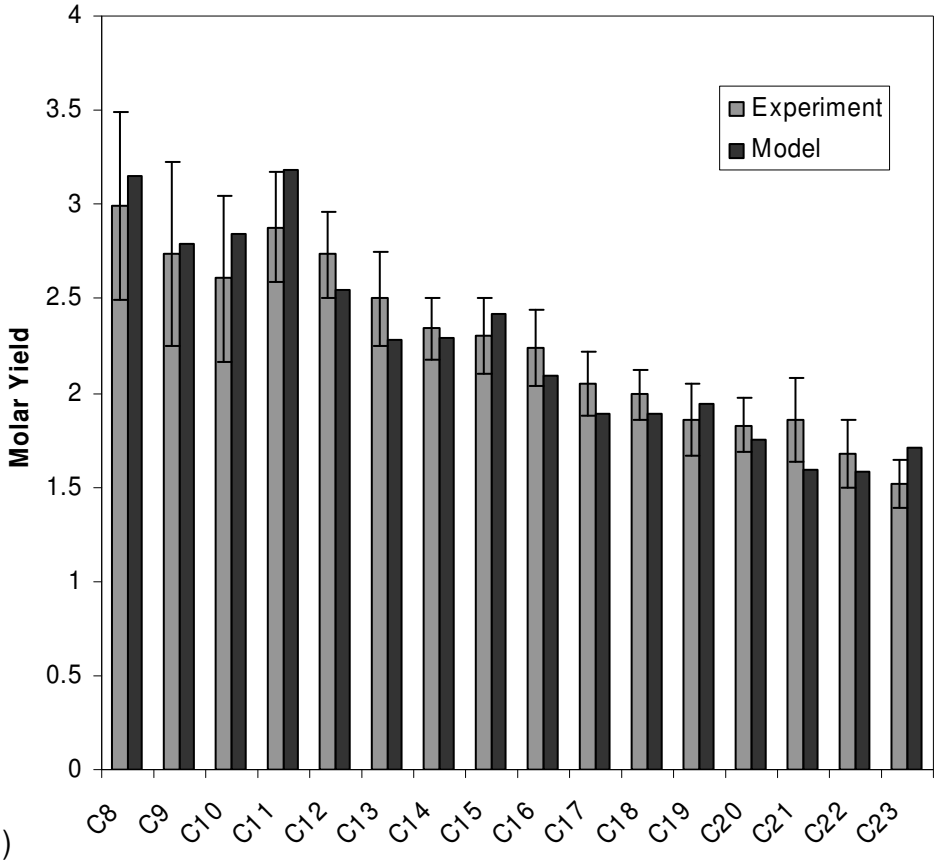

b)

Figure 5.5: Continued

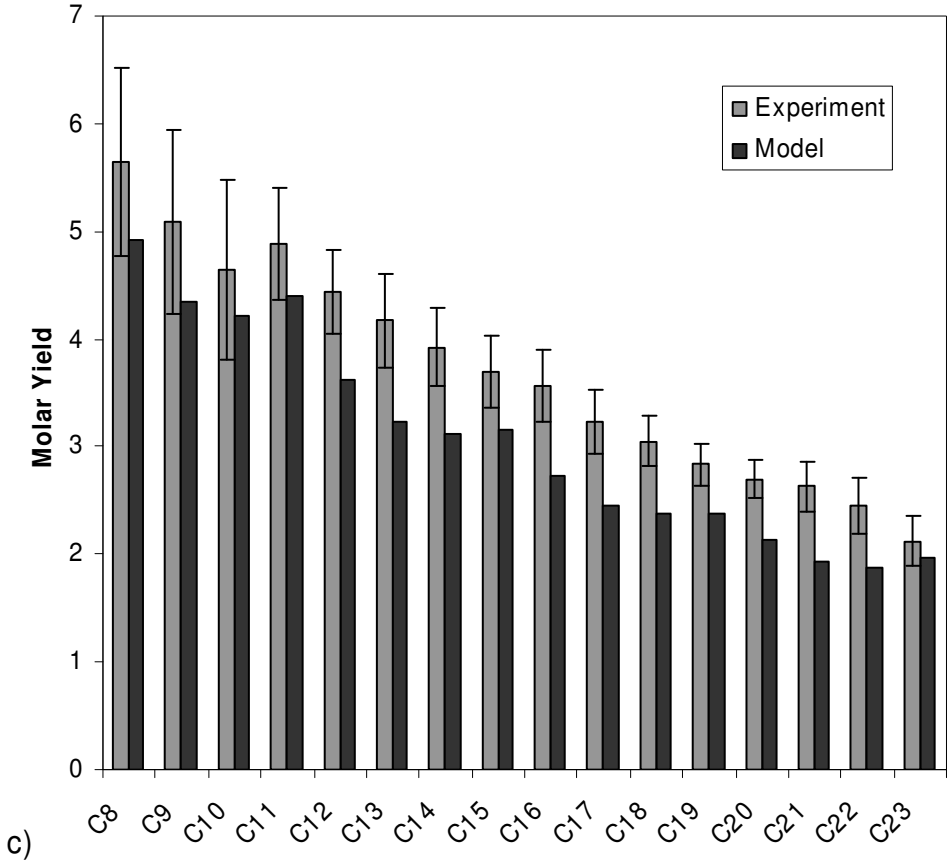

c)

Figure 5.5: Continued

of molecular weight decay data for the experimental results examined here makes it impossible to validate the quantitative results of the model for M_n and M_w explicitly.

The experimental and model results for the gaseous products obtained during HDPE pyrolysis are compared in a parity plot in Figure 5.6. The agreement between the experimental values and the model results is fair. In the experimental study, it was noted that measurement of the yields of the gaseous products formed during pyrolysis was more difficult than for the condensable products, so the lack of better agreement is not surprising. The three gaseous products that the model has the most trouble capturing are C1, C3=, and C4=. Propylene (C3=) is often found to be the most abundant product formed during HDPE pyrolysis. The model under-predicts the formation of propylene compared to experiment. We observed that the model yield for propylene can be significantly increased by enhancing the rate of allyl bond fission of polymer chains with a terminal unsaturation, but a non-physical rate parameter for this reaction family would have been required to match the experimental data. As shown in Figure 5.3, C4= and C1 are both formed via β-scission reactions of the third position mid-chain radical. The fact that both of these products are under-predicted indicates that the model has trouble accounting for the formation of this specific radical. The inclusion of 1,3-hydrogen shift would promote the formation of third position mid-chain radicals. Nevertheless, non-physical rate parameters would be required to achieve any noticeable enhancement in their formation rate. Because they are well supported, we maintained the rate parameters reported in Table 5.3.

An alternative and more plausible explanation for why the gaseous product yields are not captured as well as the yields of the condensable products is that secondary decomposition pathways in the gas phase are not included in the model. Secondary gas phase reactions may account for some of the discrepancies between the experimental product spectrum and the model

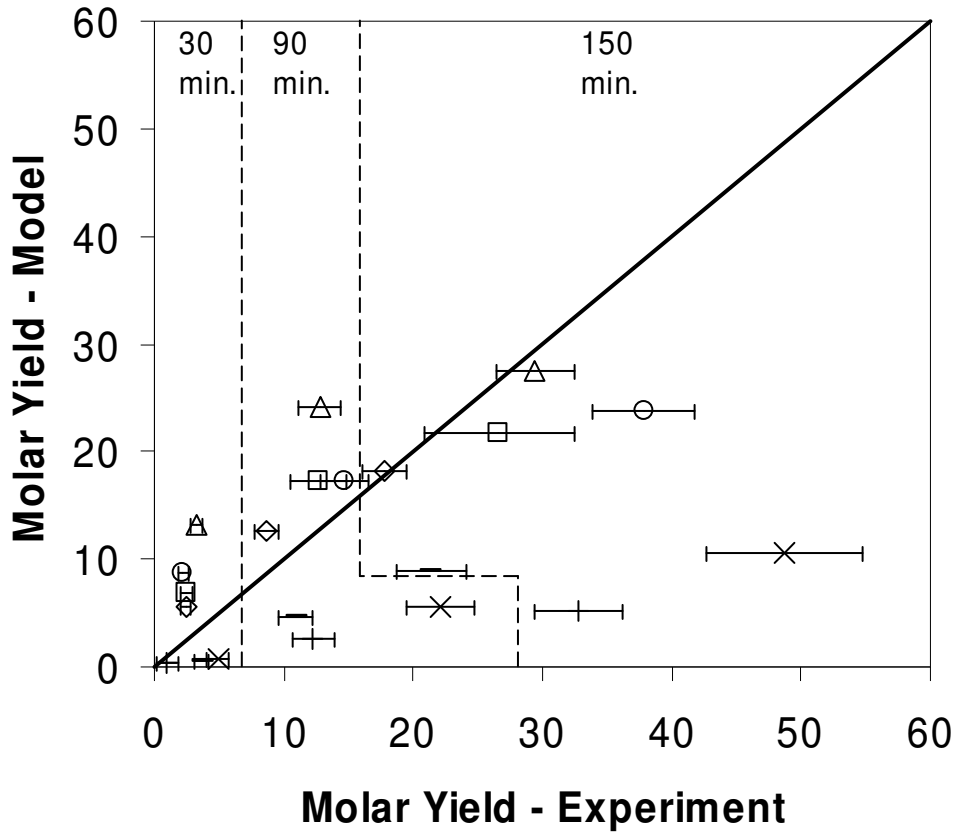

Figure 5.6: Parity plot comparing experimental and model molar yields for the gaseous products produced during pyrolysis of HDPE with M_{w0} = 125,000 at 420 °C. Gaseous products shown are C1 (+), C2= (□), C2 (○), C3= (×), C3 (△), C4= (–), and C4 (◇). The error bars reflect the standard deviation of the molar yields reported for three different initial HDPE loadings in the experimental study.

results. This is especially true at longer reaction times, when higher conversions are achieved, where the experimental technique utilized for the data set used has been shown to be affected by secondary reactions (Kruse et al. 2003b; Kruse et al. 2002). An example of possible secondary reactions would be the alkenes undergoing allyl bond fission, which would form both shorter alkyl radicals and allylic radicals. These radicals can go on to form alkanes and propylene, both of which are under-predicted at long times.

5.3.2 Time Evolution of LMWPs

The detail of our mechanistic model and the way in which it is solved gives us the ability to look at the full time evolution of the LMWP which allows for further mechanistic insight. Figure 5.7 shows the time evolution of the total LMWP as well as the total alkane and total alkene evolution. These totals include all species reported in Figures 5.4, 5.5, and 5.6. The agreement between the model and experimental results is very good, particularly for 30 and 90 minutes. The fact that the model results show that the total alkane molar yield is greater than the total alkene molar yield is in contradiction with the experimental behavior, although the deviation is caused by the errors in the model results for the gaseous products, specifically the under-prediction of C3= and C4= by the model.

The time evolution of a selection of specific alkane and alkene products is shown in Figure 5.8 and Figure 5.9, respectively. Figure 5.8 shows the time evolution of C8, C15, and C22. Figure 5.9 shows the time evolution of C9=, C14=, and C18=. The species shown demonstrate the excellent ability of the model to predict the time evolution of a broad range of specific condensable products. The behavior of the time evolution curves of the six species shown in Figure 5.8 and Figure 5.9 can be rationalized for all species. The specific condensable

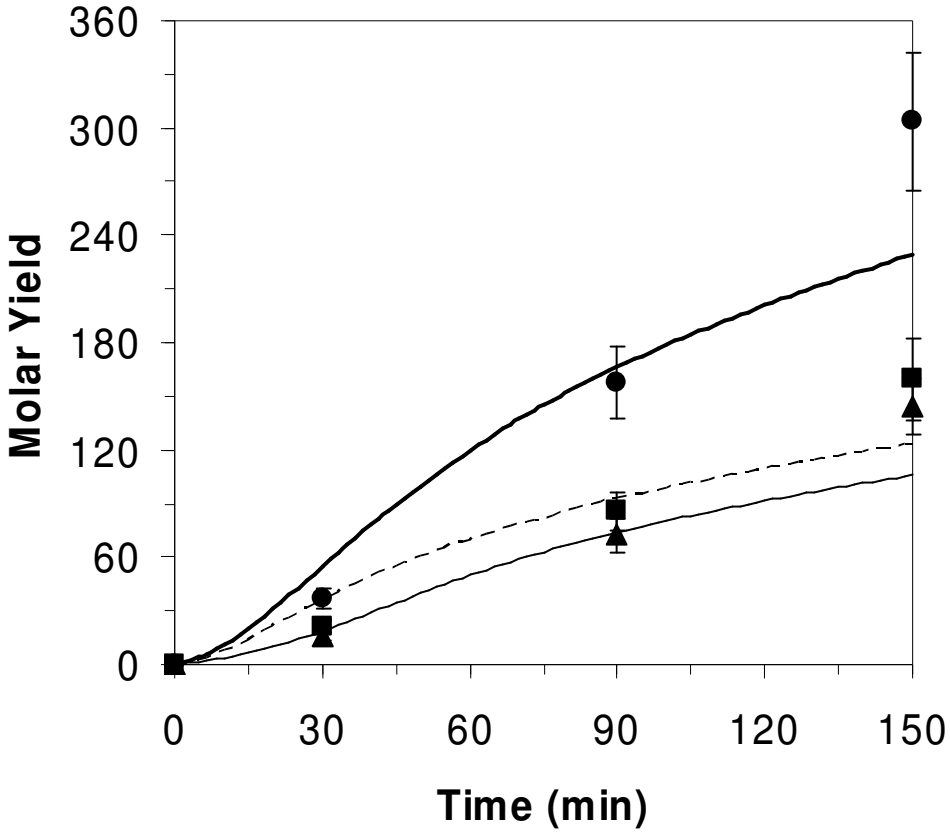

Figure 5.7: Model results compared to experimental values for 125,000 M_{w0} HDPE pyrolysis at 420 °C for the time evolution of the total LMWP, the total alkane and total alkene yields. Model results are shown as lines (——— total LMWP; – – – total alkane; —— total alkene) and experimental data as points (● total LMWP; ▲ total alkane; ■ total alkene).

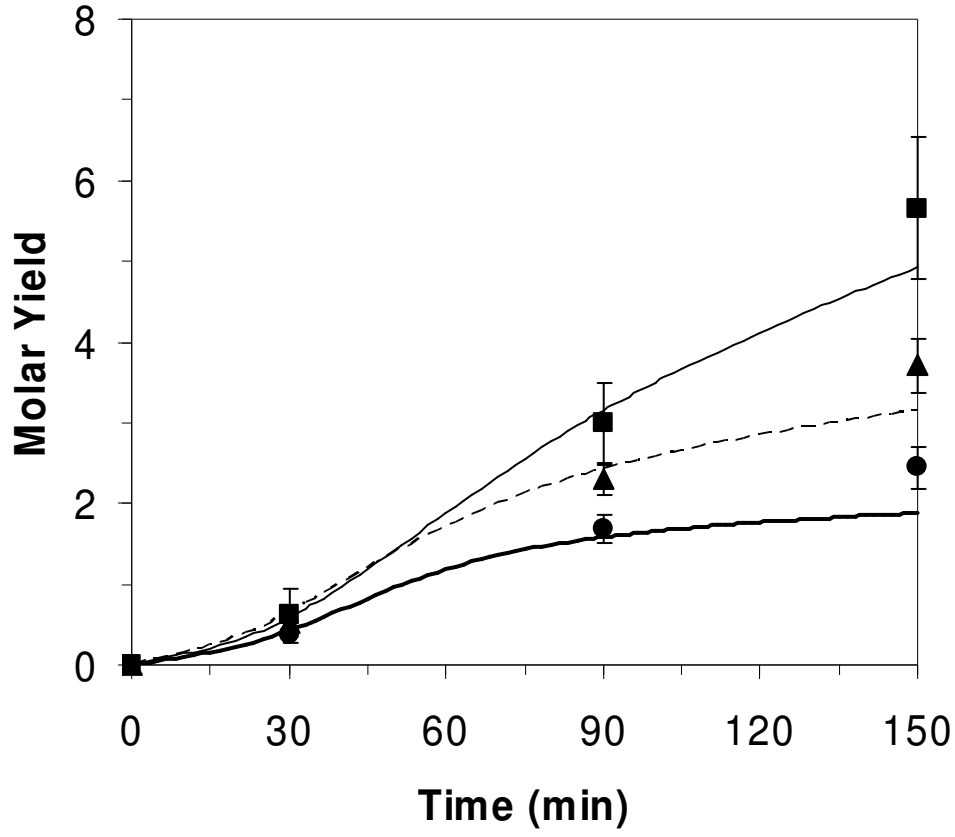

Figure 5.8: Model results compared to experimental values for 125,000 M_{w0} HDPE pyrolysis at 420 °C for the time evolution of C8, C15 and C22. Model results are shown as lines (—— C8;– – -C15; ▬ C22) and experimental data as points (■ C8; ▲ C15; ● C22).

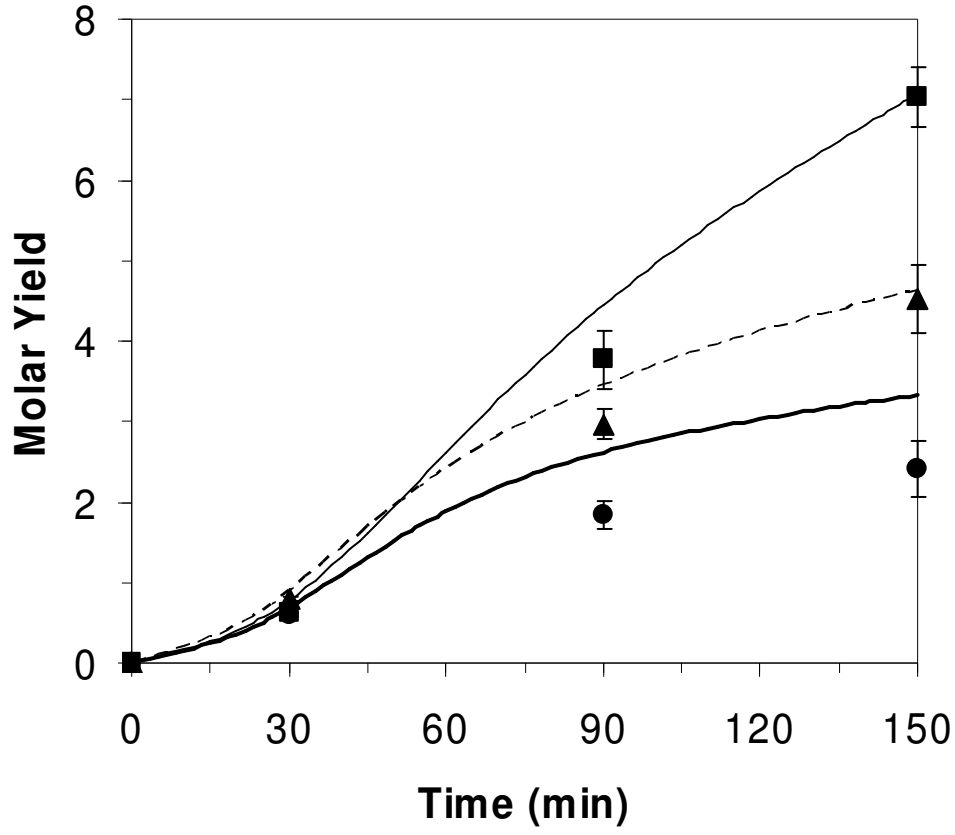

Figure 5.9: Model results compared to experimental values for 125,000 M_{w0} HDPE pyrolysis at 420 °C for the time evolution of C9=, C14= and C18=. Model results are shown as lines (—— C9=; – – - C14=; ▬ C18=) and experimental data as points (■ C9=; ▲ C14=; ● C18=).

products at the early stages of the degradation (less than 45 minutes) are formed in similar amounts for all the alkanes shown in Figure 5.8 and all the alkenes shown in Figure 5.9. This behavior indicates that the RS reaction pathway is dominant for the formation of these products because the different products exhibit statistical yields. As the degradation continues, the rates of formation of the higher carbon number species slow down compared to those for species with lower carbon numbers, which can be partially attributed to the molecular weight effects discussed in the previous section.

The time evolution of C15 and C14= at early degradation times shows that these products are formed in slightly greater yields than the other products shown in Figures 5.8 and 5.9. It should be noted that C15 and C14= are products that can be formed after successive x,x+4-hydrogen shift reactions. The x,x+4-hydrogen shift (and 1,5-hydrogen shift) reactions are the most favorable of the intramolecular hydrogen transfer reactions. The facility of these reactions suggests that the BB pathway to their formation should be more favorable than for other species. This is borne out in the early time evolution results. While the enhanced early time yields of C15 and C14= compared to the other products demonstrate that BB plays a role in specific product formation, the fact that the enhancement is relatively small indicates that this is a complementary role, and the model is able to capture these effects. It should be noted this is the first modeling study to present specific product time evolution results for HDPE pyrolysis.

5.3.3 Random Scission vs. Backbiting

The competition between the RS and BB reaction pathways can be further analyzed utilizing the model results. The BB reaction pathway is expected to produce a product distribution with peaks in the yields of specific products (Faravelli et al. 1999; Tsuchiya and

Sumi 1968a, 1968b). These peaks are expected at the products formed from specific radicals that can be formed by successive x,x+4-hydrogen shift reactions, such as C10=, C14=, C11, and C15. The peaked behavior is seen in the model results, demonstrating the importance of the BB pathways to the product distribution of HDPE pyrolysis. The high yields of products other than the ones formed by successive x,x+4-hydrogen shift reactions indicates that RS is also important. As discussed in the previous section, the similarity of the early evolution of condensable species, regardless of the facility of BB reaction pathways leading to them, indicates that RS is more controlling for product formation.

To quantify this specifically, the competition between the reaction pathways was analyzed in a more detailed fashion using net rate analysis. The net rates of end-chain β–scission, intramolecular chain transfer (all possible 1,x-hydrogen transfers), and intermolecular chain transfer by end-chain radicals is shown in Figure 5.10. These net rates allow a comparison between the three general reaction pathways to LMWP formation in HDPE pyrolysis. The figure only shows the first 45 minutes of the simulated degradation to minimize the impact of molecular weight decay effects on the results. As shown in Figures 5.8 and 5.9, the product evolution behavior is nearly identical for a variety of species over the first 45 minutes of degradation. The UZ pathway is never competitive with the other two pathways. The UZ pathway is not expected to be important during polyethylene pyrolysis because experimental results show that monomer is not formed in preference to other LMWP products. Figure 5.10 demonstrates that intermolecular hydrogen transfer (RS) is a more important reaction than intramolecular hydrogen shift (BB) for end-chain radicals. This indicates a preference for the RS reaction pathway over the BB reaction pathway. These conclusions agree with an earlier

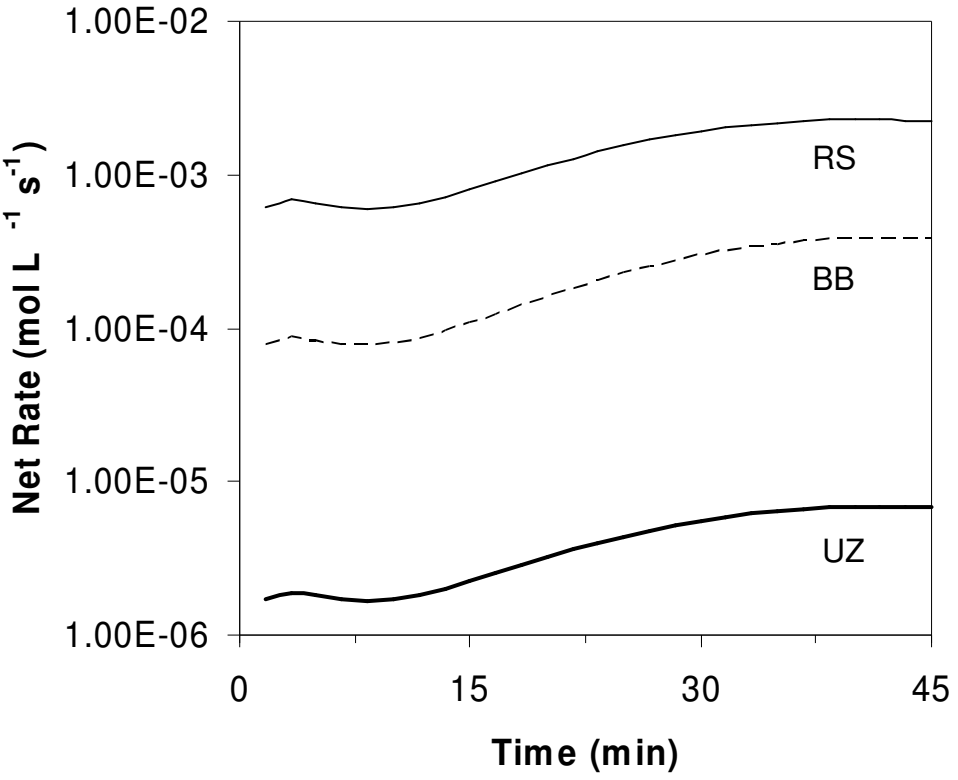

Figure 5.10: Net rates for end-chain β-scission (UZ), intramolecular hydrogen abstraction (BB), and intermolecular hydrogen abstraction (RS) for end-chain radicals during pyrolysis of HDPE with M_{w0} = 125,000 at 420 °C.

modeling study which compared the general reaction pathways for final product yields over a range of temperatures (Marongiu et al. 2007).

To examine the varied role that the BB reaction pathway can play in the formation of different products, the net rates of formation of select specific mid-chain radicals via intramolecular hydrogen shift was analyzed. Figure 5.11 shows the net rates of formation of the 5^{th} position mid-chain radical, the 13^{th} position mid-chain radical, and the 18^{th} position mid-chain radical via intramolecular hydrogen shift reactions. Each specific mid-chain radical position can have up to six intramolecular shift reactions leading to its formation. A general schematic of these reactions is shown in Figure 5.12. The 5^{th} position mid-chain radical has the largest rate of formation via intramolecular hydrogen shift. This is driven by the relative ease of 1,5-hydrogen shift, which overwhelms the other intramolecular hydrogen shift reactions that have a net consumption of the 5^{th} position mid-chain radical. The 13^{th} position mid-chain radical has a net rate of formation via intramolecular hydrogen shift in between those for 5^{th} and 18^{th} position mid-chain radicals. This is expected because, while there is not a direct 1,x-hydrogen shift to form the 13^{th} position mid-chain radical, it is formed as part of the successive x,x+4-hydrogen shift series of reactions (1,5-, followed by 5,9-, followed by 9,13-hydrogen shift). The 18^{th} position mid-chain radical has the lowest net rate of formation via intramolecular hydrogen shift reactions. There is no direct route to the 18^{th} position mid-chain radical that uses either a single 1,x-hydrogen shift reaction or only utilizes the favored x,x+4-hydrogen shift reactions, which causes it to be more difficult to form via BB reactions. The net rates presented in Figure 5.11 demonstrate the various levels of importance the BB reaction pathways have on the formation of different specific mid-chain radicals, and hence to the formation of different species. It should be noted that the difference in the shapes of the three net rate curves shown in Figure 5.11 is

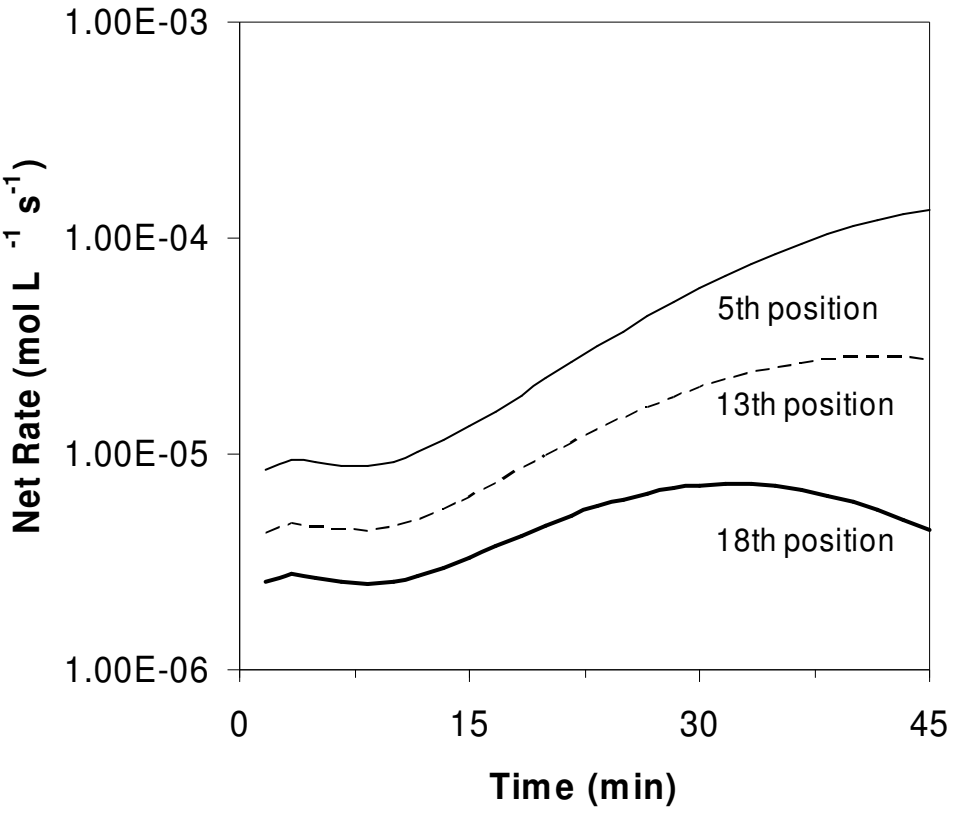

Figure 5.11: Net rates for the formation of 5th position, 13th position, and 18th position mid-chain radicals via intramolecular hydrogen shift (BB) during pyrolysis of HDPE with M_{w0} = 125,000 at 420 °C.

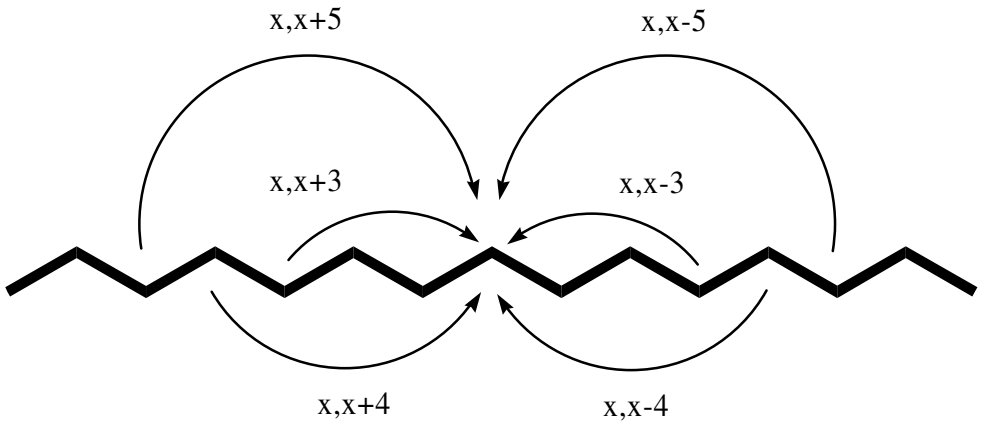

Figure 5.12: General schematic of possible intramolecular hydrogen shift reactions to form a specific mid-chain radical during HDPE pyrolysis.

related to the differences in the radical concentrations that comprise the specific net rates. While RS is dominant for the formation of mid-chain radicals as shown in Figure 5.10, the contribution from BB varies depending on the ease of intramolecular shift reactions to form a given specific mid-chain radical. This varying contribution of BB causes the characteristic peaked behavior seen in the product yield spectra (Figures 5.4 and 5.5). As discussed in the previous section, the equivalence of the temporal evolution of different products at early degradation times, regardless of the facility of BB reactions to the specific product formation, indicates that RS is more controlling for specific product formation while BB pathways are complementary. The net rates presented in Figure 5.11 demonstrate the different degrees of importance the BB pathway can have for specific product formation.

While net rate analysis of HDPE pyrolysis provides valuable insight into the competition between RS and BB in HDPE, it cannot be seen as completely definitive. Due to the diversity of reactions that can take place, radicals that form specific LMWP are not just formed via direct BB or RS reactions of the end-chain radicals that are created from bond fission, but are also formed from pathways comprised of multiple steps that shuffle the position of a radical center via BB and/or RS. As shown in the example in Figure 5.13, the 13^{th} position mid-chain radical has several different pathways to form it, including a series of BB reactions and direct formation via RS. However, there are also more convoluted pathways such as the one shown, which involves 1,6-hydrogen shift (BB), followed by intermolecular hydrogen transfer to form a 17^{th} position mid-chain radical (RS), which is then followed by a x,x-4-hydrogen shift reaction (BB). The net rate analysis provided is able to quantify the relative contributions of BB and RS among the steps that directly form the 13^{th} position mid-chain radical, but it does not trace back through all the possible pathways to the initial formation of a radical, which may involve many steps of RS and

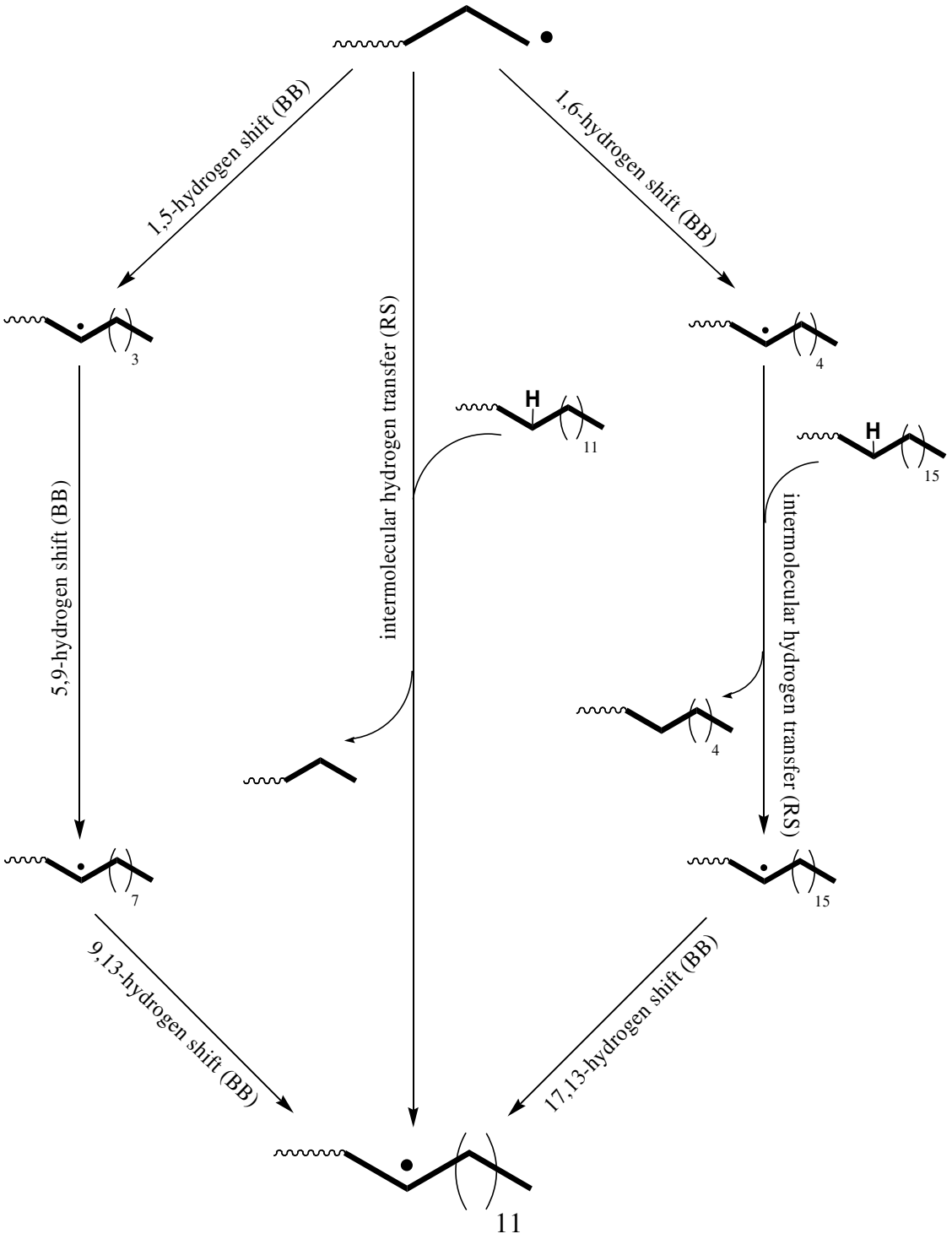

Figure 5.13: Examples of possible reaction pathways for the formation of the 13th position mid-chain radical.

BB in different combinations. A full map of the reaction network and the net rates associated with each step would be required to quantify the contributions of RS and BB in detail. It is clear from the net rate analysis performed, however, that direct RS is important for the formation of all mid-chain positions, and the contribution of BB can vary from position to position.

5.4 CONCLUSIONS

A detailed mechanistic model of HDPE pyrolysis was developed utilizing a framework based on the method of moments. Rate parameters were specified based on both literature values as well as parameters utilized in our previous work (Kruse et al. 2003b; Levine and Broadbelt 2008). Three frequency factors for β-scission reactions were obtained using parameter estimation, but the final values were very close (differing by less than a factor of 10) to their initial values and were within typical ranges for β-scission frequency factors. The model tracked 151 species and included over 11,000 reactions. The model was compared with experimental data for pyrolysis of HDPE with M_{w0} = 125,000 at 420 °C which had been previously collected in our research group (De Witt and Broadbelt 2000). Model results were found to be in excellent agreement with the experimental data for the molar yields of the condensable LMWP and in fair agreement for the molar yields of the gaseous LMWP. The time evolution curves for condensable LMWP were similar over a wide range of n-alkane and 1-alkene products. Specifically, the first 45 minutes of degradation showed similar amounts of product evolution for a variety of products, indicating the dominance of the RS pathway. The model results were further analyzed using net rate analysis to understand the competition between the major reaction pathways to LMWP formation. The UZ pathway was found to be of minimal significance compared to the BB and RS pathways. Both the BB and RS pathways were shown to be

important for LMWP formation, with the RS pathway being more dominant based on the net rates of reactions of end-chain radicals. Net rates for the formation of specific mid-chain radicals via intramolecular hydrogen transfer demonstrated that the role of BB in the formation of specific products varies with radical position, favoring the formation of specific mid-chain radicals that have more facile BB pathways involving x,x+4-intramolecular hydrogen transfer reactions that lead to them.

CHAPTER 6

INCREASED STRUCTURAL DETAIL IN A POLYSTYRENE PYROLYSIS MECHANISTIC MODELING: TRACKING OF BACKBONE TRIADS

6.1 INTRODUCTION

Mechanistic modeling of polymer pyrolysis has been shown to be a powerful tool for increasing mechanistic and kinetic understanding of these complex reaction systems (Kruse et al. 2005; Kruse et al. 2003b; Kruse et al. 2001; Levine and Broadbelt 2008; Marongiu et al. 2007). Polymer pyrolysis is characterized by a large free-radical reaction network, which often yields a diverse product spectrum. The high molecular weight, polydisperse nature of polymers and the large number of reaction channels available to free radicals cause these reaction networks to involve thousands of species and reactions. The size of these reaction systems has forced mechanistic modeling efforts to minimize the structural detail included in the model as well as utilize lumping schemes to avoid tracking the range of polymer chain lengths explicitly.

The method of moments has been the primary lumping technique utilized in polymer pyrolysis modeling (Kodera and McCoy 1997; Kruse et al. 2005; Kruse et al. 2003b; Kruse et al. 2001; Levine and Broadbelt 2008; Marongiu et al. 2007; Wang et al. 1995), but other techniques, such as simply dividing the molecular weight distribution into bins, have been utilized (Faravelli et al. 2001; Marongiu et al. 2007). Early polymer degradation models developed using the

method of moments further simplified the system by lumping some reactions together as well as invoking the quasi steady state approximation (QSSA) (Kodera and McCoy 1997; Madras and McCoy 1999; Wang et al. 1995). The most detailed method of moments models developed to date utilize only elementary reactions and do not invoke the QSSA (Kruse et al. 2005; Kruse et al. 2003b; Kruse et al. 2001; Levine and Broadbelt 2008). These models, while comprehensive, are still limited by the level of structural detail tracked. The most detailed models track different end types as well as mid-chain radical types to distinguish polymeric species. They also track different bond types that exist in the system. For some polymers, such as copolymers or those with structural heterogeneities, it would be useful to be able to track polymer backbone features that are less local than a single bond in these models.

In this work, we devised a method to track backbone triads within a method of moments model for polystyrene pyrolysis. A triad is defined as a sequence of three consecutive backbone atoms. Polystyrene pyrolysis was utilized to demonstrate this method because it has a smaller product spectrum and reaction network size compared to polypropylene and polyethylene pyrolysis. The inclusion of triads can aid in the explicit tracking of some structural heterogeneities, such as peroxide bonds, within the model. The method of tracking triads in the polystyrene pyrolysis model as well as a comparison between a version of the polystyrene model which includes the tracking of triads and the latest version developed without the tracking of triads (Levine and Broadbelt 2008) are presented below.

6.2 MODELING FRAMEWORK

6.2.1 General Modeling Framework

To capture a high level of detail while maintaining a manageable model size, the method of moments is utilized in our modeling framework. The method of moments uses a series of moments to describe the chain length distribution instead of explicitly tracking every possible chain length. To fully determine the chain length distribution an infinite series of moments would be required, but a substantial amount of information about the distribution can be maintained from only the first few moments (Grinstead and Laurie 1997). The number and weight average molecular weights can be determined from the zeroth, first, and second moments (Dotson et al. 1996). Building on the work of McCoy and coworkers (Kodera and McCoy 1997; Madras and McCoy 1999; McCoy 1993; Sterling and McCoy 2001; Wang et al. 1995), we have developed a method of moments-based modeling framework to build detailed mechanistic models for reactions of polymers. This framework has been previously applied to polystyrene pyrolysis, polypropylene pyrolysis, binary pyrolysis of polystyrene and polypropylene, and living free-radical polymerization of polystyrene (Kruse et al. 2005; Kruse et al. 2003a; Kruse et al. 2003b, 2003c; Kruse et al. 2001; Kruse et al. 2002; Levine and Broadbelt 2008).

The mechanistic chemistry of the system is incorporated by allowing all the species in the system to react according to a set of elementary reactions. For polystyrene pyrolysis the following reaction families are utilized (1) chain fission, (2) radical recombination, (3) allyl chain fission, (4) hydrogen abstraction, (5) mid-chain β-scission, (6) radical addition, (7) end-chain β-scission, (8) disproportionation, and (9) intramolecular hydrogen transfer (1,3-, 1,5-, 1,7-, and 7,3-hydrogen shift). Polymeric species within the model were distinguished based on structural characteristics of the chain including radical position, end type, and chain structure.

Low molecular weight products (LMWP) and their corresponding radicals were tracked explicitly.

The specification of rate parameters for the polystyrene pyrolysis model has been discussed previously in Chapter 3. Rate parameters are specified for each reaction in the model. To minimize the number of parameters needed while maintaining a connection between the chemical structure and thermodynamics of the reactants and products and their reactivity, the Evans-Polanyi (Evans and Polanyi 1938) and Blowers-Masel (Blowers and Masel 1999) relationships were used. A hierarchical approach was utilized to parameterize the model where reliable experimental values for polymer reactions are utilized first, followed by reliable experimental values based on small molecule chemistry. In the absence of any reliable experimental value, various estimation techniques are utilized, including parameter estimation (Stewert et al. 1992), polymer mimic modeling studies (Woo et al. 1998), and Benson group additivity (Benson 1976). The parameter set developed for polystyrene pyrolysis has been validated against a wide range of experimental data (Levine and Broadbelt 2008).

To help manage the assembly of the large number of reactions and species in our polymer pyrolysis models, PERL scripts were developed to automate model construction. The PERL scripts create lists of reactions, species, necessary rate constants, variables, and algebraic equations. The list of reactions is converted by the PERL scripts into population balance equations which use moment operations to convert reaction terms into proper moment equations for each polymeric species. Differential equations for the zeroth, first, and second moments are developed for each polymeric species. The final set of stiff differential equations and algebraic equations for other key variables was solved using DASSL (Petzold 1983).

6.2.2 Method of Tracking Triads

A triad is defined as any combination of three consecutive backbone atoms. In polystyrene, the backbone is composed of all carbon atoms, but there are both benzylic (head) and non-benzylic (tail) carbon atoms, which were tracked separately and used to define the triads. The possible triads for polystyrene are shown in Figure 6.1. The hhh and ttt triads were excluded from the model because they are extremely unlikely to form during polystyrene pyrolysis. A differential equation for the concentration of each triad was formulated based on the reactions that form or break a given triad. For example, bond fission reactions break two triads and radical recombination reactions form two triads. The differential equations are formulated using the same PERL scripts that construct the moment differential equations for polymeric species and the explicit differential equations for LMWP concentrations.

Incorporating triads into the model introduces a degree of uncertainty into certain reactions in the model. This is because the structural detail of reactant species for certain reactions does not fully define the triads involved in the reaction. To account for this uncertainty, all combinations of allowed triads that are possible for a reaction must be included in the model. This involved splitting each reaction that had an uncertainty about which triads were involved into multiple reactions. To ensure that the mass balance for the system was maintained, it was critical that proper partitioning of each reaction that was split be performed.

For polymer pyrolysis the only reaction families that have an uncertainty for the triads involved are bond fission, β-scission, and hydrogen abstraction. Figure 6.2 depicts the general form of these three reaction families and which positions make up the triad or triads involved in the reaction.

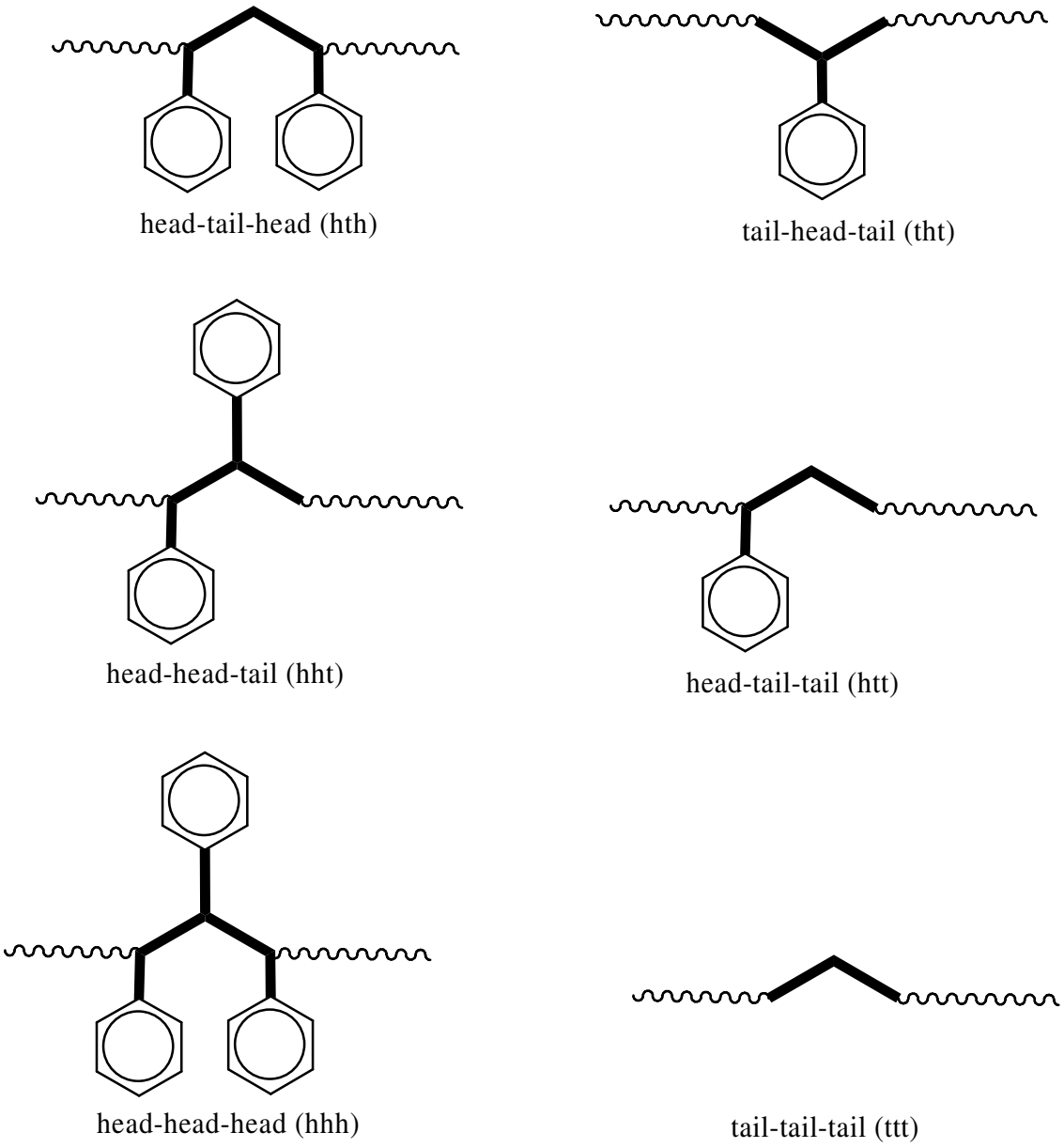

Figure 6.1: Structure of the six possible triads in polystyrene. Head-head-head and tail-tail-tail triads were excluded from the modeling study.

bond fission: b and c are known

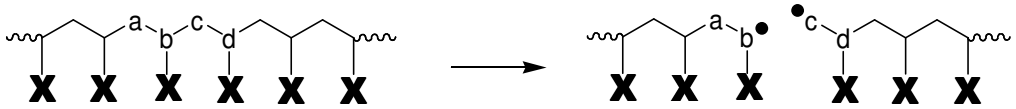

β-scission: b,c, and d are known

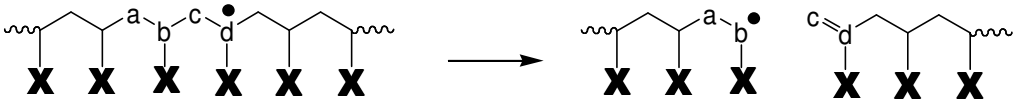

Hydrogen abstraction: b is known

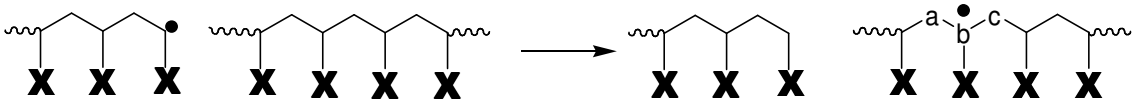

Figure 6.2: Three reaction families that include a level of uncertainty of the triads involved.

For bond fission two triads are consumed in the reaction. As shown in Figure 6.2 these triads are abc and bcd where b and c are defined by the bond undergoing fission. The reaction for a given combination of triads is split based on the conditional probability that abc exists given that bc is part of the triad and that bcd exists given that bc is part of the triad. This conditional probability is shown in equation 6.1:

$$b_{ij} = \frac{[a_i bc]}{\sum_x [a_x bc]} * \frac{[bcd_j]}{\sum_y [bcd_y]} \tag{6.1}$$

where b_{ij} is the conditional probability for a bond fission reaction with unknown neighboring atoms a_i and d_j. This probability, b_{ij}, is multiplied by the existing rate coefficient for the bond fission of bond bc to partition each set of triads possible for the fission of bond bc. This allows for the differential equations describing the triad concentrations to include the proper bond fission terms for a given triad. It also means that the existing species and moment differential equations will have the correct total rate of bond fission reactions over counted because the sum of all b_{ij} terms equals one.

For β-scission, while two triads are consumed in the reaction only one has a degree of uncertainty. As depicted in Figure 6.2 the triads involved are abc and bcd, where b, c, and d are defined by the type of β-scission reaction occurring. The conditional probability that the triad abc exists given that bc is part of the triad is used to split all the possible β-scission reactions. This conditional probability is shown in equation 6.2:

$$s_i = \frac{[a_i bc]}{\sum_x [a_x bc]} \tag{6.2}$$

were s_i is the conditional probability for a β-scission reaction with unknown neighboring atom a_i. The conditional probability s_i is used in a similar fashion to b_{ij} where it is multiplied by the existing β-scission rate coefficient.

For hydrogen abstraction no triads are formed or consumed, but the atoms neighboring the position being abstracted from can affect the reactivity by either stabilizing or destabilizing the radical being formed. While this effect is negligible for polystyrene pyrolysis it was important to include all of these possible reactions to demonstrate the capability to link triad structure to reactivity for future systems. As depicted in Figure 6.2 the triad involved in a hydrogen abstraction reaction is abc where only b is defined by the reaction. The conditional probability that triad abc exists given that b is the central atom of the triad is used to partition the hydrogen abstraction reactions. This conditional probability is shown in equation 6.3:

$$h_{ij} = \frac{[a_i bc_j]}{\sum_x \sum_y [a_x bc_y]} \tag{6.3}$$

where h_{ij} is the conditional probability for a hydrogen abstraction reaction with unknown neighboring atoms a_i and c_j. The probability h_{ij} is used in the same fashion as s_i and b_{ij} to partition the hydrogen abstraction reactions. By utilizing the above conditional probabilities the additional reactions needed to track triads can be properly incorporated into the mechanistic model.

6.4 RESULTS AND DISCUSSION

In order to validate the methodology for tracking triads within the modeling framework a polystyrene pyrolysis model that included the above algorithm was developed. The model tracked 85 species and included over 10,000 reactions. The model was solved for pyrolysis of

polystyrene with an initial M_n of 113,000 and an initial M_w of 280,000 at 350 °C. The model was compared against both experimental data previously collected in our research group (Kruse et al. 2005) as well as the previously validated polystyrene pyrolysis model that did not include the triad tracking methodology (Levine and Broadbelt 2008). The results of both models compared to the experimental data are shown in Figure 6.3.

Both models are in excellent agreement with the experimental data for both the molecular weight decay as well as for the evolution of the various low molecular weight products (LMWP). It should be noted that the total LMWP data includes not only the three most abundant products of polystyrene pyrolysis, styrene monomer, dimer and trimer, but also the minor products α-methylstyrene, diphenylpropane, and toluene. Both sets of model results overlay each other making it difficult to tell them apart in Figure 6.3. This is the behavior that is expected if the triad tracking methodology has been properly implemented, because for polystyrene the different triads do not lead to different reactivities in the reactions that involve them. The overlay of the two sets of model results is a demonstration of the validity of the triad tracking methodology described in the previous section.

Finally, the concentrations for the four triads that were included in the polystyrene model can be analyzed. The triad and bond concentration profiles can be seen in Figure 6.4. Since the model is initialized assuming that all polystyrene chains are made up of only head-to-tail bonds, it is expected that the majority of bonds and triads in the system throughout the degradation will be head-to-tail bonds and head-tail-head or tail-head-tail triads. Head-to-head and tail-to-tail bonds are considered structural anomalies and should be formed in much smaller quantities. More head-to-head bonds than tail-to-tail bonds are expected in the system because of the larger concentration of head radicals due to the stability of benzylic radicals. Figure 6.4 clearly shows

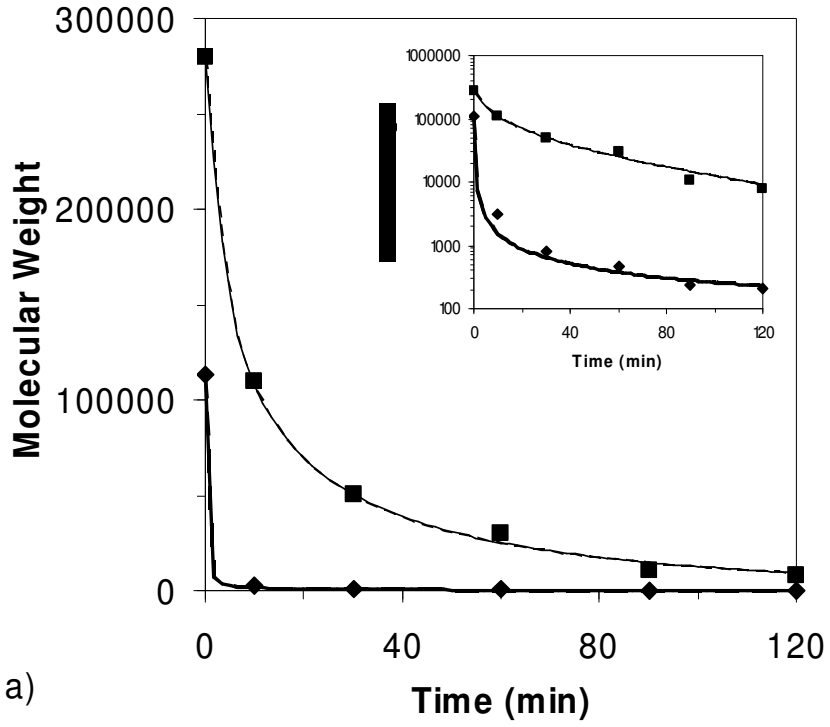

Figure 6.3: Model results for pyrolysis of polystyrene with M_{n0} = 113,000 and M_{w0}= 280,000 at 350 °C for both the model that includes tracking of triads and the original model which does not track triads. The molecular weight changes are shown in (a) with model results as lines (—— $M_{n\text{-w/o triads}}$; – – $M_{n\text{-w/ triads}}$; —— $M_{w\text{-w/o triads}}$; – – $M_{w\text{-w/ triads}}$) and the experimental data as points (◆ M_n; ■ M_w). The total LMWP and styrene yields are shown in (b) with model results as lines (—— $styrene_{\text{-w/o triads}}$; – – $styrene_{\text{-w/ triads}}$; —— total $LMWP_{\text{-w/o triads}}$; – – total $LMWP_{\text{-w/ triads}}$) and the experimental data as points (◆ styrene; ■ total LMWP). The dimer and trimer yields are shown in (c) with model results as lines (—— $trimer_{\text{-w/o triads}}$; – – $trimer_{\text{-w/ triads}}$; —— $dimer_{\text{-w/o triads}}$; – – $dimer_{\text{-w/ triads}}$) and the experimental data as points (◆ dimer; ■ trimer). The inset in (a) is the molecular weight change results plotted on a logarithmic scale to demonstrate the capture of the M_n experimental data by the model.

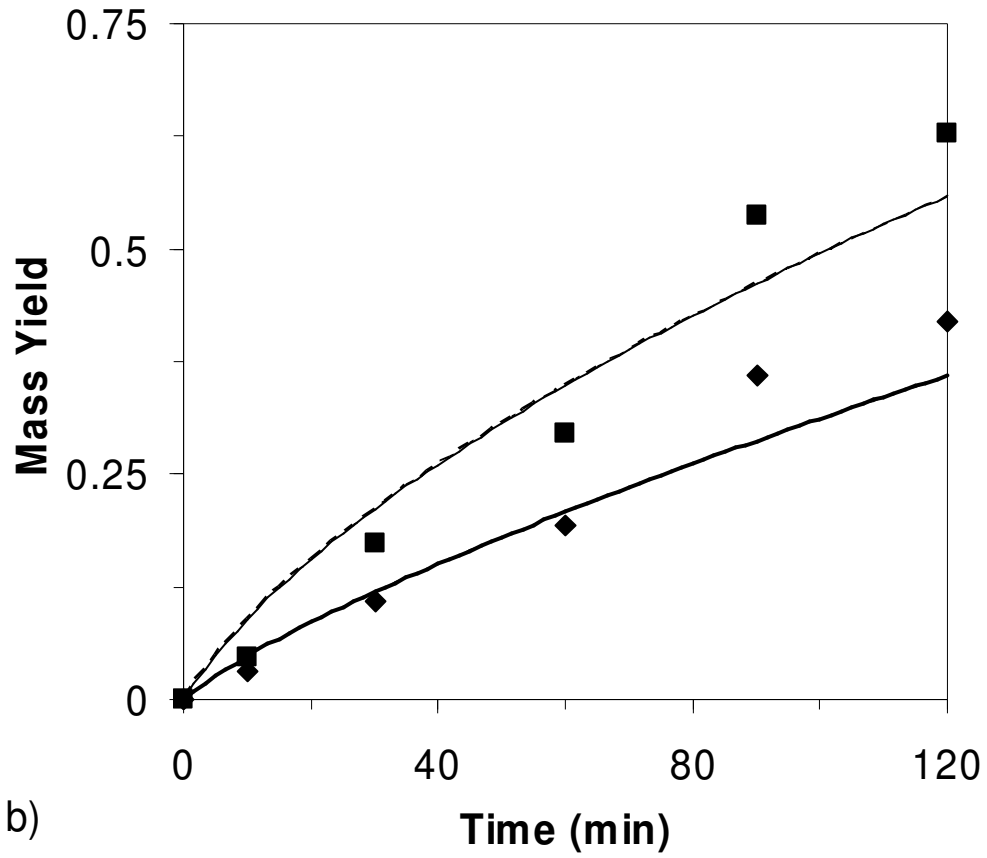

b)

Figure 6.3: Continued

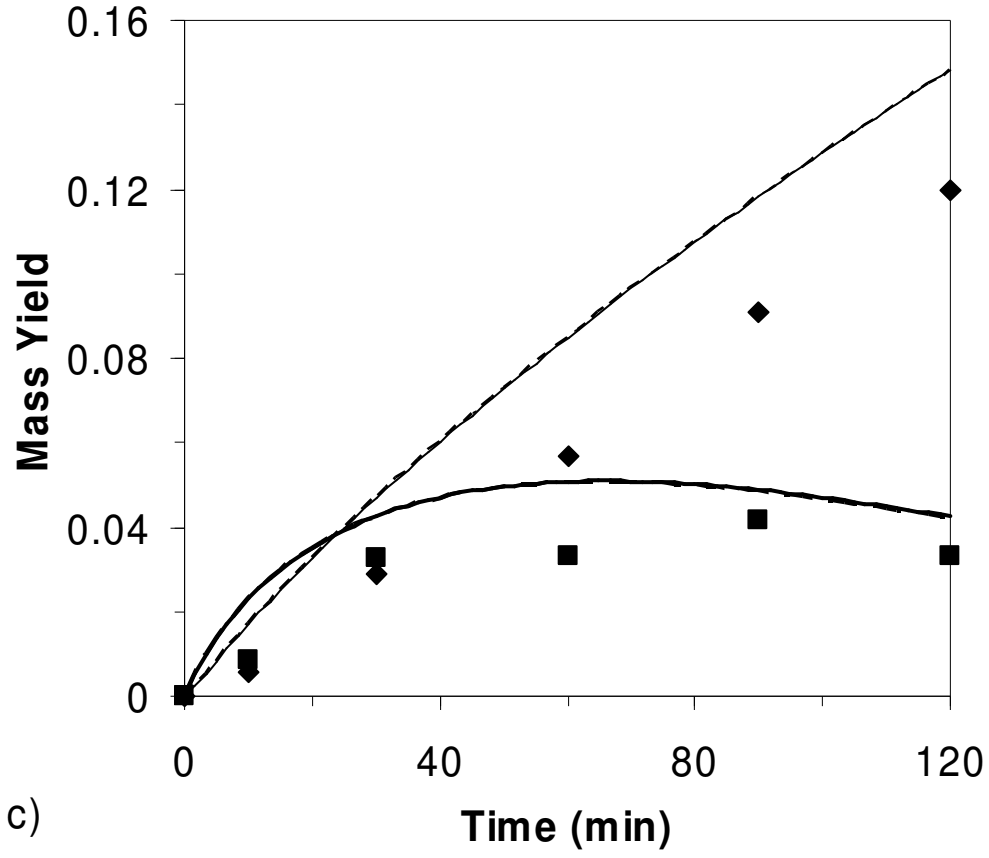

c)

Figure 6.3: Continued

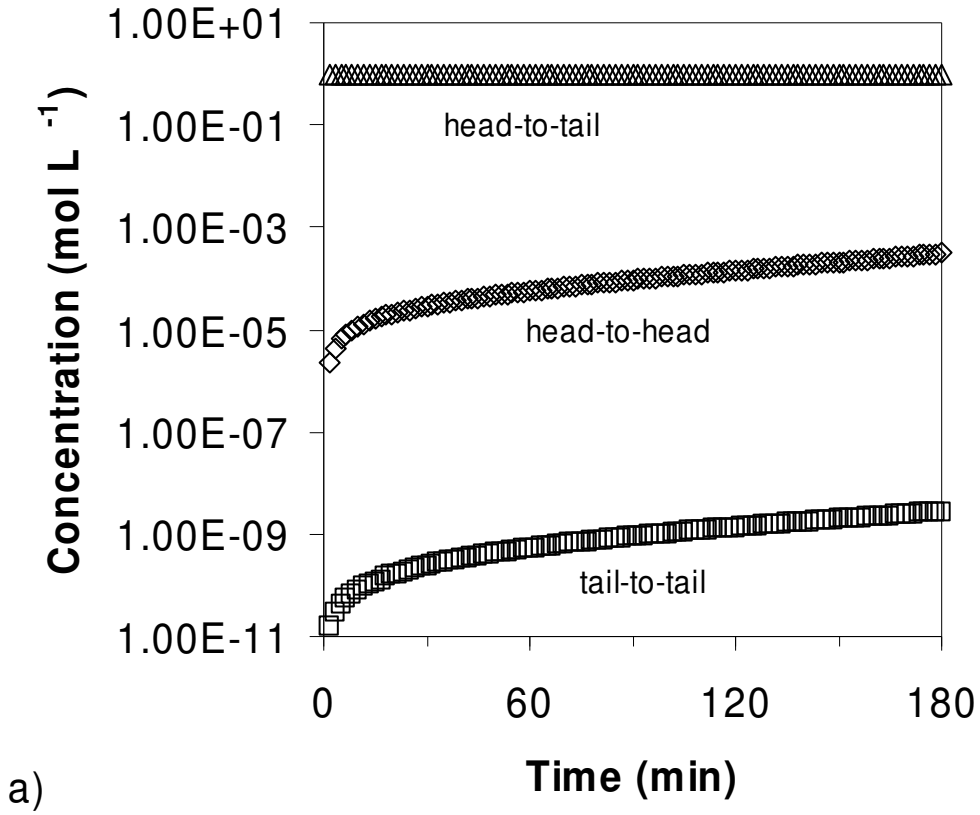

Figure 6.4: Concentration profiles for (a) bonds and (b) triads for pyrolysis of polystyrene with a M_{n0} = 113,000 and M_{w0} = 280,000 at 350 °C.

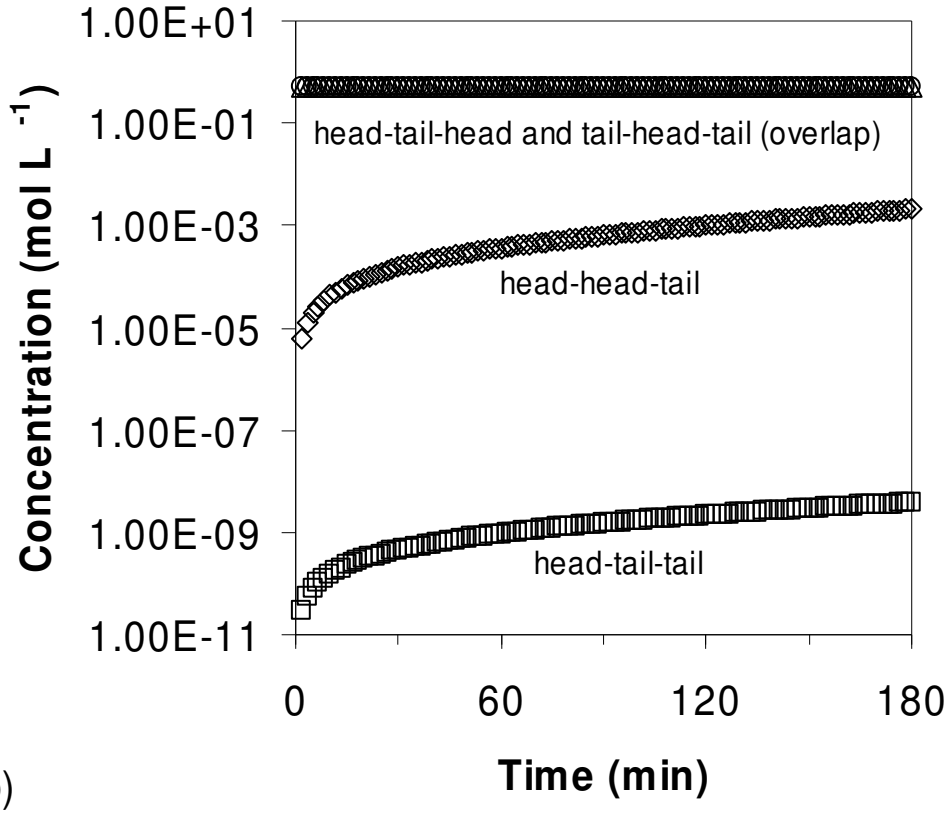

b)

Figure 6.4: Continued

that the triads demonstrate the same behavior as the bonds in their concentration profiles, as expected. The majority of the triads in the systems are hth and tht triads, each making up close to 50% of the total triads in the system, with smaller amounts of hht and htt triads in the expected order.

To test how the model size expands with the inclusion of more backbone atom types, a model for poly(styrene peroxide) pyrolysis was constructed. The inclusion of oxygen into the backbone of polystyrene allows for 15 triads, excluding the triads that include three of the same backbone atom. This additional variety of triads causes the model size to increase substantially because of the additional combinations of triads involved in various reactions. Table 6.1 shows the way the model scales going from the original polystyrene pyrolysis model without triads to the polystyrene pyrolysis model that includes triads to the poly(styrene peroxide) model. The majority of the model size growth is in the number of reactions included in the model which is not as computationally expensive as increasing the number of species tracked within the model. Nevertheless, it was not possible to solve the moment-based poly(styrene peroxide) model due to the level of stiffness in the model equations, due to the thermal lability of the peroxide bonds.

6.4 CONCLUSIONS

An algorithm for tracking increased structural detail in a method of moments polymer pyrolysis model was developed. This methodology relied on properly partitioning newly included reactions that were necessary to capture the uncertainty about the triads involved in some reaction types. Conditional probabilities were utilized for bond fission, β-scission, and hydrogen abstraction reactions to partition reactions based on the likelihood that they would

Table 6.1: Model size characteristics for addition of triad tracking to polystyrene and poly(styrene peroxide) pyrolysis mechanistic models

Model	Backbone Atom Types	Track Triads?	# of species	# of ODEs	# of Reactions
Polystyrene	Head, Tail	No	75	82	>3,500
Polystyrene	Head, Tail	Yes	85	98	>10,000
Poly(styrene peroxide)	Head, Tail, Oxygen	Yes	157	214	>78,000

occur involving a given triad or triads. The algorithm was validated using a polystyrene pyrolysis model. The model results matched those from a previous version of the polystyrene pyrolysis model that did not include the triad tracking algorithm. The results were also in excellent agreement with experimental data for pyrolysis of polystyrene with M_{n0} = 113,000 and M_{w0} = 280,000 at 350 °C. The bond and triad concentration profiles predicted by the model were consistent with each other and followed expected behavior. The increase in model size that included triad tracking was reported for both the polystyrene model and for a poly(styrene peroxide) model. While the poly(styrene peroxide) model was still a manageable size, it could not be solved to any appreciable extent of degradation due to model stiffness. The application of kinetic Monte Carlo to remedy this is described in the next chapter.

CHAPTER 7

A KINETIC MONTE CARLO MECHANISTIC MODEL OF POLY(STYRENE PEROXIDE) PYROLYSIS

7.1 INTRODUCTION

Polyperoxides are an interesting class of materials which have applications as solid fuels and macroinitiators (Kishore and Mukundan 1986; Subramanian 2003). Unlike conventional peroxides which have one peroxy linkage, polyperoxides contain multiple peroxide bonds in a polymer chain. While they have been extensively studied, a recent review indicated that their reactivity requires further study to allow this class of materials to reach its full potential (Subramanian 2003). Vinyl polyperoxides, alternating copolymers of a vinyl monomer and oxygen, are an important sub-class of polyperoxides. Poly(styrene peroxide) (PSP) is the most extensively studied vinyl polyperoxide, even though it can be difficult to work with because it can become explosive above 100 °C. Additionally, PSP provides a model for studying how peroxide bonds affect polystyrene pyrolysis.

The thermal degradation of PSP was initially studied over 50 years ago by Mayo and Miller (1956). Their early work studied the pyrolysis of PSP under a wide range of conditions including temperature, pressure, and solvent. Their results showed that there were two major pyrolysis products from PSP: benzaldehyde and formaldehyde, which made up at least 80 wt. % of the products during pyrolysis of PSP without a solvent. They also identified two minor products from PSP pyrolysis: α-hydroxy acetophenone and phenyl glycol, which were found to

make up from 2 - 10 wt. %, with the majority being α-hydroxy acetophenone. Their results led to the proposal of a basic mechanism of degradation, which involved unzipping of radical chains to form benzaldehyde and formaldehyde. To form the minor products, Mayo and Miller (1956) proposed a mechanism of successive disproportionation reactions. These proposed mechanisms can be seen in Figure 7.1.

The pyrolysis of PSP has been studied since the work of Mayo and Miller primarily by Kishore and coworkers (Kishore 1981; Kishore and Mukundan 1986; Kishore et al. 1980; Kishore and Ravindran 1982, 1983; Singh et al. 2002). The activation energy for PSP pyrolysis was calculated using TGA and DSC techniques to be between 30 and 32.5 kcal mol^{-1} which is in agreement with reported values for the bond dissociation energy for peroxide bonds (Kishore 1981; Kishore et al. 1980). In another study, the thermal degradation of PSP was examined at temperatures up to 450 °C, and the basic product spectrum was analyzed with a focus on the major products, benzaldehyde and formaldehyde (Kishore and Ravindran 1983). This study showed similar product spectra over a wide range of temperatures suggesting that the mechanism does not change at temperatures up to 450 °C. Their product yields were similar to those seen by Mayo and Miller, where benzaldehyde and formaldehyde made up the majority of the products, i.e., up to 97 wt. %. The split between the two major products was shown to approximately correspond to an equimolar product distribution, which is ~78 wt. % benzaldehyde and ~22 wt. % formaldehyde. While these studies offered many important details about PSP pyrolysis, they did not challenge nor confirm the mechanism proposed by Mayo and Miller. The Mayo and Miller mechanism has never been rigorously tested utilizing a detailed mechanistic model for PSP pyrolysis.

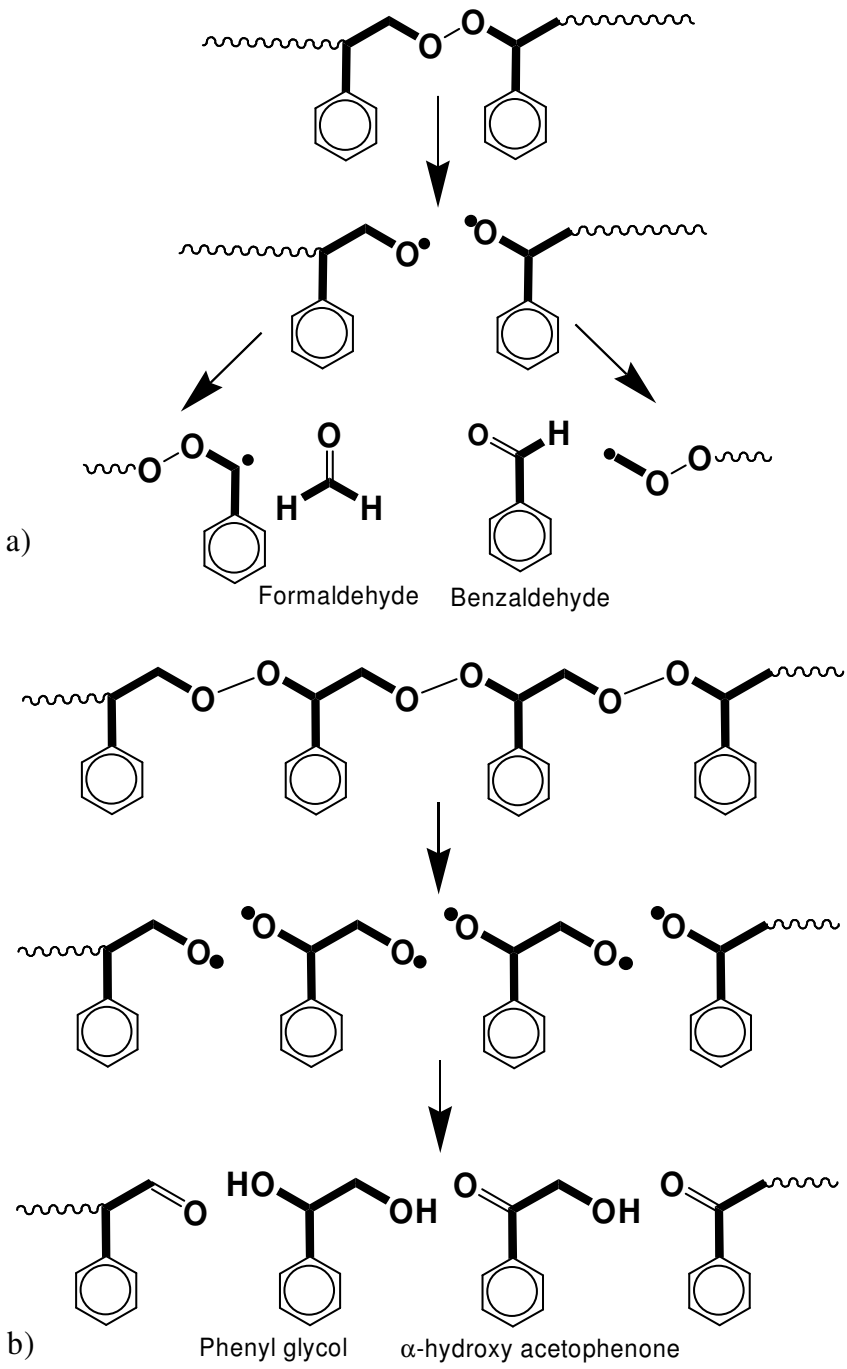

Figure 7.1: (a) Unzipping mechanism and (b) disproportionation mechanism for product formation during poly(styrene peroxide) pyrolysis proposed by Mayo and Miller (1956).

Kinetic Monte Carlo (KMC) modeling is an alternative approach to traditional continuum modeling which utilizes a stochastic approach originally developed by Gillespie (1976). While traditional deterministic models for polymer degradation systems are forced to use lumping techniques, such as the method of moments, because of the large number of species and reactions involved, a KMC model explicitly tracks every species in the system. KMC models track discrete particles in a scaled homogeneous reaction volume instead of overall species' concentrations. Traditional continuum models for polymer degradation require the use of numerical solvers to solve very stiff sets of differential equations that make up these models. In KMC models an iterative approach is utilized which does not require the simultaneous solution of multiple differential and algebraic equations so difficulties like the stiffness of the system are not encountered.

KMC models have rarely been utilized to study polymer degradation systems. This is because the size of polymer degradation systems often makes the formulation of a KMC model difficult. The possible reaction channels specific to every species in the system must be included in the KMC model. As one increases the number of reactants and reaction channels, the solution of a KMC model becomes slower and more computationally prohibitive (Gillespie 2007; McDermott et al. 1990). The work of McDermott et al. (1990) is one of the earliest uses of a KMC model for a polymer degradation system. McDermott et al. utilized a KMC model to study the degradation of the model lignin polymer, poly(veratryl β-guaiacyl ether). Their simulation was based on fixed time steps and was carried out allowing one chain to decompose independently at a time since only unimolecular decomposition steps were considered. Pinto and Kaliaguine (1991) applied a KMC framework similar to that of McDermott et al. to model acid hydrolysis of polysaccharides. Libanati and coworkers (1993) developed a KMC model using a

dynamic reaction lattice to study the pyrolysis of poly(arylether sulfones). The use of a lattice-based simulation allowed gelation to be modeled, which was characterized using percolation theory. Additionally, general polymer degradation Monte Carlo models have been used to study the evolution of the polymer molecular weight distribution (Bose and Git 2004; Giudici and Hamielec 1996; Tobita 1996a, 1996b). These studies make use of chain scission probabilities to study the breakdown of polymeric chains, but these chain scission probabilities are not related to rate coefficients of elementary reaction steps. KMC modeling has also been used to look into peroxide-initiated degradation of polypropylene to refine estimation techniques for the scission rate constant and the initiator efficiency (Huang et al. 1997; Huang et al. 1995). While these studies demonstrated the value of KMC models for understanding polymer degradation systems, the application of the technique to specific polymer degradation systems to test mechanistic assumptions has been limited.

In this research, a KMC model for PSP pyrolysis was developed, based on the modeling framework first formulated by Gillespie (1976). The model results were compared to existing data for PSP pyrolysis in the literature. The model allowed for the existing mechanistic assumptions about product formation during PSP pyrolysis to be tested. Additionally, alternative reaction pathways were included in the model to demonstrate the ability of these new reaction pathways to account for experimentally observed products. Finally, the role that trace peroxide bonds may play as a structural heterogeneity in polystyrene pyrolysis is discussed in light of the PSP mechanism of degradation.

7.2 MODELING FRAMEWORK

7.2.1 Kinetic Monte Carlo Formulation

The simple stochastic framework formulated by Gillespie (1976) is the basis of most KMC models. Reactions are defined by how they explicitly alter the number of species of different types in a scaled homogeneous reaction volume. Each reaction is assigned a probability based on its current reaction rate and the sum of the rates of all possible reactions, as shown in Equation 7.1:

$$p_r = \frac{R_r}{\sum_{i=1}^{T} R_i} \tag{7.1}$$

where p_r is the probability of reaction r occurring, R_i is the reaction rate for reaction i, and T is the total number of all possible reactions. The probabilities for each possible reaction in the system make up a reaction probability distribution. A reaction is chosen by selecting a random number between zero and one and determining to which reaction in the reaction probability distribution it corresponds. This stochastic reaction selection procedure is described by Equation 7.2:

$$\sum_{i=1}^{r-1} p_i < x_1 < \sum_{i=1}^{r} p_i \tag{7.2}$$

where x_1 is the random number and r is the index of the selected reaction. The time step of the selected reaction is based on another random number between zero and one and the sum of all possible reaction rates. Gillespie (1976) derived Equation 7.3 to determine the time step for a stochastic reaction event:

$$\tau = \frac{1}{\sum_{r=1}^{T} R_i} \ln\left(\frac{1}{x_2}\right) \qquad (7.3)$$

where τ is the time step and x_2 is the second random number. These equations for selecting reactions and stepping through time provide the basic framework for a KMC model.

7.2.2 Level of Detail

The KMC modeling framework utilizes explicit species in a scaled homogeneous reaction volume. Species in our PSP pyrolysis model were either polymer chains or low molecular weight products (LMWP). LMWP tracked included the major products, benzaldehyde and formaldehyde, as well as the minor products α-hydroxy acetophenone and phenyl glycol. Additional LMWP derived from methyl and benzyl radicals were allowed to form. Methyl and benzyl radicals were formed based on the initial chain ends specified for the polymeric species in the model. The products derived from methyl and benzyl radicals were lumped together as product species which did not have any experimental data available for comparison. Polymeric chains were divided into separate species based on their chain end types. Within a species, each individual chain was tracked explicitly. Each chain tracked the explicit number of benzylic and non-benzylic carbons as well as oxygen atoms bound to benzylic and non-benzylic carbons. The number of peroxide bonds in each chain was also tracked. The chain end types used to separate polymeric species are shown in Figure 7.2. To limit the demand on computer memory required by the model, the explicit chain topology of polymer chains was not tracked.

In the first generation model, the reactions necessary to fully implement the traditional mechanism found in the literature were included in the model. These included the elementary

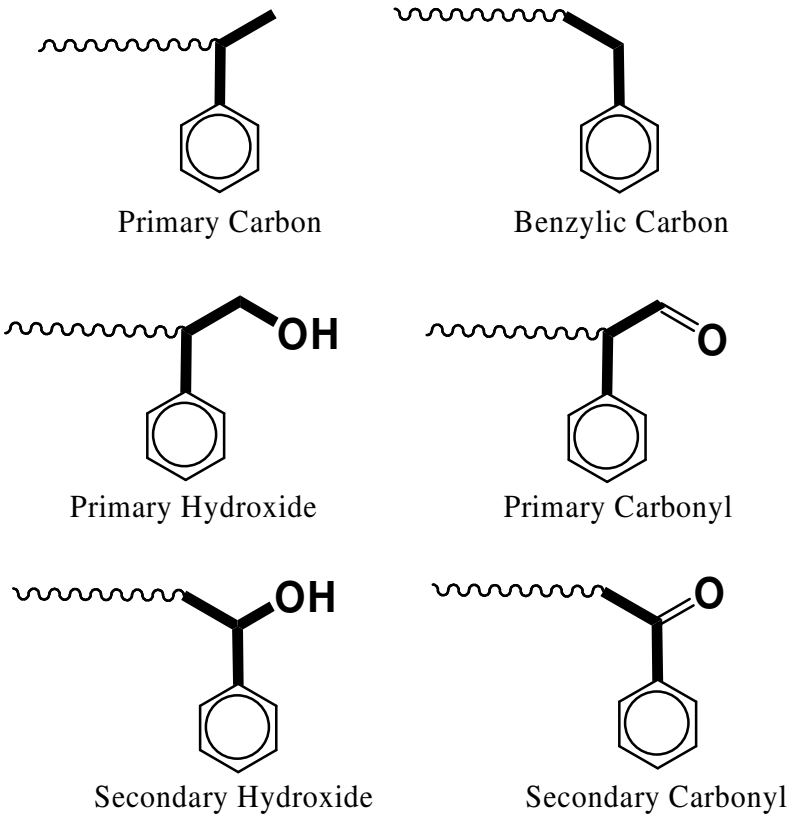

Figure 7.2: Chain end types used to describe polymeric species in the poly(styrene peroxide) pyrolysis model. Individual chains were tracked explicitly in the model.

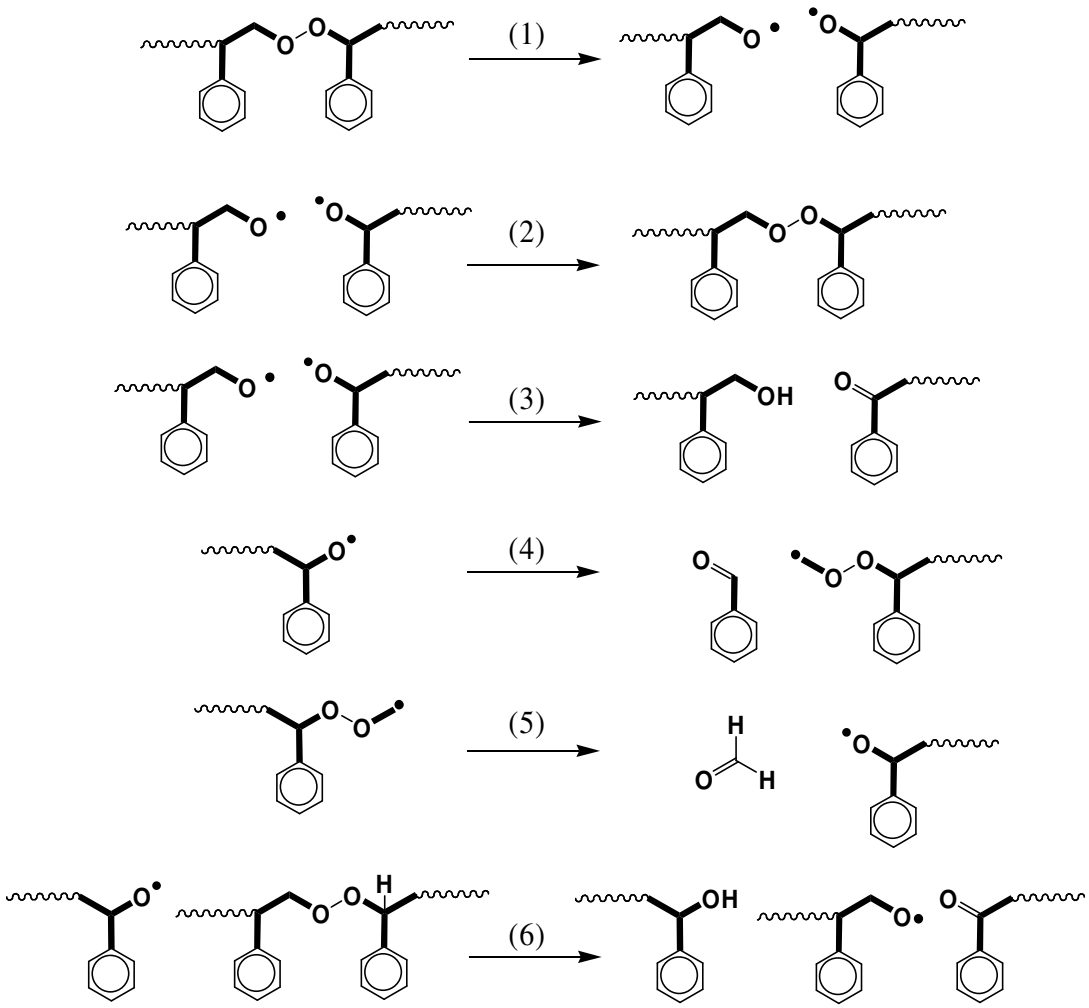

Figure 7.3: Examples of reaction types utilized in the KMC model for poly(styrene peroxide) pyrolysis: (1) peroxide bond fission; (2) alkoxy radical recombination; (3) alkoxy radical disproportionation; (4) alkoxy radical β-scission; (5) peroxide bond β-scission; (6) hydrogen abstraction/mid-chain peroxide β-scission

reaction families (1) peroxide bond fission, (2) alkoxy radical recombination, (3) alkoxy radical disproportionation, (4) alkoxy radical β-scission, and (5) peroxide bond β-scission. Examples of these reactions are shown in Figure 7.3. Peroxide β-scission is used to describe the β-scission of a carbon radical that results in cleavage of a peroxide bond. In the second generation model, a reaction that lumps hydrogen abstraction of a mid-chain benzylic hydrogen and mid-chain peroxide β-scission was included to test alternative routes to the formation of the minor products. These two reactions were lumped together to maintain a manageable model size. By grouping the reactions together mid-chain radicals do not need to be tracked. Combining the reactions was justified by comparing the rate of mid-chain peroxide β-scission to the rates of other reactions possible for mid-chain radicals. The β-scission reaction rate was typically found to be over ten orders of magnitude higher than the other possible reactions because of the facile cleavage of peroxide bonds. An example of the lumped reaction is shown as reaction six in Figure 7.3.

7.2.3 Rate Parameter Specification

Rate parameters were specified using an approach that is similar to the one our research group has utilized in our previous continuum modeling of polymer pyrolysis (Kruse et al. 2005; Kruse et al. 2003b; Kruse et al. 2002). Rate parameters were not only dependent on the reaction type but were also linked to the structure and thermodynamics of the reactants and products. To establish this link between structure and reactivity, the Evans-Polanyi relationship (Evans and Polanyi 1938) and the Blowers-Masel relationship (Blowers and Masel 1999) were used. These correlations relate the activation energy of a reaction to the heat of reaction. The Blowers-Masel

relationship was used for hydrogen abstraction reactions, while the Evans-Polanyi relationship was utilized for the other reaction families included in the model.

Arrhenius behavior was assumed for all reactions, requiring a frequency factor and the parameters for either the Evans-Polanyi or Blowers-Masel relationship be specified. Frequency factors and the Evans-Polanyi and Blowers-Masel parameters were assumed to be constant for a given reaction family. Table 7.1 summarizes the rate parameters utilized in the KMC model. The majority of these parameters were taken from our previous values that were developed for polystyrene pyrolysis (Levine and Broadbelt 2008). All heats of reaction other than the heat of reaction for peroxide bond fission were calculated using Benson group additivity (Benson 1976). The heat of reaction for peroxide bond fission was varied within a range determined from experimentally reported bond dissociation energies for peroxide bonds of 32-37 kcal mol^{-1} (Dean 1973; Weast et al. 1986). The heats of reaction calculated for the peroxide β-scission reactions combined with the Evans-Polanyi parameters utilized for β-scission reactions yielded negative activation energies. This is not unexpected based on the instability of carbon radicals when the radical center neighbors a peroxide bond. Previous work in our research group studying lubricant degradation found similar behavior. In this earlier work, DFT calculations were unable to find an optimized geometry for C•OOH radicals; instead the more stable β-scission products were obtained (Pfaendtner and Broadbelt 2008). The standard procedure when an Evans-Polanyi correlation yields a negative activation energy is to assume the reaction is unactivated. Thus, end-chain peroxide β-scission was assigned an activation energy of zero and mid-chain peroxide β-scission was lumped in with the hydrogen abstraction reaction that formed the unstable mid-chain radical that neighbored a peroxide bond. Additionally, end-chain primary and benzylic

Table 7.1: Rate parameters utilized in the poly(styrene peroxide) pyrolysis KMC model

Reaction Type	Frequency Factor, A (s^{-1} or L mol^{-1} s^{-1})	Intrinsic barrier, E_0 (kcal mol^{-1})	Transfer Coefficient, α	ΔH_{rxn} (kcal mol^{-1})	Activation Energy, E_a (kcal mol^{-1})
Peroxide bond fission	$1.00x10^{16}$ [a]	2.3 [a]	1	32 – 37 [c]	34.3 – 39.3
Alkoxy radical recombination	$1.10x10^{11}$ [a]	2.3 [a]	0	-32 – -37 [c]	2.3
Alkoxy radical disproportionation	$1.65x10^{10}$ [a] [b]	2.3 [a]	0	NA	2.3
Primary alkoxy radical β-scission	$3.10x10^{12}$ [a]	11.4 [a]	0.76	-6.45 [d]	6.5
Secondary alkoxy radical β-scission	$3.10x10^{12}$ [a]	11.4 [a]	0.76	4.3 [d]	14.7
Peroxide β-scission	$3.10x10^{12}$ [a]	11.4 [a]	0.76	-36.5 [d]	0 [e]
Alkoxy radical hydrogen abstraction [f] [g]	$2.10x10^{6}$ [a]	12 [a]	NA	-20.1 [d]	4.0
Benzyl radical hydrogen abstraction [g]	$2.10x10^{6}$ [a]	12 [a]	NA	-0.3 [d]	11.9

[a] Parameters taken from previous polystyrene pyrolysis modeling work (Levine and Broadbelt 2008)
[b] Disproportionation was assumed to be 15% of recombination based on Schreck et al. (1989)
[c] Peroxide bond fission varied within reported range of peroxide bond dissociation energies (Dean 1973; Weast et al. 1986)
[d] Heats of reaction estimated using Benson group additivity (Benson 1976)
[e] Peroxide β-scission assumed to be unactivated because Evans-Polanyi predicts a negative activation energy
[f] The alkoxy radical hydrogen abstraction rate parameters were also used for methyl radicals, based on the similarity of the group additivity estimations of their ΔH_{rxn} values
[g] Only alkoxy, methyl, and benzyl radicals were allowed to undergo hydrogen abstraction due to the facility of the peroxide β-scission reaction available to long-chain carbon radicals

carbon polymeric radicals were not allowed to undergo hydrogen abstraction based on the facility of the competing peroxide β-scission reaction. The specified rate parameters were developed on a macroscopic per volume basis, but for KMC models the reaction rates need to be based on the total number of molecules in the scaled volume used in the model. In KMC models the explicit number of reactant molecules is used in place of concentration to calculate reaction rates. Gillespie (1976) derived conversions between macroscopic rate constants and the stochastic rate constants required by the KMC model. These relationships are shown in Equations 7.4, 7.5, and 7.6:

$$k_i^{KMC} = k_i^{macro} \tag{7.4}$$

$$k_{ii}^{KMC} = \frac{2k_{ii}^{macro}}{VN_A} \tag{7.5}$$

$$k_{ij}^{KMC} = \frac{k_{ij}^{macro}}{VN_A} \tag{7.6}$$

where k_i is a rate constant for a first order reaction, k_{ii} is a rate constant for a second order reaction between the same species, k_{ij} is a rate constant for a second order reaction between different species, V is the scaled reaction volume, N_A is Avogadro's number, and the superscripts *KMC* and *macro* indicate if the rate constant is the stochastic or macroscopic version, respectively.

7.2.4 Model Assembly and Solution

The model was constructed using the C++ programming language. All possible reaction events that could occur based on the reaction types allowed and the species included in the model were specified, and how a given reaction would alter the makeup of the explicit species in the

scaled reaction volume was defined. The model was initialized with a specific number of PSP chains. All initial PSP chains were assumed to have a molecular weight of 5002 and to be capped with styrene units, so that one end was a benzylic carbon and one end was a primary carbon. This meant that all initial PSP chains had 36 peroxide bonds. The initial molecular weight was chosen based on typical molecular weights in studies of PSP polymerization that have been reported, which have indicated that it is difficult to synthesize PSP with molecular weights above about 5000 (Subramanian 2003). Most studies of PSP pyrolysis do not present any molecular weight data for the polymer used. The scaled volume of the system was determined based on a volume per chain calculated from the density of polystyrene at 100 °C equal to 841 g L^{-1}, since density data for PSP was unavailable. All model results presented in this work used an isothermal temperature of 100 °C. As discussed in the results, the initial number of PSP chains in the system was increased until the results converged.

To solve the model, the basic procedure outlined by Gillespie (1976) was used. First, the rates for all reactions specified in the model were calculated based on the current explicit species makeup using Equation 7.1. A random number from zero to one was generated to select which reaction occurs using Equation 7.2. For the given reaction, the species that undergo the reaction were randomly selected from the relevant reactant molecules currently in the system. The explicit species' makeup was then altered according to the rules of the chosen reaction. Another random number from zero to one was generated and used to determine the size of the time step for this reaction event using Equation 7.3. These steps were repeated to move through time until a specified time was reached. For the PSP pyrolysis simulations performed in this work, the model was run to six hours of degradation.

Certain reactions have reaction path degeneracy that needed to be taken into account when their reaction rates were calculated. For peroxide bond fission and hydrogen abstraction reactions, there is reaction path degeneracy based on the number of peroxide bonds and the number of abstractable hydrogens, respectively. For these reactions, the number of reactant species was replaced by the number of reactive moieties, either peroxide bonds or abstractable hydrogens, to calculate the reaction rates. When these types of reactions were selected, the species that underwent the reaction was randomly chosen based on weighting the possible reactants according to the number of relevant reactive moieties in each individual species.

7.3 RESULTS AND DISCUSSION

7.3.1 Traditional Mechanism

The KMC model for PSP pyrolysis was initially constructed utilizing only reactions involved in the traditional mechanism described by Mayo and Miller (1956) as shown in Figure 7.1. This version of the model utilized reactions one through five as depicted in Figure 7.3. The model included 147 specific reaction events. The model was initially solved using a heat of reaction for peroxide bond fission of 37 kcal mol^{-1}, and the number of initial PSP chains in the system was varied until the model converged. These results are compared with the percentage of peroxide bonds remaining as a function of time reported in the experimental data of Mayo and Miller (1956) in Figure 7.4. It can be seen that the model results converged, based on the overlay of the curves, with the initial number of polymer chains set to $1x10^5$ based on the similarity between the results for $1x10^5$ and $1x10^6$ initial polymer chains. It is also clear from these results that the rate of degradation predicted by the model is too slow compared to the experimental results.

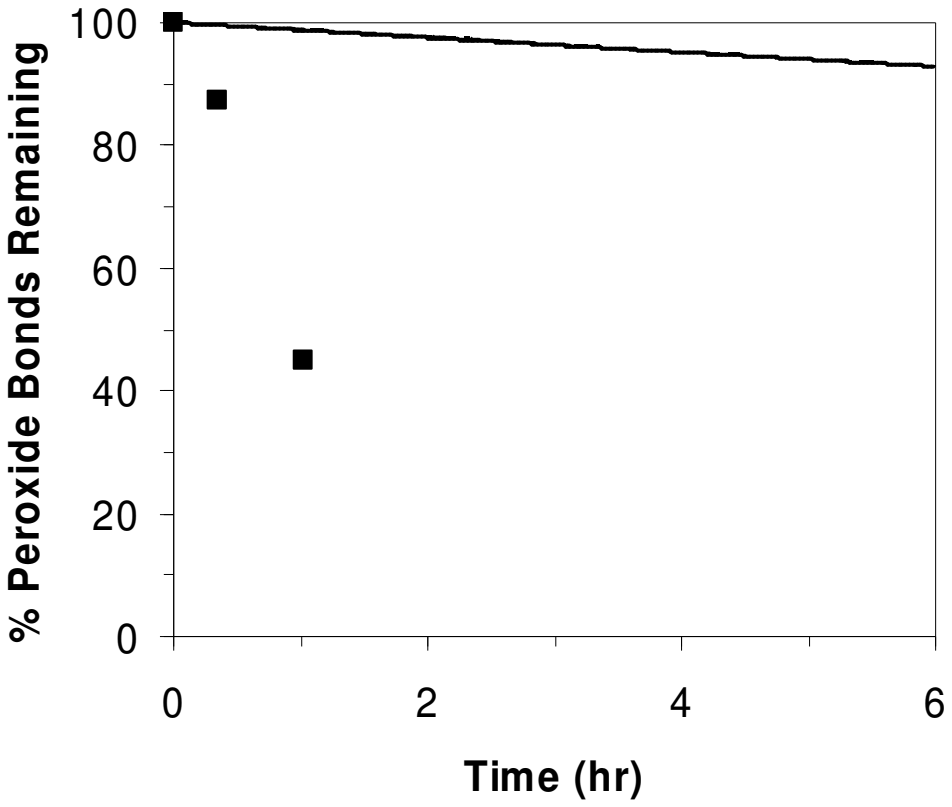

Figure 7.4: KMC model results for the pyrolysis of PSP at 100 °C using a heat of reaction for peroxide bond fission of 37 kcal mol^{-1} and an initial number of PSP chains in the system of $1x10^4$ (——), $1x10^5$ (– –), and $1x10^6$ (——) compared with the experimental data (■) of Mayo and Miller (1956). It should be noted that all three model curves overlay with each other.

To achieve better agreement with the experimental results, the heat of reaction for peroxide bond fission was lowered within the acceptable range shown in Table 7.1. It was found that a heat of reaction of 34 kcal mol^{-1} for peroxide bond fission achieved excellent agreement of the model results with the experimental data of Mayo and Miller (1956) as shown in Figure 7.5. The model results still converged with an initial number of chains of $1x10^5$. It should be noted that the Mayo and Miller data set includes one more data point for the percentage of peroxide bonds remaining during PSP pyrolysis at 18 hours that indicates near complete degradation at that time. While the model was not run out to 18 hours, it can be seen from Figure 7.5 that if the model results were extrapolated to 18 hours, close to zero percent peroxide bonds remaining would be predicted.

Given that the overall rate of degradation is captured very well by the model, the model results were next analyzed to quantify the product distribution that was predicted. The results obtained with $1x10^6$ initial chains revealed that only the major products, benzaldehyde and formaldehyde, were formed. The two major products were formed in near equimolar amounts, resulting in 78 wt. % benzaldehyde and 22 wt. % formaldehyde. There was no formation of the minor products. While these results supported the unzipping mechanism to form the major products, they also showed that the alkoxy radical termination reactions were not competitive with the unzipping reactions. Instead, the kinetic chain was controlled by termination reactions between methyl and benzyl radicals formed when a PSP chain fully unzips, which were present based on the chain architecture assumed in the initial PSP chains.

These results indicated that the mechanism of successive disproportionation reactions to form phenyl glycol and α-hydroxy acetophenone proposed by Mayo and Miller (1956) was

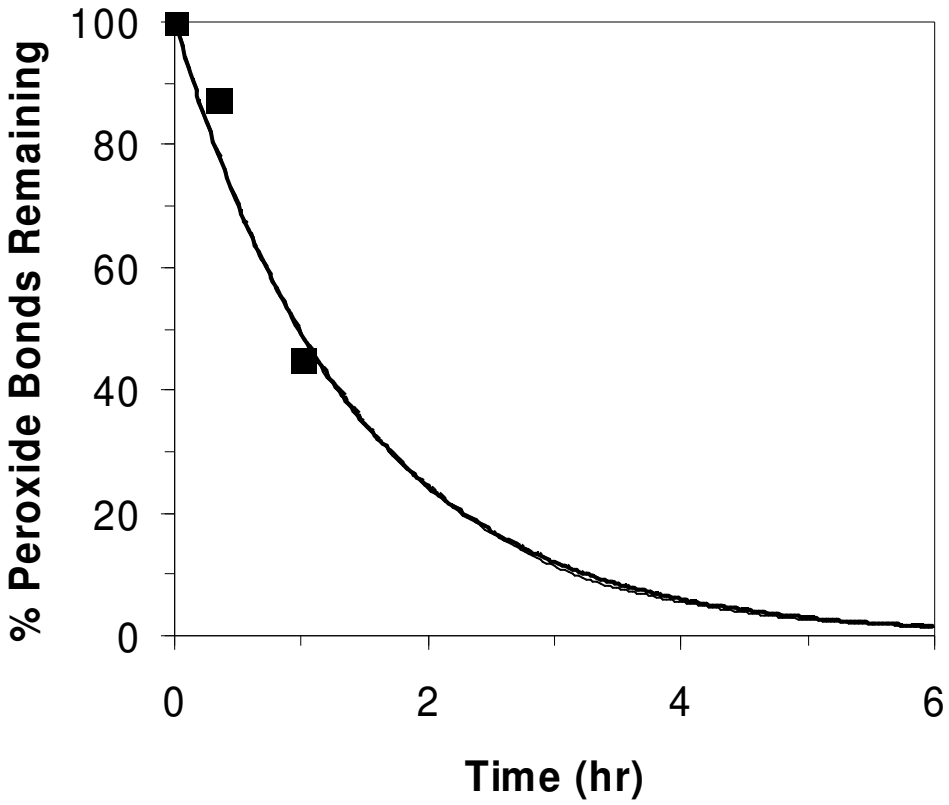

Figure 7.5: KMC model results for the pyrolysis of PSP at 100 °C using a heat of reaction for peroxide bond fission of 34 kcal mol^{-1} and an initial number of PSP chains in the system of $1x10^4$ (——), $1x10^5$ (– –), and $1x10^6$ (▬) compared with the experimental data (■) of Mayo and Miller (1956). It should be noted that the experimental data set includes a point at 18 hours indicating near total degradation (not shown). It should be noted that the model curves overlay each other.

insufficient. As indicated in Table 7.1, disproportionation was assumed to be 15% of the recombination rate based on the work of Schreck et al. (1989). To further test the successive disproportionation mechanism, the rate coefficient for alkoxy radical disproportionation was increased to ten times the original rate coefficient for alkoxy radical recombination, while alkoxy radical recombination was not allowed. The rate of degradation results were still in good agreement with the data of Mayo and Miller, but even with artificially inflated disproportionation rates, only negligible amounts of the minor products were formed after six hours of degradation. The two minor products made up less then 0.003 wt. % of the pyrolysis products, while the expected yield of the minor products is 2-10 wt. %. Increasing the disproportionation rate constant even more significantly would increase the yield of the minor products further, but a rate constant above the Smoluchowski limit would be required (Cussler 1997). These results indicate that alternative routes to the formation of the observed minor products of PSP pyrolysis are necessary.

7.3.2 Role of Hydrogen Abstraction

The minor products, α-hydroxy acetophenone and phenyl glycol, can be formed by successive hydrogen abstraction reactions as an alternative to the traditional successive disproportionation mechanism. Examples of these new reaction pathways are provided in Figure 7.6. All possible hydrogen abstraction reactions for small radicals and alkoxy radicals were included in the model. Polymeric carbon radicals were not allowed to undergo hydrogen abstraction because of the facility of the peroxide β-scission reaction. The inclusion of these reactions resulted in a total of 287 specific types of reaction events in the model. Because these reactions provide additional facile channels that lead to peroxide bond cleavage, their

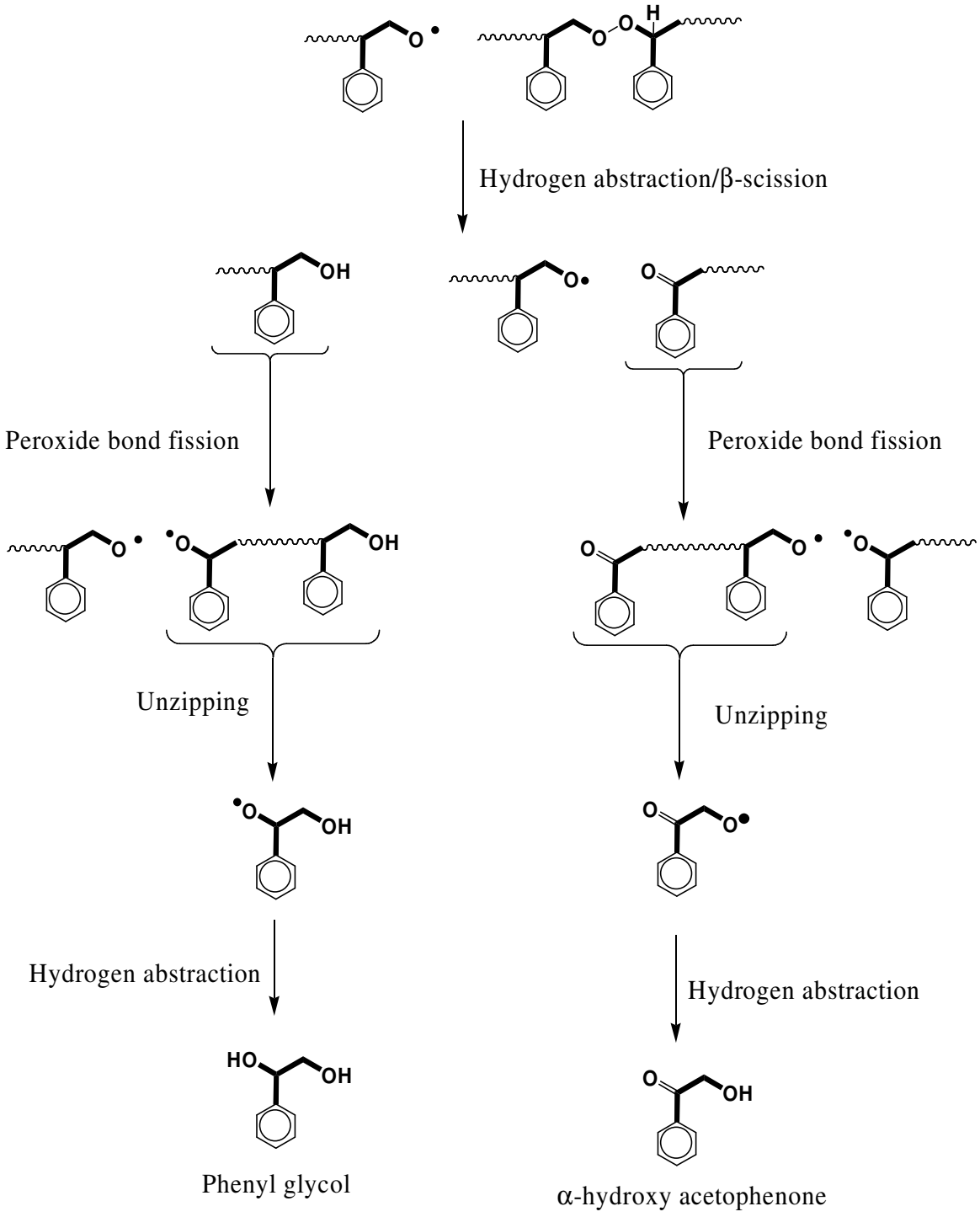

Figure 7.6: Examples of new reaction pathways to phenyl glycol and α-hydroxy acetophenone utilizing hydrogen abstraction reactions.

implementation altered the rate of degradation in the model results. To once again obtain good agreement with the experimental data of Mayo and Miller (1956), the heat of reaction for peroxide bond fission was varied. It was found that a heat of reaction of 34.2 kcal mol^{-1} resulted in excellent agreement between the model results and the experimental data. This value is very similar to the value of 34 kcal mol^{-1} used for the model that did not include hydrogen abstraction, but the model results are very sensitive to the peroxide bond fission kinetics. The convergence of this expanded model was more difficult to achieve because of the increased complexity of the model and its associated increase in computational time. An initial number of chains of $1x10^5$ was found to be insufficient, as revealed by the large deviation of the results obtained with $1x10^5$ and $1x10^6$ initial PSP chains. Preliminary results with $1x10^7$ initial PSP chains indicate that the model may converge around $1x10^6$ initial chains; however, complete runs with $1x10^7$ and $1x10^8$ initial chains are still in progress. The model results compared with the experimental data are shown in Figure 7.7.

The model results for the simulations with $1x10^6$ initial PSP chains with the hydrogen abstraction reactions included were analyzed to quantify the product spectrum. The yields of the four experimentally observed products at the end of six hours were 72.7 wt.% benzaldehyde, 21.2 wt. % formaldehyde, 1.3 wt. % phenyl glycol and 4.8 wt. % α-hydroxy acetophenone. These are in very good agreement with the typical product yields that have been observed experimentally from PSP pyrolysis (Kishore and Ravindran 1983; Mayo and Miller 1956; Subramanian 2003). Benzaldehyde and formaldehyde are still formed in a near equimolar ratio, but the unzipping products are no longer the only products formed in the model. The model results are also nicely consistent with the experimental observation that the yield of α-hydroxy

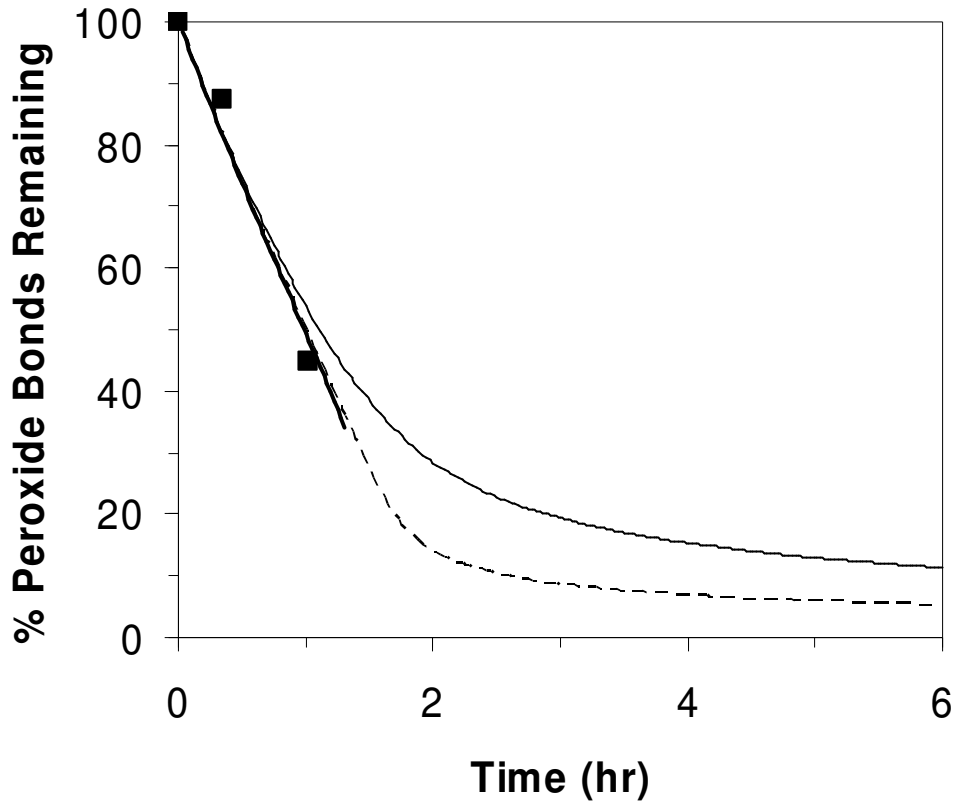

Figure 7.7: KMC model results including hydrogen abstraction reactions for the pyrolysis of PSP at 100 °C using a heat of reaction for peroxide bond fission of 34.2 kcal mol^{-1} and an initial number of PSP chains in the system of $1x10^5$ (——), $1x10^6$ (– –), and $1x10^7$ (▬) compared with the experimental data (■) of Mayo and Miller (1956). It should be that noted the experimental data set includes a point at 18 hours indicating near total degradation (not shown).

acetophenone is higher than that of the other minor product, phenyl glycol. It is clear from these results that the hydrogen abstraction pathways can yield significant amounts of the minor products of PSP pyrolysis.

7.3.3 Role of Peroxide Bonds in Polystyrene Pyrolysis

Although only a regular copolymer was studied here, the behavior of the alkoxy radicals formed from peroxide bond fission during PSP pyrolysis can be illustrative of the role of trace peroxide bonds in polystyrene during pyrolysis. The PSP mechanistic model discussed above demonstrated that the alkoxy radicals formed from peroxide bond fission primarily undergo alkoxy β-scission or hydrogen abstraction. Both of these reactions will yield carbon radicals which can undergo (de)propagation reactions found in polystyrene pyrolysis to further the degradation. This indicates that the presence of peroxide bonds in polystyrene should result in an increase in the initial rate of degradation, because the peroxide bonds are much more thermally labile than the carbon-carbon bonds comprising the polystyrene backbone. Peroxide bonds, if present at all, would be expected only in trace quantities in polystyrene. This would result in only trace amounts of the unzipping products, benzaldehyde and formaldehyde, or trace amounts of hydroxide chain ends, depending on which propagation reaction an alkoxy radical undergoes. Thus, an increased rate of degradation may be the only sign of the presence of peroxide bonds in polystyrene because the yields of products derived from peroxide bonds would be too low to be detected experimentally. Although the model would be more complex because the structure and composition of the initial chains would be polydisperse, it is conceivable that

the KMC modeling framework presented here would allow the role of trace peroxide bonds in polystyrene pyrolysis to be explored quantitatively.

7.4 CONCLUSIONS

A KMC model for PSP degradation was developed utilizing the traditional mechanism found in the literature as well as including hydrogen abstraction and mid-chain peroxide β-scission reactions which are not part of the traditional mechanism. The model that only included the traditional mechanism used 147 specific reaction events. The full model with the hydrogen abstraction reactions used 287 specific reaction events. Both versions of the model were able to capture experimental data in the literature for overall degradation, shown as the percentage of peroxide bonds remaining (Mayo and Miller 1956). The model utilizing only the traditional mechanism utilized a heat of reaction for peroxide bond fission of 34 kcal mol^{-1}, while the model including hydrogen abstraction utilized a heat of reaction for peroxide bond fission of 34.2 kcal mol^{-1}, both of which sit squarely in the range of peroxide bond strengths reported experimentally. In both models, the majority of the products formed were benzaldehyde and formaldehyde. The unzipping reaction pathway was found to be sufficient to form these products. However, the model utilizing only the traditional mechanism was unable to produce significant amounts of the minor products that are observed experimentally, phenyl glycol and α-hydroxy acetophenone. The traditional mechanism relies on successive disproportionation steps to form these products. Even a version of the model with enhanced rates of disproportionation was unable to produce more than trace amounts of the minor products, which is not in agreement with the experimental results in the literature.

Successive hydrogen abstraction reactions were proposed as an alternative pathway to the formation of these minor products. The version of the model including hydrogen abstraction reactions was able to produce significant amounts of the minor products. The final product spectrum predicted by the model after six hours of pyrolysis was 72.7 wt% benzaldehyde, 21.2 wt% formaldehyde, 1.3 wt% phenyl glycol and 4.8 wt% α-hydroxy acetophenone, which is in agreement with typical product spectra observed experimentally (Kishore and Ravindran 1983; Mayo and Miller 1956; Subramanian 2003). Thus, we propose that the successive hydrogen abstraction reaction pathway, which is a very typical step in polymer pyrolysis in general, is a viable route for the production of the minor products formed during PSP pyrolysis.

The details of the mechanism of PSP pyrolysis were used to gain insight into the role that trace peroxide bonds can play in polystyrene pyrolysis. Based on the degradation behavior seen during PSP pyrolysis, thermally labile peroxide bonds would be expected to enhance the initial rate of degradation of polystyrene pyrolysis, but the formation of other small products or chain ends associated with the peroxide bonds would be negligible.

This study has demonstrated the power of KMC models of polymer degradation to offer valuable mechanistic insight. They are especially applicable for polymer degradation systems where continuum models are difficult to solve due to the stiffness of the model equations. The application of KMC models to specific polymer degradation systems provides a powerful tool for studying these complex reaction networks.

CHAPTER 8

CONCLUSIONS AND RECOMMENDATIONS

8.1 CONCLUSIONS

Pyrolysis is a promising recycling technique for treating polymeric waste. Polymer pyrolysis systems are characterized by large free radical reaction networks, which often yield diverse product spectra. Even though there is a long history of study, the complexity of polymer pyrolysis systems has made fully understanding the kinetics and mechanisms of these systems difficult. Increased understanding of the kinetic and mechanistic details of polymer degradation systems is critical to the further development of polymer pyrolysis technologies. This work has demonstrated the power of mechanistic modeling of complex polymer degradation systems to provide valuable insight into their kinetic and mechanistic details. We have utilized mechanistic models to probe the kinetics and mechanisms of polystyrene, polyethylene, and poly(styrene peroxide) pyrolysis. Method of moments-based models were used to study polystyrene and polyethylene pyrolysis, while a kinetic Monte Carlo-based model was used to investigate poly(styrene peroxide) pyrolysis.

8.1.1 Polystyrene Pyrolysis Mechanistic Modeling

The research presented in Chapters 3 and 4 discusses the development and utilization of a detailed mechanistic model for polystyrene pyrolysis to study the reaction pathway for formation of styrene dimer (Chapter 3) and the calculation of an overall activation energy free of heat and

mass transfer limitations (Chapter 4). This work demonstrated the power of mechanistic models to provide valuable insight into the kinetic and mechanistic details of complex polymer degradation reaction networks.

The reaction pathway leading to the formation of styrene dimer in polystyrene pyrolysis was traditionally thought to utilize 1,3-hydrogen shift, but recently this hypothesis was abandoned because of the high energy barrier this reaction needs to overcome (Poutsma 2006). Two alternate reaction pathways were recently proposed to account for the formation of styrene dimer: the benzyl radical addition pathway (Ohtani et al. 1990; Poutsma 2006) and the 7,3-hydrogen shift pathway (Moscatelli et al. 2006). By incorporating the relevant reaction families, our mechanistic model for polystyrene pyrolysis was utilized to understand the competition between these reaction pathways, as well as the traditional 1,3-hydrogen shift pathway. The rate parameters for the polystyrene model were updated based on recent work in the literature (Moscatelli et al. 2006; Pfaendtner et al. 2006; Poutsma 2006). The model results were validated against an extensive set of experimental data collected in our research group (Kruse et al. 2002) as well as taken from the literature (Bockhorn et al. 1998; Bouster et al. 1980). Net rate analysis was performed, utilizing the extensive information tracked in the model, to analyze the competition between the three reaction pathways to dimer. The 1,3-hydrogen shift reaction pathway was found to be noncompetitive with the other two reaction pathways. The 7,3-hydrogen shift reaction pathway was dominant over the benzyl radical addition reaction pathway at the conditions studied. The benzyl radical addition pathway became more competitive with increasing temperature due to the rapid increase in the concentration of benzyl radicals as temperature rises.

While the overall activation energy for polystyrene pyrolysis has been determined by numerous experimental studies, an exact value has been difficult to obtain. The range of values reported in the literature for the overall activation energy is over 85 kcal mol^{-1} which cannot be explained by simple experimental error. Heat and mass transport effects have been shown to affect polymer pyrolysis experiments even when conducted with relatively small samples sizes (Szekely et al. 1987). These effects are often assumed to be the cause of much of the large disparity between reported overall activation energies (Westerhout et al. 1997). Our mechanistic model does not include the heat and mass transfer limitations that can complicate the kinetic results of experimental studies. By constructing Arrhenius plots for varying initial degrees of degradation an overall intrinsic activation energy of 53.3 +/- 1.3 kcal mol^{-1} was determined for polystyrene pyrolysis. This value was found to be in good agreement with activation energies derived using Rice-Herzfeld kinetic analysis, demonstrating the importance of the formation of LMWP to the overall polymer degradation. Our definitive activation energy can be used to demonstrate which experimental studies in the literature were the least affected by transport limitations. An additional comparison with experimental data collected by our collaborators using a unique technique that has been shown to be free of transport limitations (Zhao and Bar-Ziv 2000; Zhao et al. 1998) is underway.

8.1.2 Polyethylene Pyrolysis Mechanistic Modeling

Polyethylene pyrolysis has an extremely diverse product spectrum making the competition between the general reaction pathways for product formation difficult to understand. We developed a detailed mechanistic model for HDPE pyrolysis utilizing the method of moments framework. This model was utilized to gain insight into the competition of different

reaction pathways in Chapter 5. The model tracked 151 species, including 48 specific low molecular weight products, and included over 11,000 reactions. The model results were in very good agreement with experimental data for pyrolysis of HDPE with M_{w0} = 125,000 at 420 °C which had been previously collected in our research group (De Witt and Broadbelt 2000). The model was able to predict the time evolution of the formation of specific products, which had not been previously presented by earlier mechanistic models for this polymer degradation system.

Utilizing the detailed information tracked in the model, net rate analysis was done to compare the general reaction pathways: unzipping (UZ), backbiting (BB), and random scission (RS). It was found that UZ was not significant for product formation compared to BB and RS. Overall, RS was more important than BB to the formation of specific products. The contribution of the BB reaction pathway to specific product formation was shown to vary depending on the relative ease of the intramolecular hydrogen shift(s) needed to form different specific mid-chain radicals.

8.1.3 Tracking Additional Structural Detail in Polymer Pyrolysis Mechanistic Models

An algorithm was developed to track backbone triad concentrations in method of moments-based mechanistic models for polymer pyrolysis in Chapter 6. Polymer degradation models are often limited in the level of detail that can be tracked in the model because of the large number of species and reactions involved in the reaction networks. The methodology utilized conditional probabilities to properly partition new reactions in the model. These new reactions were required to remove a level of uncertainty about the triads involved in a given reaction for certain reaction families. The algorithm was validated by constructing a version of the polystyrene pyrolysis model including this algorithm and comparing its results with the

results of the polystyrene pyrolysis model which did not track backbone triads. The bond and triad concentration profiles matched expected behavior. The triad algorithm was found to cause a large increase in the number of reactions included in a model but not to a point of making the models unmanageable. A poly(styrene peroxide) method of moments model was constructed but could not be solved due to the stiffness of the model equations.

8.1.4 Poly(styrene peroxide) Pyrolysis Mechanistic Modeling

The difficulty modeling poly(styrene peroxide) (PSP) pyrolysis using method of moments-based models due to the stiffness of the model equations was overcome by developing a kinetic Monte Carlo (KMC) mechanistic model for PSP pyrolysis. The KMC model was utilized to test the longstanding mechanism for product formation proposed in the literature. The results of the KMC model were in excellent agreement with the limited degradation data available in the literature, as measured by the percentage of peroxide bonds remaining. The lack of detailed data available for the product spectrum obtained during PSP pyrolysis only allowed for qualitative comparison between the model product spectrum and literature data. A version of the PSP pyrolysis model that only utilized the proposed mechanisms in the literature was unable to achieve significant formation of the minor products seen during PSP pyrolysis. The traditional mechanism for minor product formation relied on successive disproportionation reactions. Significant amounts of phenyl glycol and α-hydroxy acetophenone were not obtained even when disproportionation was the only termination reaction allowed. To form these products, successive hydrogen abstraction reactions as well as β-scission of the mid-chain radicals formed as a result of hydrogen abstraction were proposed. The addition of these reaction pathways to the KMC model significantly increased the amount of the minor products

formed during PSP pyrolysis. The final product spectrum of 72.7 wt % benzaldehyde, 21.2 wt % formaldehyde, 1.3 wt % phenyl glycol, and 4.8 wt % α-hydroxy acetophenone is in good agreement with a typical product spectrum for PSP pyrolysis (Subramanian 2003). The need for hydrogen abstraction reactions to form the minor products is a new insight into the degradation behavior of PSP.

The increased understanding of PSP pyrolysis was also used to gain insight into the role of trace peroxide bonds in polystyrene (PS) pyrolysis. The alkoxy radicals formed during the rupture of a peroxide bond in PSP will either abstract hydrogen or undergo end-chain β-scission. Similar behavior would be expected for trace peroxide bonds during PS pyrolysis. This would result in an increase in the observed initial degradation rate because the alkoxy radicals will undergo propagation reactions yielding either end-chain or mid-chain carbon radicals. Trace peroxide bonds in polystyrene would yield only trace quantities of hydroxide chain ends or benzaldehyde and formaldehyde, making their presence difficult to observe experimentally.

8.2 RECOMMENDATIONS FOR FUTURE WORK

While the research discussed in this dissertation has demonstrated the wealth of information that can be gained from the development and utilization of detailed mechanistic models for polymer pyrolysis, there are still many areas where additional research would be beneficial. The tools developed and utilized in the above work can help address additional research questions relating both to polymer degradation systems and to other macromolecular degradation systems.

As discussed in Chapter 1 the makeup of polymeric waste is extremely heterogeneous. Sorting of the plastic waste is one of the most expensive steps involved in polymer recycling

(Aguado 1999). By understanding mixed polymer pyrolysis systems, valuable insight can be gained that will aid in developing pyrolysis technologies for polymer recycling. The models developed in Chapters 3 and 5 for polystyrene and polyethylene coupled with previous research developing a detailed mechanistic model for polypropylene (Kruse et al. 2003b) provide the basis for a model for the mixed pyrolysis of these three major components of polymeric waste. Binary pyrolysis modeling has already been done for polyethylene and polystyrene (Faravelli et al. 2003) and for polypropylene and polystyrene (Kruse et al. 2005) providing guidance for the interactions between the polymers in this mixed pyrolysis system. If this mixed system can be better understood, it would allow the study of pyrolysis of polymers that make up over 65% of polymeric waste.

The development of a binary pyrolysis model for polyethylene and polypropylene would be a key first step in understanding the binary interactions between these two materials. Polypropylene and polyethylene are not miscible so the interactions should be limited to the diffusion of low molecular weight radicals between the two polymer melt phases. This type of interaction has been captured previously for the binary pyrolysis of polypropylene and polystyrene (Kruse et al. 2005). Once the interactions between polypropylene and polyethylene during pyrolysis are understood, the modeling of the mixed system that includes polyethylene, polypropylene and polystyrene can be developed. This model can be used to understand how the polymers in this mixture enhance or retard each other's degradation.

The development of a KMC model for a polymer pyrolysis system provides a large opportunity to further boost our understanding of polymer pyrolysis. The explicit tracking of not only species but also what reactions occur in the KMC framework provides detailed information that was not previously available about these complex reaction systems. I recommend the

development of a KMC model for HDPE pyrolysis. The KMC model would be able to utilize the rate parameters developed for the moment-based model discussed in Chapter 5. This model would be more complicated than the poly(styrene peroxide) pyrolysis KMC model developed in Chapter 7. The simplicity of the polyethylene chain should limit the structural details that need to be tracked for each chain in the system to chain ends, radical position, and chain length, making a KMC model of manageable size possible. Additionally, if the computational time to solve such a model becomes overwhelming there have been numerous techniques developed to accelerate KMC models that may allow the model to be solved faster (Cao et al. 2006; Gillespie 2001, 2007). A polyethylene pyrolysis KMC model would allow the competition between the random scission and backbiting general reaction pathways to be studied explicitly by analyzing specific kinetic chains that occur in the KMC model.

The power of mechanistic models for understanding polymer degradation systems has been demonstrated. I recommend extending the tools utilized in these mechanistic models to other macromolecular degradation systems. The utilization of biomass as a feedstock for fuels and chemicals has received a significant amount of attention recently as a solution to political and environmental concerns over fossil fuel-derived fuels and chemicals (Huber et al. 2006). Pyrolysis to bio-oil is one attractive method of converting biomass to a chemical and fuel feedstock (Mohan et al. 2006). The pyrolysis of biomass is extremely complex making a detailed mechanistic understanding of these systems difficult. Biomass feeds are heterogeneous, being mainly made up of cellulose, hemicellulose, and lignin. I propose that a model for cellulose pyrolysis be developed. Since cellulose is a regular polymer of anhydroglucose units, its structural detail can be tracked in a similar fashion to how structural details of synthetic polymers are tracked in our modeling framework.

Cellulose is the largest single component in biomass, making up 40-50% of most biomass (Mohan et al. 2006). The product spectrum obtained during pyrolysis of cellulose is complex but is mainly made up of levoglucosan (up to 60% of the product), other anhydrosugars, furan/pyran derivatives such as furfural, and small products made up of two to four carbons. While this product spectrum is broad, it could initially be incorporated into a mechanistic model in lumped groups, focusing on capturing the formation of the major product, levoglucosan.

Currently, there are no detailed mechanistic models for cellulose pyrolysis. The kinetic models that have been developed are highly empirical and rely on only a few highly lumped reaction steps. The most commonly used model for cellulose pyrolysis is the Broido-Shafizadeh model (Bradbury et al. 1979; Broido and Nelson 1975) which involves only three reactions and utilizes empirically-derived rate constants. While this model has been useful for predicting the overall degradation behavior, it provides almost no insight into how the various products are formed during cellulose pyrolysis. The most recent model for cellulose pyrolysis was developed by Wooten et al. (2004) and involves only six reactions. The specific mechanistic nature of these reactions is not detailed in this work and so minimal mechanistic understanding of how the various lumped species used in the model are formed is possible.

There is controversy in cellulose pyrolysis over whether it is a homolytic or heterolytic reaction system (Essig et al. 1988; Kislitsyn et al. 1971). This question can initially be avoided through the development of a pathways-level model. The method of moments framework can be utilized to develop a pathways-level model that will predict the formation of levoglucosan as well as other important products of cellulose pyrolysis. The pathways utilized in the model can be influenced based on the extensive experimental work that has been done on a range of glucans (Ponder and Richards 1994) and glucose (Paine III et al. 2008a, 2008b). The model proposed

here would be the most detailed model for cellulose pyrolysis developed to date and would provide valuable insight into this complex process. By including the proper level of detail, the model would allow a study of the decay of the cellulose degree of polymerization, the role of crystallinity, and the role of trace metal species in the cellulose. These areas have been difficult to understand using experimental techniques.

REFERENCES

Aguado, J. (1999). *Feedstock recycling of plastic wastes*. Cambridge: Royal Society of Chemistry.

Aguado, R., Olazar, M., Gaisan, B., Prieto, R., and Bilbao, J. (2003). Kinetics of polystyrene pyrolysis in a conical spouted bed reactor. *Chemical Engineering Journal* **92**: 91-99.

Al-Harthi, M., Cheng, L. S., Soares, J. B. P., and Simon, L. C. (2007). Atom-transfer radical polymerization of styrene with bifunctional and monofunctional initiators: Experimental and mathematical modeling results. *Journal of Polymer Science A: Polymer Chemistry* **45**: 2212-24.

Al-Harthi, M., Soares, J. B. P., and Simon, L. C. (2006). Dynamic Monte Carlo simulation of atom-transfer radical polymerization. *Macromolecular Materials and Engineering* **291**: 993-1003.

Anderson, D. A., and Freeman, E. S. (1961). The kinetics of the thermal degradation of polystyrene and polyethylene. *Journal of Polymer Science* **54**: 253-60.

Ballice, L., Yuksal, M., and Saglam, M. (1998). Classification of volatile products from the temperature-programmed pyrolysis of low- and high-density polyethylene. *Energy and Fuels* **12**: 925-28.

Benson, S. W. (1976). *Thermochemical kinetics: Methods for the estimation of thermochemical data and rate parameters*. 2nd ed. New York: John Wiley and Sons.

Beuermann, S., and Buback, M. (2002). Rate coefficients of free-radical polymerization deduced from pulsed laser experiments. *Progress in Polymer Science* **27**: 191-254.

Blowers, P., and Masel, R. I. (1999). An extension of the Marcus equation for atom transfer reactions. *Journal of Physical Chemistry A* **103** (35): 7047-54.

Bockhorn, H., Hentschel, J., Hornung, A., and Hornung, U. (1999). Environmental engineering: Stepwise pyrolysis of plastic waste. *Chemical Engineering Science* **54**: 3043-51.

Bockhorn, H., Hornung, A., and Hornung, U. (1998). Gasification of polystyrene as initial step in incineration, fires, or smoldering of plastics. *Proceedings of the Combustion Institute* **27**: 1343-49.

Bose, S. M., and Git, Y. (2004). Mathematical modeling and computer simulation of linear polymer degradation: Simple scissions. *Macromolecular Theory and Simulation* **13**: 453-73.

Bouster, C., Vermande, P., and Veron, J. (1980). Study on the pyrolysis of polystyrenes i. Kinetics of thermal decomposition. *Journal of Analytical and Applied Pyrolysis* **2**: 297-313.

Bradbury, A. G. W., Sakai, Y., and Shafizadeh, F. (1979). A kinetic model for pyrolysis of cellulose. *Journal of Applied Polymer Science* **23** (11): 3271-80.

Brandrup, J., and Immergut, E. H., eds. (1999). *The polymer handbook*. 4th ed. New York: Wiley-Interscience.

Broido, A., and Nelson, M. A. (1975). Char yield on pyrolysis of cellulose. *Combustion and Flame* **24** (2): 263-68.

Buback, M., Gilbert, R. G., Hutchinson, R. A., Klumperman, B., Kuchta, F.-D., Manders, B. G., O'Driscoll, K. F., Russell, G. T., and Schweer, J. (1995). Critically evaluated rate coefficients for free-radical polymerization, 1 propagation rate coefficient for styrene. *Macromolecular Chemistry and Physics* **196**: 3267-80.

Cameron, G. G., Bryce, W. A. J., and McWalter, I. T. (1984). Thermal degradation of polystyrene - 5: Effects of initiator residues. *European Polymer Journal* **20** (6): 563-69.

Cameron, G. G., and Kerr, G. P. (1968). Thermal degradation of polystyrene - 1: Chain scission at low temperatures. *European Polymer Journal* **4** (6): 709-17.

Cameron, G. G., and Kerr, G. P. (1970). Thermal degradation of polystyrene - 2: The role of abnormalities. *European Polymer Journal* **6** (2): 423-33.

Cameron, G. G., and MacCallum, J. R. (1967). The thermal degradation of polystyrene. *Journal of Macromolecular Science Part C - Polymer Reviews* **C1** (2): 327-59.

Cameron, G. G., and McWalter, I. T. (1970). On transfer reactions during vacuum pyrolysis of polystyrene. *European Polymer Journal* **6**: 1601-03.

Cameron, G. G., and McWalter, I. T. (1982). Thermal degradation of polystyrene - 4: Decomposition of oxygen-containing polymers. *European Polymer Journal* **18**: 1029-32.

Cameron, G. G., Meyer, J. M., and McWalter, I. T. (1978). Thermal degradation of polystyrene - 3: A reappraisal. *Macromolecules* **11** (4): 696-700.

Cao, Y., Gillespie, D. T., and Petzold, L. R. (2006). Efficient step size selection for the tau-leaping simulation method. *The Journal of Chemical Physics* **124**: 044109-1-11.

Cascaval, C. N., Vasile, C., and Schneider, I. A. (1970). Kinetic of the thermal degradation of polystyrene. *Macromolecular Chemistry and Physics* **131**: 55-62.

Conesa, J. A., Font, R., and Marcilla, A. (1997). Comparison between pyrolysis of two types of polyethylenes in a fluidized bed reactor. *Energy and Fuels* **11**: 126-36.

Cussler, E. L. (1997). *Diffusion: Mass transfer in fluid systems*. Cambridge: Cambridge University Press.

Daoust, D., Bormann, S., Legras, R., and Mercier, J. P. (1981). Thermal degradation of polystyrene: Changes in molecular composition. *Polymer Engineering and Science* **21** (11): 721-26.

De Witt, M. J., and Broadbelt, L. J. (2000). Binary interactions between high-density polyethylene and 4-(1-napthylmethyl)bibenzyl during low-pressure pyrolysis. *Energy and Fuels* **14**: 448-58.

Dean, J. A., ed. (1973). *Lange's handbook of chemistry*. 11th ed. New York: McGraw-Hill.

Dotson, N. A., Galvan, R., Laurence, R. L., and Tirrell, M. (1996). *Polymerization process modeling*. New York: Wiley-VCH.

EPA. (1996). *Municipal solid waste in the United States: 1995 facts and figures*. Washington, DC: United States Environmental Protection Agency.

EPA. (2006). *Municipal solid waste in the United States: 2005 facts and figures*. Washington, DC: United States Environmental Protection Agency.

Essig, M., Richards, G. N., and Schenk, E. (1988). Mechanisms of formation of the major volatile products from the pyrolysis of cellulose. *Cellulose and Wood - Chemistry and Technology*. Proceedings of the Tenth Cellulose Conference, Syracuse, New York, May 29-June 2, 1988.

Evans, M. G., and Polanyi, M. (1938). Inertia and driving force of chemical reactions. *Transactions of the Faraday Society* **34**: 11-29.

Faravelli, T., Bozzano, G., Colombo, M., Ranzi, E., and Dente, M. (2003). Kinetic modeling of the thermal degradation of polyethylene and polystyrene mixtures. *Journal of Analytical and Applied Pyrolysis* **70**: 761-77.

Faravelli, T., Bozzano, G., Scassa, C., Perego, M., Fabini, S., Ranzi, E., and Dente, M. (1999). Gas product distribution from polyethylene pyrolysis. *Journal of Analytical and Applied Pyrolysis* **52**: 87-103.

Faravelli, T., Pinciroli, M., Pisano, G., Bozzano, G., Dente, M., and Ranzi, E. (2001). Thermal degradation of polystyrene. *Journal of Analytical and Applied Pyrolysis* **60**: 103-21.

Fuoss, R. M., Salyer, I. O., and Wilson, H. S. (1964). Evaluation of rate constants from thermogravimetric data. *Journal of Polymer Science Part A* **2**: 3147-51.

Gillespie, D. T. (1976). A general method for numerically simulating the stochastic time evolution of coupled chemical reactions. *Journal of Computational Physics* **22**: 403-34.

Gillespie, D. T. (2001). Approximate accelerated stochastic simulation of chemically reacting systems. *Journal of Chemical Physics* **115** (4): 1716-33.

Gillespie, D. T. (2007). Stochastic simulation of chemical kinetics. *Annual Review of Physical Chemistry* **58**: 35-55.

Giudici, R., and Hamielec, A. E. (1996). A simulation study on random scission of branched chains. *Polymer Reaction Engineering* **4** (1): 73-101.

Grinstead, C. M., and Laurie, S. J. (1997). *Introduction to probability*. Providence: American Mathematical Society.

Habibi, A., and Vasheghani-Farahani, E. (2007). Bayesian modeling and Markov chain Monte Carlo simulations for a kinetic study of homo- and co- polymerization systems. *Macromolecular Theory and Simulation* **16**: 269-94.

Huang, C., Duever, T. A., and Tzoganakis, C. (1997). Kinetic parameter estimation in peroxide initiated degradation of polypropylene. *Polymer Reaction Engineering* **5**: 1-24.

Huang, C., Tzoganakis, C., and Duever, T. A. (1995). Monte Carlo simulation of peroxide initiated degradation of polypropylene. *Polymer Reaction Engineering* **3**: 43-63.

Huber, G. W., Iborra, S., and Corma, A. (2006). Synthesis of transportation fuels from biomass: Chemistry, catalysts, and engineering. *Chemical Reviews* **106** (9): 4044-98.

Jalil, P. A. (2002). Investigations on polyethylene degradation into fuel oil over tungstophosphoric acid supported on MCM-41 mesoporous silica. *Journal of Analytical and Applied Pyrolysis* **65**: 185-95.

Jellinek, H. H. G. (1944). On the degradation of long chain molecules part i. *Transactions of the Faraday Society* **40**: 266-73.

Jellinek, H. H. G. (1948a). On the degradation of long chain molecules part ii. *Transactions of the Faraday Society* **44**: 345-49.

Jellinek, H. H. G. (1948b). Thermal degradation of polystyrene part i. *Journal of Polymer Science* **3** (6): 850-65.

Jellinek, H. H. G. (1949a). Thermal degradation of polystyrene and polyethylene. Part iii. *Journal of Polymer Science* **4**: 13-36.

Jellinek, H. H. G. (1949b). Thermal degradation of polystyrene part ii. *Journal of Polymer Science* **4**: 1-12.

Kim, Y.-C., Kim, S., and Chung, S.-H. (2005). Estimation of the kinetic triplet of polystyrene pyrolysis from isothermal kinetic results. *Journal of Industrial and Engineering Chemistry* **11** (6): 857-63.

Kim, Y. S., Hwang, G. C., Bae, S. Y., Yi, S. C., Moon, S. K., and Kumazawa, H. (1999). Pyrolysis of polystyrene in a batch-type stirred vessel. *Korean Journal of Chemical Engineering* **16** (2): 161-65.

Kiran, E., and Gillham, J. K. (1976). Pyrolysis-molecular weight chromatography: A new on-line system for analysis of polymers. ii. Thermal decomposition of polyolefins: Polyethylene, polypropylene, polyisbutylene. *Journal of Applied Polymer Science* **20**: 2045-68.

Kishore, K. (1980). Spectral and thermal data on poly(styrene peroxide). *Journal of Chemical and Engineering Data* **25**: 92-94.

Kishore, K. (1981). Mechanism of the thermal decomposition of polystyrene peroxide. *Journal of Thermal Analysis* **21**: 15-19.

Kishore, K., and Bhanu, V. A. (1985). Maximum degradation rates in vinyl polymers. *Journal of Polymer Science: Polymer Letters* **23**: 567-71.

Kishore, K., and Mukundan, T. (1986). Poly(styrene peroxide): An auto-combustible polymer fuel. *Nature* **324** (6093): 130-31.

Kishore, K., Pai Verneker, V. R., and Gayathri, V. (1980). Kinetic study on thermal decomposition of polystyrene peroxide. *Journal of Analytical and Applied Pyrolysis* **1**: 315-22.

Kishore, K., Pai Verneker, V. R., and Nair, M. N. R. (1976). Thermal degradation of polystyrene. *Journal of Applied Polymer Science* **20**: 2355-65.

Kishore, K., Paramasivam, S., and Sandhya, T. E. (1996). High-pressure kinetics of vinyl polyperoxides. *Macromolecules* **29** (22): 6973-78.

Kishore, K., and Ravindran, K. (1982). Thermal reactivity of poly(styrene peroxide): A thermodynamic approach. *Macromolecules* **15**: 1638-39.

Kishore, K., and Ravindran, K. (1983). Effect of temperature, pressure and additives on pyrolysis of polystyrene peroxide. *Journal of Analytical and Applied Pyrolysis* **5**: 363-70.

Kislitsyn, A. N., Rodionova, Z. M., Savinykh, V. I., and Guseva, A. V. (1971). Study of the mechanism of thermal decomposition of cellulose. *Zhurnal Prikladnoi Khimii* **44** (11): 2518-24.

Kodera, Y., and McCoy, B. J. (1997). Distribution kinetics of radical mechanisms: Reversible polymer decomposition. *AIChE Journal* **43** (12): 3205-14.

Kotka, B. V., Valade, J. L., and Martin, W. N. (1973). Dynamic thermogravimetric analysis of polystyrene: Effect of molecular weight on thermal decomposition. *Journal of Applied Polymer Science* **17**: 1-19.

Krstina, J., Moad, G., and Solomon, D. H. (1989). "Weak links" in polystyrene - thermal degradation of polymers prepared with AIBN or benzoyl peroxide as initiator. *European Polymer Journal* **25** (7/8): 767-77.

Kruse, T. M., Levine, S. E., Wong, H.-W., Duoss, E., Lebovitz, A. H., Torkelson, J. M., and Broadbelt, L. J. (2005). Binary mixture pyrolysis of polypropylene and polystyrene: A modeling and experimental study. *Journal of Analytical and Applied Pyrolysis* **73**: 342-54.

Kruse, T. M., Souleimonova, R., Cho, A., Gray, M. K., Torkelson, J. M., and Broadbelt, L. J. (2003a). Limitations in the synthesis of high molecular weight polymers via nitroxide-mediated controlled radical polymerization: Modeling studies. *Macromolecules* **36** (20): 7812-23.

Kruse, T. M., Wong, H.-W., and Broadbelt, L. J. (2003b). Mechanistic modeling of polymer pyrolysis: Polypropylene. *Macromolecules* **36** (25): 9594-607.

Kruse, T. M., Wong, H.-W., and Broadbelt, L. J. (2003c). Modeling the evolution of the full polystyrene molecular weight distribution during polystyrene pyrolysis. *Industrial and Engineering Chemistry Research* **42** (12): 2722-35.

Kruse, T. M., Woo, O. S., and Broadbelt, L. J. (2001). Detailed mechanistic modeling of polymer degradation: Application to polystyrene. *Chemical Engineering Science* **56**: 971-79.

Kruse, T. M., Woo, O. S., Wong, H.-W., Khan, S. S., and Broadbelt, L. J. (2002). Mechanistic modeling of polymer degradation: A comprehensive study of polystyrene. *Macromolecules* **35** (20): 7830-44.

Kuroki, T., Ikemura, T., Ogawa, T., and Sekiguchi, Y. (1982). Kinetic study on the first stage during thermal degradation of polystyrene. *Polymer* **23**: 1091-94.

Levine, S. E., and Broadbelt, L. J. (2008). Reaction pathways to dimer in polystyrene pyrolysis: A mechanistic modeling study. *Polymer Degradation and Stability* **93** (5): 941-51.

Li, N., Cho, A., Broadbelt, L. J., and Hutchinson, R. A. (2006). Low conversion 4-acetoxystyrene free-radical polymerization kinetics determined by pulsed-laser and thermal polymerization. *Macromolecular Chemistry and Physics* **207**: 1429-38.

Libanati, C., Broadbelt, L. J., LaMarca, C., Klein, M. T., Andrews, S. M., and Cotter, R. J. (1993). Mechanistic modeling of polymer pyrolysis using Monte-Carlo methods. *Molecular Simulation* **11** (2-4): 187-204.

MacCallum, J. R. (1965). The occurrence of weak links in vinyl polymers undergoing thermal degradation. *Makromolekulare Chemie* **83**: 129-36.

Madorsky, S. L. (1953). Rates and activation energies of thermal degradation of styrene and acrylate polymers in a vacuum. *Journal of Polymer Science* **11** (5): 491-506.

Madorsky, S. L. (1964). *Thermal degradation of organic polymers*. New York: John Wiley and Sons.

Madorsky, S. L., and Straus, S. (1948). High vacuum pyrolytic fractionation of polystyrene. *Industrial and Engineering Chemistry* **40**: 848-52.

Madorsky, S. L., Straus, S., Thompson, D., and Williamson, L. (1949). Pyrolysis of polyisobutene (vistanex), polyisoprene, polybutadiene, GR-S, and polyethylene in a high vacuum. *Journal of Polymer Science* **4**: 639-64.

Madras, G., Chung, G. Y., Smith, J. M., and McCoy, B. J. (1997a). Molecular weight effect on the dynamics of polystyrene degradation. *Industrial Engineering and Chemistry Research* **36**: 2019-24.

Madras, G., and McCoy, B. J. (1999). Distribution kinetics for polymer mixture degradation. *Industrial Engineering and Chemistry Research* **38**: 352-57.

Madras, G., Smith, J. M., and McCoy, B. J. (1997b). Thermal degradation kinetics of polystyrene in solution. *Polymer Degradation and Stability* **58**: 131-38.

Maholtra, S. L., Hesse, J., and Blanchard, L.-P. (1975). Thermal decomposition of polystyrene. *Polymer* **16**: 81-93.

Marongiu, A., Faravelli, T., and Ranzi, E. (2007). Detailed kinetic modeling of the thermal degradation of vinyl polymers. *Journal of Analytical and Applied Pyrolysis* **78**: 343-62.

Mastral, J. F., Berrueco, C., and Ceamanos, J. (2007). Modeling of the pyrolysis of high density polyethylene product distribution in a fluidized bed reactor. *Journal of Analytical and Applied Pyrolysis* **79**: 313-22.

Mayo, F. R., and Miller, A. A. (1956). Oxidation of unsaturated compounds ii: Reactions of styrene peroxide. *Journal of the American Chemical Society* **78**: 1023-34.

McCoy, B. J. (1993). Continuous-mixture kinetics and equilibrium for reversible oligomerization reactions. *AIChE Journal* **39** (11): 1827-33.

McDermott, J. B., Libanati, C., LaMarca, C., and Klein, M. T. (1990). Quantitative use of model compound information: Monte Carlo simulation of the reactions of complex macromolecules. *Industrial and Engineering Chemistry Research* **29**: 22-29.

Mehmet, Y., and Roche, R. S. (1976). A study of the thermal degradation of polystyrene by thermal volatization analysis. *Journal of Applied Polymer Science* **20**: 1955-65.

Mohan, D., Pittman Jr., C. U., and Steele, P. H. (2006). Pyrolysis of wood/biomass for bio-oil: A critical review. *Energy and Fuels* **20**: 848-89.

Moscatelli, D., Cavallotti, C., and Morbidelli, M. (2006). Prediction of molecular weight distributions based on ab initio calculations: Application to the high temperature styrene polymerization. *Macromolecules* **39**: 9641-53.

Nanda, A. K., and Kishore, K. (2000a). Semiemperical and thermodynamic calculations on the exothermic degradation of vinyl polyperoxides. *Indian Journal of Chemistry* **39A** (6): 631-33.

Nanda, A. K., and Kishore, K. (2000b). Thermal-initiating potentialities of vinyl polyperoxides: Transmutation of block-into-block copolymer and an exploratory investigation of surface texture and morphology. *Journal of Polymer Science A: Polymer Chemistry* **38**: 3665-73.

Ohtani, H., Yuyama, T., Tsuge, S., Plage, B., and Schulten, H.-R. (1990). Study of thermal degradation of polystyrenes by pyrolysis-gas chromatography and pyrolysis-field ionization mass spectrometry. *European Polymer Journal* **26** (8): 893-99.

Paine III, J. B., Pithawalla, Y. B., and Naworal, J. D. (2008a). Carbohydrate pyrolysis mechanisms from isotope labeling part 2. The pyrolysis of D-glucose: General disconnective analysis and the formation of C_1 and C_2 carbonyl compounds by electrocyclic fragmentation mechanisms. *Journal of Analytical and Applied Pyrolysis* **82**: 10-41.

Paine III, J. B., Pithawalla, Y. B., and Naworal, J. D. (2008b). Carbohydrate pyrolysis mechanisms from isotopic labeling part 3. The pyrolysis of D-glucose: Formation of C_3 and C_4 carbonyl compounds and cyclopentenedione isomer by electrocyclic fragmentation mechanisms. *Journal of Analytical and Applied Pyrolysis* **82**: 42-69.

Petzold, L. R. (1983). *DASSL differential/algebraic system solver*. Livermore, CA: Sandia National Laboratories.

Pfaendtner, J., and Broadbelt, L. J. (2008). Mechanistic modeling of lubricant degradation. 1. Structure-reactivity relationships for free-radical oxidation. *Industrial and Engineering Chemistry Research* **47** (9): 2886-96.

Pfaendtner, J., Yu, X., and Broadbelt, L. J. (2006). Quantum chemical investigation of low-temperature intramolecular hydrogen transfer reactions of hydrocarbons. *Journal of Physical Chemistry A* **110** (37): 10863-71.

Pinto, J.-H. Q., and Kaliaguine, S. (1991). A Monte Carlo analysis of acid hydrolysis of glycosidic bonds in polysaccharides. *AIChE Journal* **37** (6): 905-14.

Ponder, G. R., and Richards, G. N. (1994). A review of some recent studies on mechanisms of pyrolysis of polysaccharides. *Biomass and Bioenergy* **7** (1-6): 1-24.

Poutsma, M. L. (2003). Reexamination of the pyrolysis of polyethylene: Data needs, free-radical mechanistic considerations, and thermochemical kinetic simulation of initial product-forming pathways. *Macromolecules* **36** (24): 8931-57.

Poutsma, M. L. (2006). Mechanistic analysis and thermochemical kinetic simulation of the pathways for volatile product formation from pyrolysis of polystyrene, especially for the dimer. *Polymer Degradation and Stability* **91**: 2979-3009.

Ranzi, E., Dente, M., Faravelli, T., Bozzano, G., Fabini, S., Nava, R., Cozzani, V., and Tognotti, L. (1997). Kinetic modeling of polyethylene and polypropylene thermal degradation. *Journal of Analytical and Applied Pyrolysis* **40-41**: 305-19.

Rice, F. O., and Herzfeld, K. F. (1934). The thermal decomposition of organic compounds from the standpoint of free radicals. vi. The mechanism of some chain reactions. *Journal of the American Chemical Society* **56**: 284-89.

Richards, D. H., and Salter, D. A. (1967). Thermal degradation of vinyl polymers iii - a radiochemical study of intermolecular chain transfer in the thermal degradation of polystyrene. *Polymer* **8**: 153-59.

Risby, T. H., and Yergey, J. A. (1982). Linear programmed thermal degradation mass spectrometry of polystyrene and poly(vinyl chloride). *Analytical Chemistry* **54**: 2228-33.

Rosen, S. L. (1993). *Fundamental principles of polymeric materials*. 2nd ed. New York: John Wiley & Sons, Inc.

Saidel, G. M., and Katz, S. (1968). Dynamic analysis of branching in radical polymerization. *Journal of Polymer Science A-2: Polymer Physics* **6**: 1149-60.

Scheirs, J., and Kaminsky, W., eds. (2006). *Feedstock recycling and pyrolysis of waste plastics: Converting waste plastics into diesel and other fuels*. West Sussex: John Wiley & Sons Ltd.

Schreck, V. A., Serelsi, A. K., and Solomon, D. H. (1989). Self-reactions of 1,3-diphenylpropyl and 1,3,5-triphenylpentyl radicals: Models for termination in styrene polymerization. *Australian Journal of Chemistry* **42** (3): 375-93.

Seeger, M., and Cantow, H.-J. (1975). Thermal scission mechanisms in homo and copolymers of alpha-olefins. 1. Fundamental mechanisms and pyrolysis of linear polyethylene. *Makromolekulare Chemie* **176** (5): 1411-25.

Sezgi, N. A., Cha, W. S., Smith, J. M., and McCoy, B. J. (1998). Polyethylene pyrolysis: Theory and experiments for molecular-weight distributions kinetics. *Industrial and Engineering Chemistry Research* **37**: 2582-91.

Singh, R. P., Desai, S. M., Sivaram, S., and Kishore, K. (2002). A novel synthesis of poly(styrene peroxide) with controlled peroxy linkages at room temperature. *Macromolecular Chemistry and Physics* **203** (15): 2163-69.

Sterling, W. J., and McCoy, B. J. (2001). Distribution kinetics of thermolytic macromolecular reactions. *AIChE Journal* **47** (10): 2289-303.

Stewart, W. E., Caracotsios, M., and Sorensen, J. P. (1992). Parameter estimation from multiresponse data. *AIChE Journal* **38** (5): 641-50.

Subramanian, K. (2003). Formation, degradation, and applications of polyperoxides. *Journal of Macromolecular Science C: Polymer Reviews* **C43** (3): 323-83.

Szekely, T., Varhegyi, G., Till, F., Szabo, P., and Jakab, E. (1987). The effects of heat and mass transport on the results of thermal decomposition studies part 2. Polystyrene, polytetrafluoroethylene, and polypropylene. *Journal of Analytical and Applied Pyrolysis* **11**: 83-92.

Tobita, H. (1996a). Random degradation of branched polymers. 1. Star polymers. *Macromolecules* **29**: 3000-09.

Tobita, H. (1996b). Random degradation of branched polymers. 2. Multiple branches. *Macromolecules* **29**: 3010-21.

Tsuchiya, Y., and Sumi, K. (1968a). Thermal decomposition products of polyethylene. *Journal of Polymer Science A-1: Polymer Chemistry* **6**: 415-24.

Tsuchiya, Y., and Sumi, K. (1968b). Thermal decomposition products of polymethylene. *Journal of Polymer Science B: Polymer Letters* **6**: 357-61.

Wall, L. A., Madorsky, S. L., Brown, D. W., Straus, S., and Simha, R. (1954). Depolymerization of polymethylene and polyethylene. *Journal of the American Chemical Society* **76**: 3430-37.

Wang, M., Smith, J. M., and McCoy, B. J. (1995). Continuous kinetics for thermal degradation of polymer in solution. *AIChE Journal* **41** (6): 1521-33.

Weast, R. C., Astle, M. J., and Beyer, W. H., eds. (1986). *CRC handbook of chemistry and physics*. 67 ed. Boca Raton: CRC Press, Inc.

Westerhout, R. W. J., Kuipers, J. A. M., and van Swaaij, W. P. M. (1998). Experimental determination of the yield of pyrolysis products of polyethene and polypropene. Influence of reaction conditions. *Industrial and Engineering Chemistry Research* **37**: 841-47.

Westerhout, R. W. J., Waanders, J., Kuipers, J. A. M., and van Swaaij, W. P. M. (1997). Kinetics of the low-temperature pyrolysis of polyethene, polypropene, and polystyrene modeling, experimental determination, and comparison with literature models and data. *Industrial and Engineering Chemistry Research* **36** (6): 1955-64.

Woo, O. S., Ayala, N., and Broadbelt, L. J. (1998). Recovery of high-valued products from styrene-based polymers through coprocessing. Experiments and mechanistic modeling. *Catalysis Today* **40**: 121-40.

Wooten, J. B., Seeman, J. I., and Hajaligol, M. R. (2004). Observation and characterization of cellulose pyrolysis intermediates by ^{13}C CPMAS NMR. A new mechanistic model. *Energy and Fuels* **18** (1): 1-15.

Zhao, B., and Bar-Ziv, E. (2000). A new look into the pyrolysis of polystyrene. *Proceedings of the Combustion Institute* **28**: 2659-66.

Zhao, B., Kantorovich, I., and Bar-Ziv, E. (1998). A new method for studying the degradation of polymers at high temperatures. *Proceedings of the Combustion Institute* **27**: 2865-71.